AD-A086 128 SOLAR TURBINES INTERNATIONAL SAN DIEGO CA F/G 11/6
COMPLEX, PRECISION CAST COLUMBIUM ALLOY GAS TURBINE ENGINE NOZZ--ETC(U)
APR 80 L HSU, W G STEVENS, A R STETSON DAAG46-76-C-0053
UNCLASSIFIED SR80-R-4444-25 USAAVRADCOM-TR-80-F-2 NL

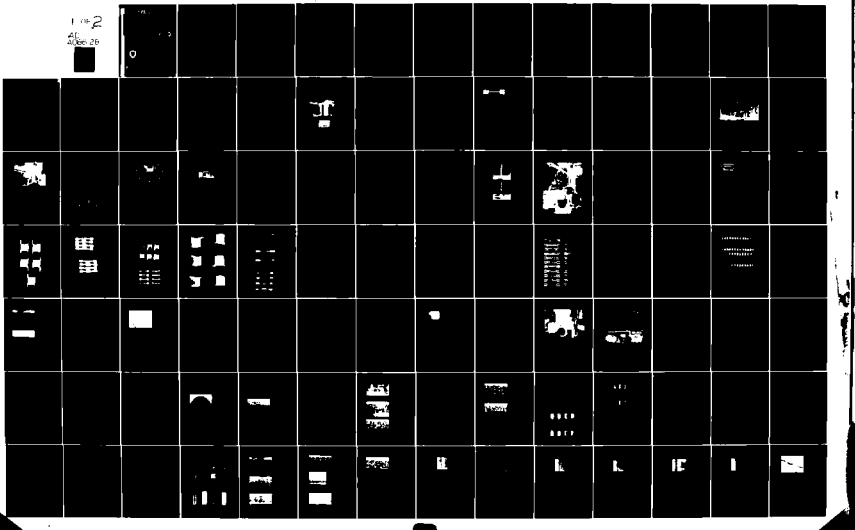

AVRADCOM
Report No. TR 80-F-2

AD

MANUFACTURING METHODS AND TECHNOLOGY (MANTECH) PROGRAM

COMPLEX, PRECISION CAST COLUMBIUM ALLOY GAS TURBINE ENGINE NOZZLES COATED TO RESIST OXIDATION

L., Hsu, W.G., Stevens and A. R., Stetson
Solar/International Harvester
2200 Pacific Highway
P.O. Box 80966
San Diego, CA 92138

March 1980

FINAL REPORT

Contract No. DAAG46-76-C-0053

United States Army
AVIATION RESEARCH AND DEVELOPMENT COMMAND

The findings in this report are not to be construed as an official Department of the Army position, unless so designated by other authorized documents.

Mention of any trade names or manufacturers in this report shall not be construed as advertising nor as an official indorsement or approval of such products or companies by the United States Government.

DISPOSITION INSTRUCTIONS

Destroy this report when it is no longer needed.
Do not return it to the originator.

SECURITY CLASSIFICATION OF THIS PAGE (When Data Entered)

REPORT DOCUMENTATION PAGE

READ INSTRUCTIONS BEFORE COMPLETING FORM

1. REPORT NUMBER: AVRADCOM Report No. TR80-F-2
2. GOVT ACCESSION NO.: AD-A086 128
3. RECIPIENT'S CATALOG NUMBER:

4. TITLE (and Subtitle): Complex, Precision Cast Columbium Alloy Gas Turbine Engine Nozzles Coated to Resist Oxidation
5. TYPE OF REPORT & PERIOD COVERED: Final Report, August 2, 1976-August 2, 1979
6. PERFORMING ORG. REPORT NUMBER: SR80-R-4444-25

7. AUTHOR(s): Hsu, L., Stevens, W.G. and Stetson, A.R.
8. CONTRACT OR GRANT NUMBER(s): DAAG46-76-C-0053

9. PERFORMING ORGANIZATION NAME AND ADDRESS: Solar Turbines International, An Operating Group of International Harvester, San Diego, California 92138
10. PROGRAM ELEMENT, PROJECT, TASK AREA & WORK UNIT NUMBERS: D/A Proj: 1758129; AMCMS Code: 1497.94.5.5411[illegible]

11. CONTROLLING OFFICE NAME AND ADDRESS: AVRADCOM, St. Louis, Missouri 63166
12. REPORT DATE: April 1980
13. NUMBER OF PAGES: 139

14. MONITORING AGENCY NAME & ADDRESS (if different from Controlling Office): Army Materials & Mechanics Research Center, Watertown, MA 02172
15. SECURITY CLASS (of this report): Unclassified
15a. DECLASSIFICATION/DOWNGRADING SCHEDULE: N/A

16. DISTRIBUTION STATEMENT (of this Report)

Approved for public release; distribution unlimited

17. DISTRIBUTION STATEMENT (of the abstract entered in Block 20, if different from Report)

18. SUPPLEMENTARY NOTES

AMMRC TR80-23

19. KEY WORDS (Continue on reverse side if necessary and identify by block number)

Columbium alloys	Oxidation	Burner rig
C129Y	Nozzle vane	NS-4 coating
Castings	Solid	Tensile
	Cored	Stress rupture

20. ABSTRACT (Continue on reverse side if necessary and identify by block number)

The objectives of this program were to produce investment cast single vane nozzle segments in C129Y alloy (Cb-10Hf-10W-0.3Y) and to coat these vanes with the NS-4 (50W-20Mo-15Ti-10V) silicide coating. Initially, both cored and solid vane segments were specified but due to problems experienced in the consumable arc process, cored vanes were deleted from the program scope.

DD FORM 1 JAN 73 1473 EDITION OF 1 NOV 65 IS OBSOLETE

UNCLASSIFIED

SECURITY CLASSIFICATION OF THIS PAGE (When Data Entered)

Block No. 20

ABSTRACT

REM Metals of Albany, Oregon was the casting subcontractor and though they have had previous experience with this alloy and other columbium alloys in general, several problems developed. The electrode material supplied was low in yttrium, which might have contributed to the poor fluidity during arc melt and incomplete fill of thin walled sections. The solid nozzles and round test bars were acceptable and were used in coating processing and testing.

Process specifications for both slurry spray and dip applications of the NS-4 modifier were prepared. Tensile and stress rupture tests of coated specimens displayed exceptional properties at elevated temperatures and showed superiority to cobalt-base vane alloys. Isothermal oxidation lives in excess of 5500 hours (at 760 and 1093°C) were exhibited by NS-4 coated C129Y specimens. In rig testing, under the severe thermal cycles and profiles imposed, the airfoil specimens typically survived about 100 hours.

FOREWORD

This final summary report covers the work performed under Contract DAAG46-76-C-0053 from August 5, 1976 to August 2, 1979. This program was sponsored by the U. S. Army Aviation Research and Development Command, St. Louis, Missouri through a contract with the Army Materials and Mechanics Research Center (AMMRC), Watertown, MA. The technical activities were performed at the Harbor Drive facilities of Solar Turbines International, an Operating Group of International Harvester. AMMRC Program Monitors were Milton Levy and Robert French.

V. S. Moore was the original Principal Investigator with A. R. Stetson as the Technical Director. With the demise of V. S. Moore, Dr. W. G. Stevens and Lulu Hsu then assumed control of the program with the assistance of A. N. Hammer in the casting phase.

Acknowledgement is extended to J. Wolman and J. Leggett for their assistance in the technical activities.

TABLE OF CONTENTS

TABLE OF CONTENTS (Cont)

LIST OF FIGURES

LIST OF FIGURES (Cont)

LIST OF FIGURES (Cont)

LIST OF FIGURES (Cont)

LIST OF FIGURES (Cont)

LIST OF TABLES

LIST OF FIGURES (Cont)

1

INTRODUCTION

1.1 BACKGROUND

Conventional superalloys and second generation materials such as directionally solidified (DS), oxide dispersion strengthened (ODS), mechanically alloyed and single crystal alloys are currently temperature limited to around 1100°C for useful, long-term service. Above 1100°C, the principal materials capable of high-temperature, high-strength performance are ceramics and refractory alloys of columbium and tantalum (Ref. 1). As a result of the efforts invested in development of columbium alloys and oxidation-resistant coatings in the last two decades, the state-of-the-art of this technology has been significantly advanced.

The application of coated columbium technology to high-temperature component fabrication must be considered critically in two important aspects:

1. Formability
2. Oxidation-resistant surface modification

1.1.1 Formability

As with any candidate alloy system, it is necessary to establish forming capabilities which, in turn, will effect the scope of its usability. Prior to investment casting of columbium alloys, columbium alloys were primarily available in wrought form, and applications were limited to simple components that can be readily fabricated. In 1971, an AMMRC sponsored investigation (Ref. 2) reported that cast alloy materials exhibited a two-fold improvement in stress rupture life at 1204°C (2200°F) when compared to equivalent wrought material. Additional work by REM Metals Corp. in 1975 (Ref. 3) demonstrated that relatively complex configurations including thin-walled components (1.02 mm) can be poured with fairly high melting, high-strength alloys such as SU31 and CB752. Significant advances were also made in foundry practice which were extremely encouraging in advancing the state-of-the-art toward the goal of production of cast engine hardware.

1.1.2 Surface Protection

The efforts expended in coating development were concurrent with casting investigations and were largely spurred on by the susceptibility of columbium alloys to catastrophic oxidation failure. Starting in the late 1950's, the development of coatings for columbium alloys has progressively evolved from relying solely on $CbSi_2$ for oxidation resistance to multi-component coating systems. Upon exposure to air at elevated temperatures, the SiO_2 scale formed from $CbSi_2$ was found to contain significant quantities of CbO_x which is highly undesirable due to the premeability of O_2 through the high anion vacancy of the columbium oxide lattice. In subsequent work, the goal has been to design and develop a coating that will furnish an adherent and continuous layer of pure SiO_2 for oxidation resistance.

Most columbium substrate alloys (and also tantalum alloys) are essentially continuous solid solutions with typically 20 percent alloying elements and vapor deposition of silicon results in formation of $CbSi_2$ at the substrate surface. In order to provide better oxidation resistance than that afforded by $CbSi_2$ alloy, the surface was modified by depositing an overlay coating that can be silicided to form a stable silicon rich layer which will continually replenish the SiO_2 scale as it is removed.

In the early 1960's, TRW developed a $(CrTiCb)Si_2$ coating that was applied in a two-stage process. Chromium and titanium were codeposited and were subsequently silicided. The resulting coating composition was much lower in columbium than the substrate itself. The presence of chromium and titanium imparted increased resistance to oxidation, 50 to 100 hours at 1316°C (2400°F) by lowering the fusion temperature of the coating for use in the range of 1316-1427°C (2400-2600°F). However, a major drawback to the widespread use of this system was the size and configuration limitations imposed by the codeposition process. This disadvantage was eliminated in a system developed at Sylvania Electric, Inc. which contained titanium and iron as the modifying constituents. The coating itself, R512E, was a fusion type and its ease of applicability coupled with its 50 to 100 hour life at 1316°C (2400°F) made this coating very attractive for applications requiring short-term (<50 hours) protection.

About the time Sylvania was working on its R512E coating, Solar was also actively pursuing a new approach to surface protection of columbium and tantalum alloys. The key concept behind Solar's approach was to minimize the presence of columbium and other undesirable elements in the coating and to maximize the elements that form outstanding oxidation-resistant silicides. In the Solar process, the slurry of the metallic modifier is applied to the substrate and vacuum sintered at temperatures between 1480 and 1700°C (2700 and 3100°F). This is followed by a pack siliciding process which essentially reduces the porosity in the coating as the formation of disilicides is accompanied by 150 percent volume growth. This reaction sintering approach produces a coating that is free of the undesirable substrate elements and can be readily modified for optimized protection in the range of 1316 to 1650°C (2400 to 3000°F) (Ref. 4). Another advantage of the Solar series of coatings is the lower coefficient of thermal expansion as noted below.

	Coefficient of Thermal Expansion (RT-1800°F) °F x 10^6
R512A (TiCrCb)Si_2 - Sylvania	6.9
R512E (TiFeCb)Si_2 - Sylvania	6.9
NS-4 (50W-20Mo-15Ti-15V)Si_2 - Solar	5.2
TNV-7 (35W-35Mo-15Ti-15V)Si_2 - Solar	5.2
TNV-12 (95Mo-5Ti)Si_2 - Solar	4.8
TNV-13 (97.5W-2.5Ti)Si_2 - Solar	4.7
Cb752 Alloy	4.3

The thermal expansion mismatch between these silicide coatings and the underlying substrate typically results in the formation of craze cracks in the coating at room temperature. At elevated temperature, the coating rapidly expands and the refractory layer softens to form a continuous protective surface. In order to increase the temperature range over which this class of coating is effective, the level of titanium and vanadium can be adjusted. The vanadium and titanium modification of the SiO_2 lattice decreases the softening temperature of the surface glass, essentially eliminating the low-temperature 649-760°C (1200-1400°F), 'pest' oxidation problem. For high-temperature application, the TNV-12 and -13 coatings are excellent while the TNV-7 and NS-4 coatings perform best at medium and lower temperatures, <1427°C (<2600°F). The NS-4 coating, in particular, has been demonstrated to be very satisfactory (Ref. 5,6). Long-term (up to 1000 hours) oxidation exposures at 1316°C (2400°F) revealed little microstructural change, indicating excellent coating stability and retained tensile properties are superior to R512E coated specimens.

1.2 PROGRAM OBJECTIVES

The goal of this program was to utilize the state-of-the-art in the columbium casting and coating technologies to produce fully coated, investment cast single vane first-stage Centaur nozzles. Figure 1 shows a paired nozzle vane although the actual configuration used in the casting sequence was essentially one half of the paired segment. The C129Y alloy (Cb-10W-10Hf) was selected for this investigation based on its superior weldability, castability, lower melting temperature and strength (Ref. 3), together with Solar's NS-4 coating.

The program was divided into two phases - Phase I was concerned with development of the casting process with establishment of process parameters for producing single vane Centaur nozzles (both cored and solid) and test specimens; Phase II was scoped to contain the coating process development work and process specification for coating application to the cast components produced in Phase I.

Mechanical property tests were used to evaluate both the quality of the cast material and also the extent of coating/substrate interaction. Finally, environmental (static and dynamic) tests were performed in Phase II on coated components to demonstrate the effectiveness of cast and coated materials under simulated service conditions.

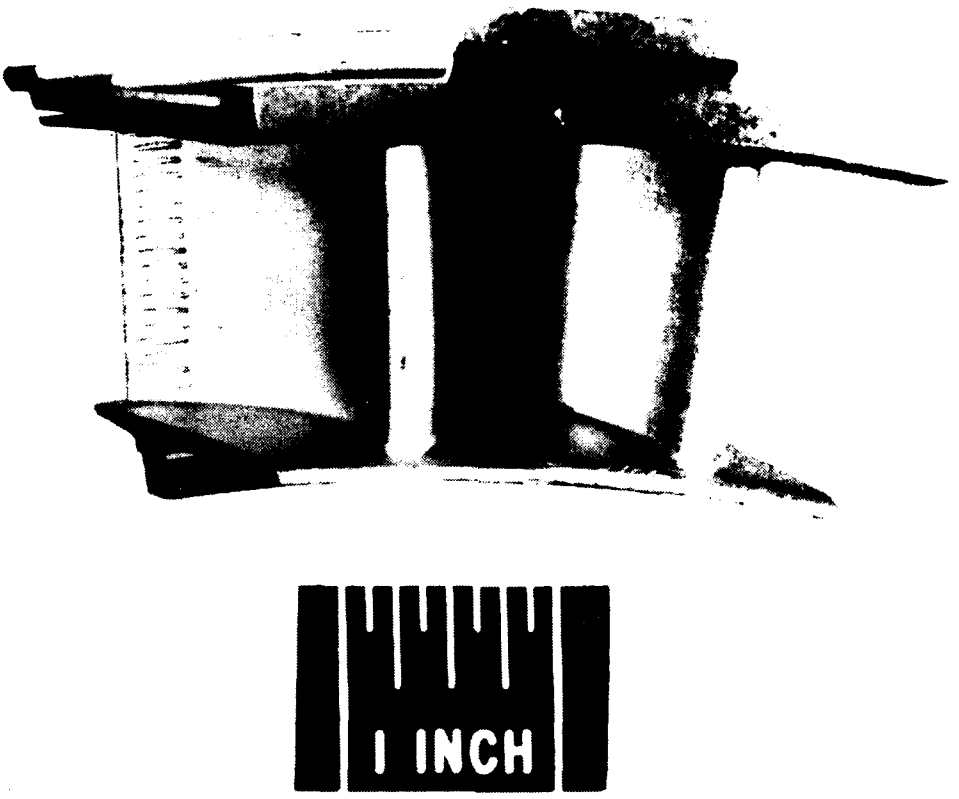

Figure 1. First-Stage Centaur Double Vane Nozzle Segment

2

EXPERIMENTAL

2.1 PROGRAM MATERIALS

The program alloy C129Y (Cb-10W-10Hf-Y) is a product of Wah Chang of Albany, Oregon and 4-inch diameter electrode and starter materials were purchased per TWCA-CB-MS-1. Lot certifiction as received from the supplier is reported in Section 3 and discussed in context with casting development.

The casting subcontractor was REM Metals Corp., an organization also located in Albany, Oregon, which has had over seven years of experience in casting of columbium alloys.

Initial work in coating development and optimization was done using pure, recrystalliized columbium sheet metal which was formed to simulate airfoil configurations.

The composition of the modifier used in the NS-4 coating was 50W-20Mo-15Ti-15V. Particle sizes of the tungsten and molybdenum powders were <5 μm. The titanium and vanadium were originally -325 and -200 mesh and were converted to their respective hydrides before grinding in Burundum mills. The hydriding procedures are descriped in Appendix A. After the metal powders were mixed together in the proper percentages, the mixture was ground to finer sizes, as described in Appendix B. A liquid-to-solid ratio of 2.5/1 to 3.0/1 by volume was used for spray applications and the modifier slurry was stored in glass bottles purged with argon prior to sealing.

The -200 mesh siicon used in the pack siliciding operations was obtained from Keokuk Electro-Metals Company as Lot No. 3991. The impurity analysis yielded 0.33% Fe, 0.04% Ca and 0.21% M.

2.2 PROGRAM SPECIMENS

At the beginning of the program, the contracted scope of work called for the following configurations to be cast, coated and tested:

- Round, 1/4-inch diameter threaded tensile bars
- Flat 0.065-inch stress-rupture bars
- 15 degree wedge shaped, thermal fatigue bars

- 30 degree wedge shaped, thermal fatigue bars
- 0.5 inch diameter oxidation coupons.

However, in the course of the program, the scope of work was changed as a result of problems encountered in the casting phase and the specimen configurations actually used are as indicated below:

- Stress-rupture specimens, Figure 2
- Tensile specimens, Figure 3
- Oxidation coupons (cut from sound sections of flat tensile specimens), Figure 4.

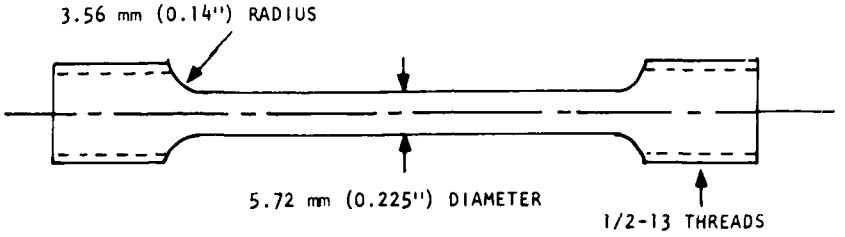

Figure 2. Stress-Rupture Test Specimen

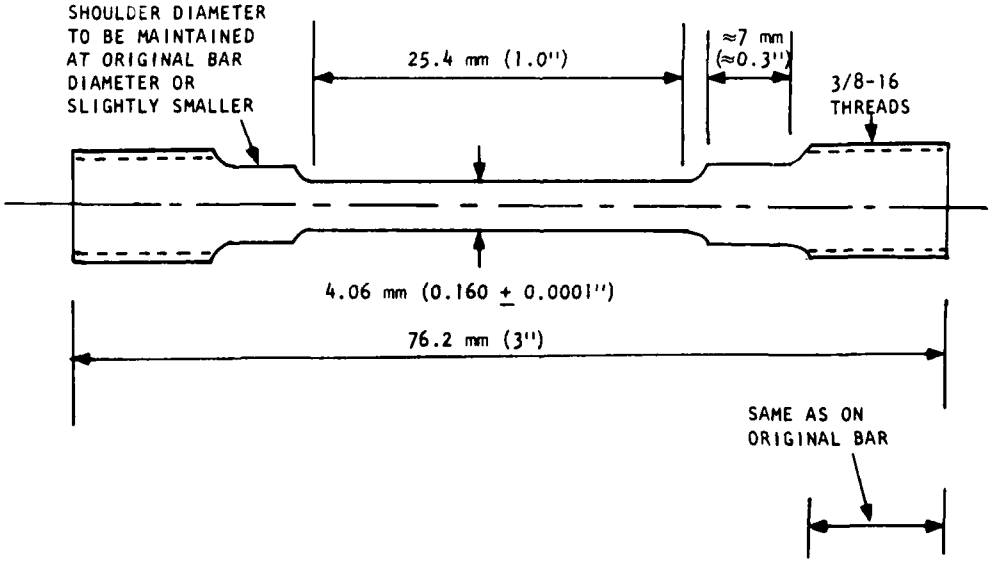

Figure 3. Tensile Test Specimen

Figure 4.

Coupon Cut From Sound Section of Casting

2.3 MECHANICAL AND ENVIRONMENTAL TESTING

The scope of testing utilized to evaluate the soundness of the cast material and the interaction of coating with substrate alloy included the following:

- Tensile (ambient, 1093°C + 1204°C)
- Stress rupture (1093°c + 1204°C)
- Furnace oxidation (760°C + 1093°C)
- Dynamic oxidation or burner rig (816°C to 1316°C).

2.3.1 Tensile Tests

The effects of the coating process and the interaction of the coating with the strength and ductility of the cast columbium alloy was evaluated in tensile tests at room temperature, 1093°C and 1204°C. Testing was done using an Instron Model TTD Universal screw-driven testing machine and load strain curves were autographically recorded from an extensometer attached to each specimen at room temperature. For elevated-temperature tests, a special setup was designed and fabricated, as illustrated in Figure 5, in order to minimize oxidation attack. A major consideration in designing the test system was the limitation imposed by the reaction of silicon with nickel forming a low melting eutectic. Therefore, couplings fabricated from molybdenum were used, both to eliminate this problem and to provide high-temperature strength. Since molybdenum has relatively poor resistance to O_2 at elevated temperatures, a special shroud was built to provide a low oxygen, argon-rich environment during testing. Tubes leading into a sleeve fitted around the extension rods fed the argon gas in around the specimen to maintain the inert atmosphere. The furnace extended past the molybdenum coupling to the extension rods and the entire shroud was kept inert by purging prior to testing and maintaining a positive pressure throughout the tests. For the elevated-temperature runs, instead of an extensometer, gage marks and heat-resistant paint were used to mark the elongation.

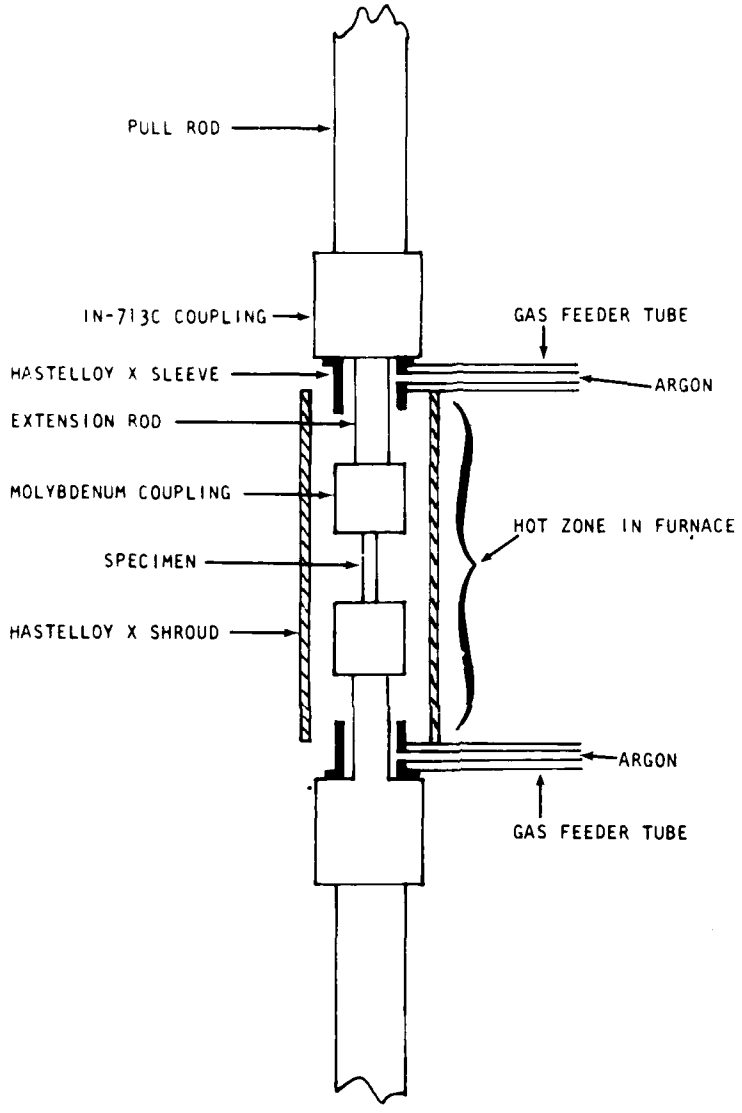

Figure 5. Tensile Test Setup

2.3.2 Stress-Rupture Tests

Elevated-temperature stress-rupture tests were performed at Southern Research Institute (SoRI) in Birmingham, Alabama. Since both uncoated and coated C129Y alloy were to be evaluated, it was decided that all tests were to be conducted in helium atmosphere.

The tests were conducted in a 12,000 pound Arcweld creep machine. The standard furnace had been removed and replaced with a specially designed environmental chamber and furnace in order to provide the controlled helium environment.

The test setup for the environmental chamber and furnace is shown schematically in Figure 6. The environmental chamber is a clear quartz tube with stainless steel endcaps. The seals between the pullrods and endcaps and the quartz tube and endcaps were made with O-rings. The helium was introduced into the chamber through the lower endcap after passing through a liquid N_2 cold trap. The helium was released from the chamber through the upper endcap where it was carried to a trap and then to a bubbler which was used to set the back pressure in the system. This back pressure was nominally 15 cm H_2O. A small tube of desiccant was placed in the purge line between the upper endcap and the bubbler to prevent the back diffusion of water vapor into the chamber. The dryer was inserted in the line after the second run. The water vapor content in the environmental chamber for the first two runs was unknown. Nominal water vapor content in the helium was 8 to 10 ppm but diffusion from the bubbler would have increased the water vapor present. After the tube with the desicant was placed in the line, the water vapor in the system was monitored on the outlet line with a Beckman Trace Moisture Analyzer. For the final seven runs the water vapor present in the system ranged from 8 to 12 ppm. After the second run a gas sample was taken. The results of the analysis of the gas sample showed less than 100 ppm of O_2 and N_2. Since the preliminary analysis showed no evidence of an air leak, the analyses were not pursued to establish actual levels.

The pullrods and threaded couplings were made of molybdenum and supplied by Solar. The threaded couplings were silicided at Solar; the pullrods were used as-machined. The surfaces of the pullrods were cleaned and polished after each run. Observation of these surfaces during a run provided a ready means of determining whether there were any air leaks into the system. No oxidation was observed on the molybdenum parts in the hot zone of the furnace. An overnight purge, was used prior to starting a run.

Dead weights were used to supply the load through a 20:1 lever arm. Strain measurements were made using dual Gaertner Filer microscopes sighting on platinum wire targets. The wires were wrapped around the gage section of the specimen, 1.52 to 1.78 cm (0.6 to 0.7 inch) apart. The gage length was measured using the traveling microscopes prior to the start of each test. The traveling microscopes can be seen in Figure 7, which is a photograph of the test setup.

Temperature was monitored using a Type S thermocouple wired in the center of the gage section. This thermocouple was used as input to an L and N Electromax III temperature controller which in turn provided control signals to a SCR power controller. A second thermocouple was also wired on the specimen for backup in case the primary thermocouple failed. The furnace was a four-element tungsten-quartz furnace and each element was rated at 2000W.

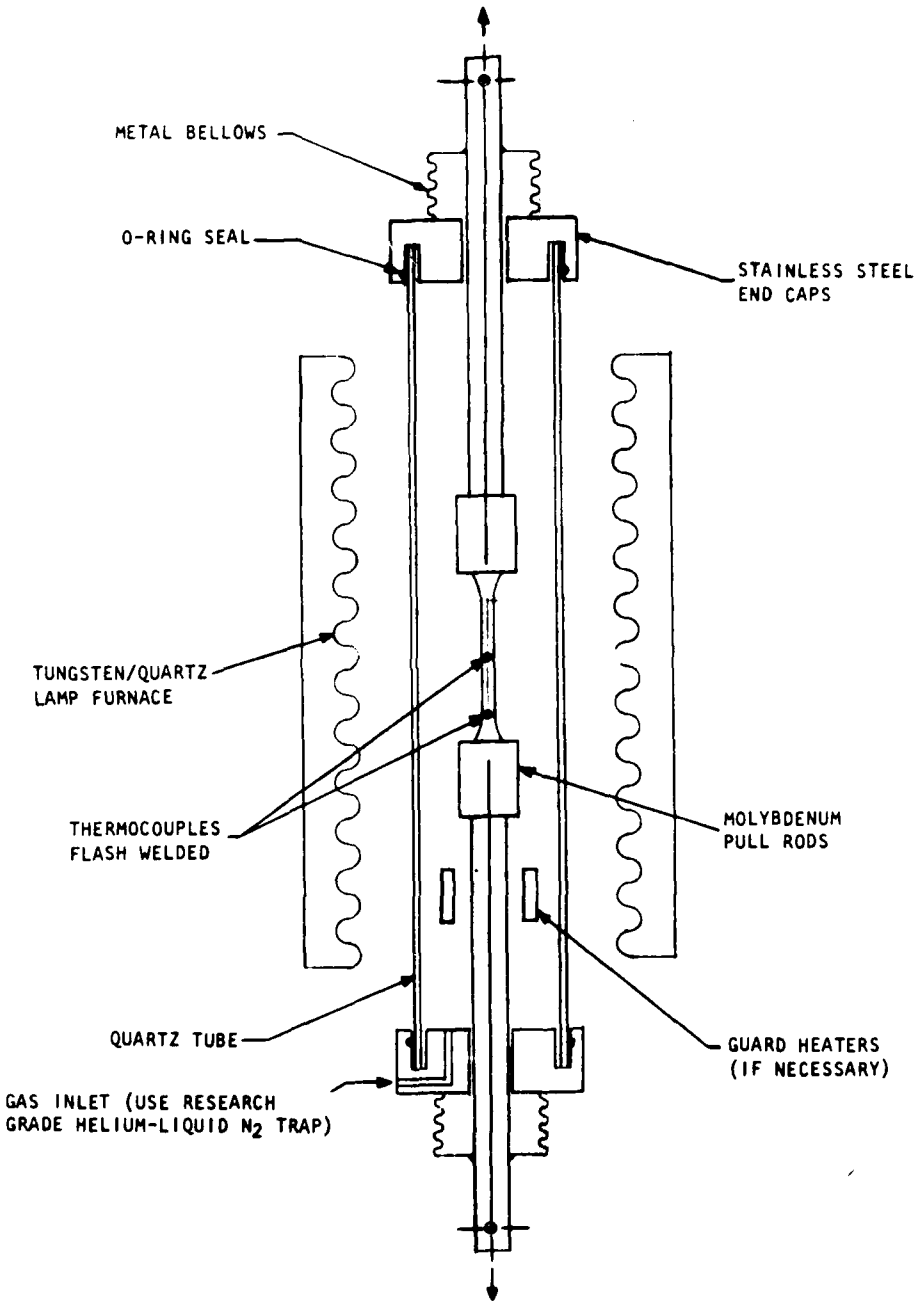

Figure 6. Schematic of Stress-Rupture Test Setup

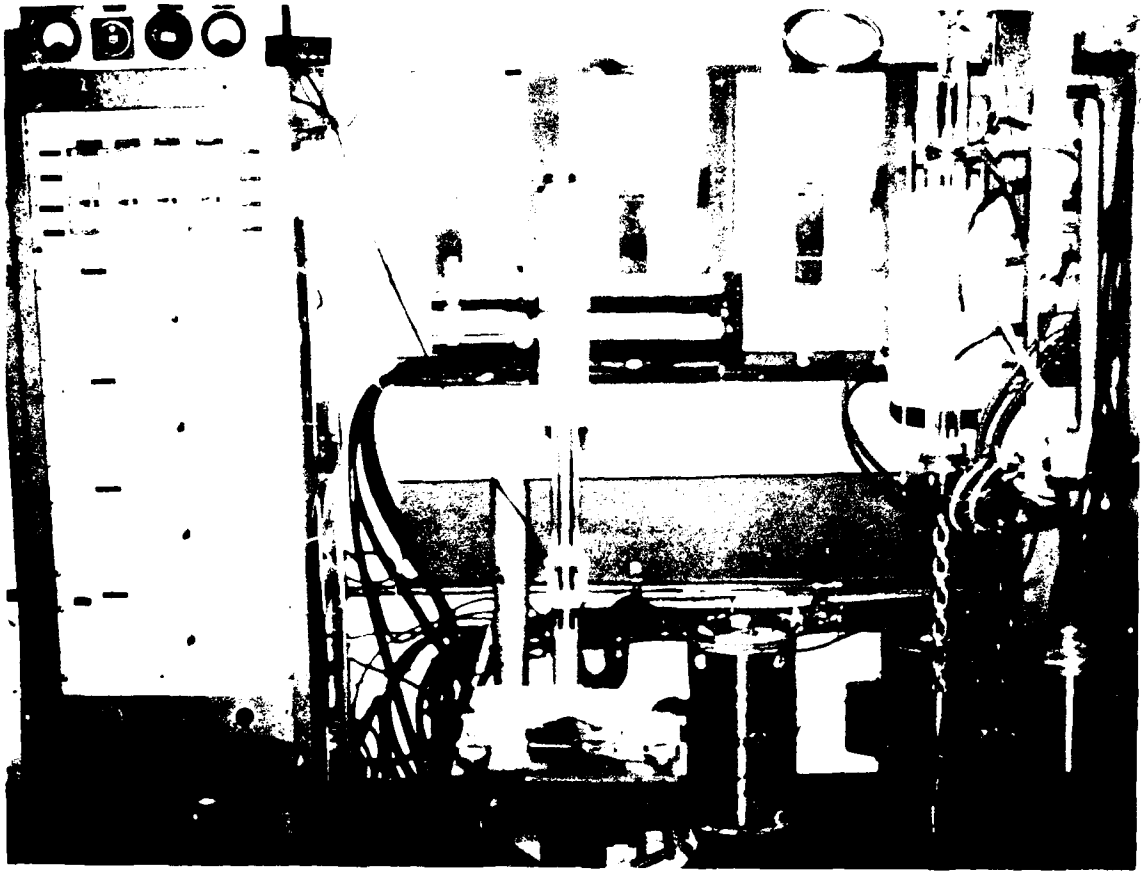

Figure 7. Setup for Stress-Rupture Evaluations on C129Y Alloy

2.3.3 Furnace Oxidation Tests

Static oxidation tests were conducted at two temperatures, 760 and 1093°C, in air. The 760°C furnace was a resistance heated, multiple unit furnace made by Hevi Duty Electric Company. A Lindberg/Hevi Duty globar furnace was used to provide the 1093°C environment. The coated specimens were placed on pieces of clean dynaquartz and were visually inspected at 24-hour intervals, except for weekends, without removal from the furnace. The specimens were allowed to cycle down to room temperature only when gravimetric measurements were to be taken.

2.3.4 Burner Rig Oxidation Tests

In order to evaluate further the performance of the NS-4/C129Y system in a dynamic oxidizing environment, environmental simulator or burner rig tests were performed. The rig itself consists of a straight-through, can-type combustor with a double liner mounted vertically such that the combustion gases can be vented to an exhaust stack, as shown in Figure 8. JP-5 fuel was used (MIL-J-5634F) and the sulfur content analyzed was 0.047 percent.

A schematic of the rig system is shown in Figure 9. The objective of this test was to subject the leading edge of the coated turbine vane (mounted on the nozzle plate of the combustor can) to 1316°C for 50 minutes followed by 10 minutes at a cooldown temperature of <816°C. The thermal cycle was achieved through control of the fuel and air supply to the combustor such that a fuel-rich, high temperature stream was produced during the high flow period of 50 minutes and a lean, secondary air diluted and cooler flame was effective for the cooldown period. Two pressure needle valves were installed on the fuel line and, with the aid of a solenoid valve mounted on one arm of the bypass, the fuel flow was controlled to alternate between high flow and low flow conditions. Similarly, a three-way solenoid on the primary air line allowed the air supply to be synchronized to the fuel flow levels. The burner rig was operated in the automatic mode with daily inspections.

Specimen leading edge temperature was read optically using a calibrated pyrometer sighted on the hot spot of the leading edge through a viewing slot cut in the specimen shroud, see Figure 10. During testing, it was found that the leading edge temperature can be directly used to control the combustion level by means of a infrared probe containing a set of thermophiles that transmitted the voltage signal to a transducer that was part of the feedback system to the fuel controller. Confirmation of leading edge temperature was made daily by means of a calibrated pyrometer.

One of the major problems encountered in the burner rig test was the mounting of the NS-4 coated single vane segment. The high-velocity gas stream and the geometry of the part were such that the part needed to be secured firmly in place. At the same time, the presence of silicon on the coating surface required that contact areas be non-reactive with silicon. Consequently, all contact surfaces on the mounted specimen were protected by a magnesium zirconia coating applied to the mounting fixture. Two specimen mount systems were tried, and these are shown in Figures 11 and 12. The latter method, which turned out to be the better one, called for welding (EB welding) a piece of FS-85 alloy onto the outboard sidewall of the vane segment which then allowed the entire specimen to be securely fastened down. The combustor nozzle orifice was 2.5 cm in diameter and the leading edge was positioned 3.1 cm above the orifice.

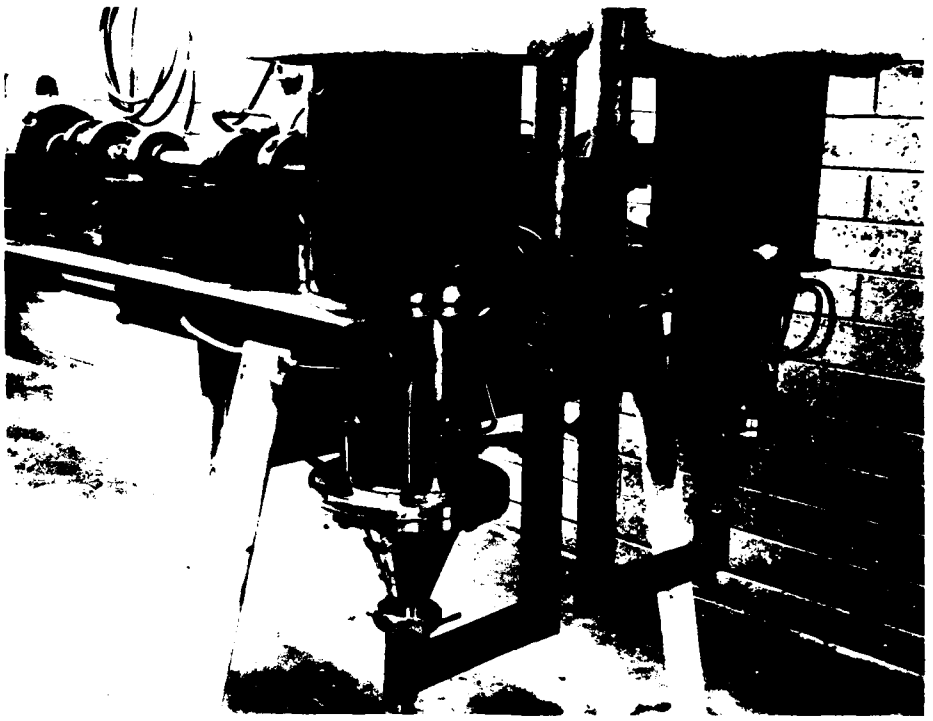

Figure 8. Gas Turbine Environmental Simulator

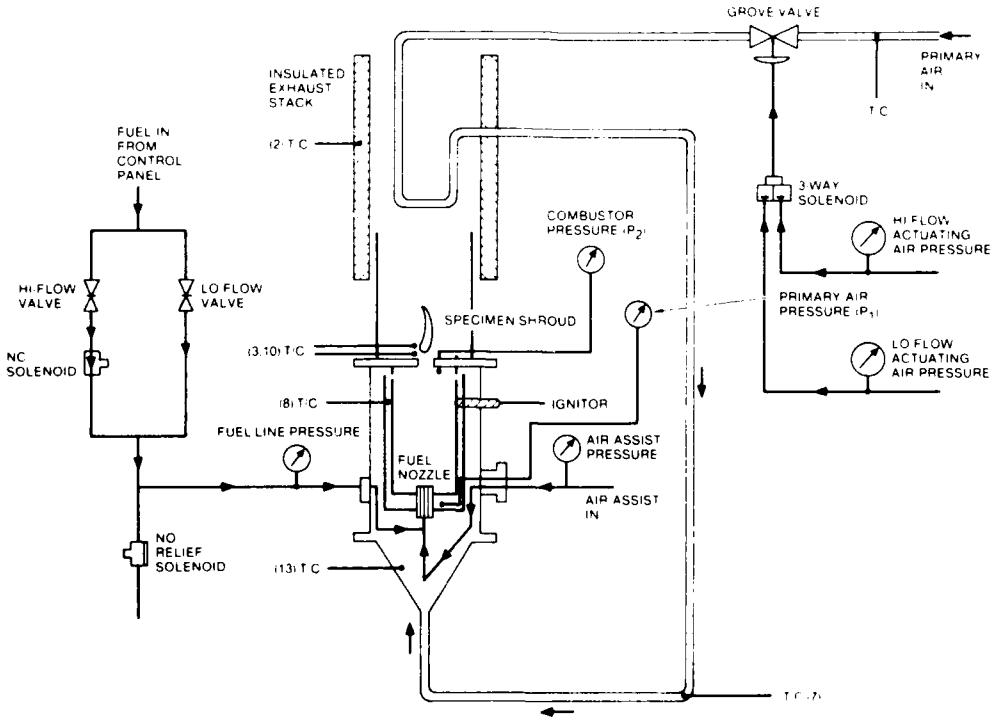

Figure 9. Schematic of Burner Rig Test

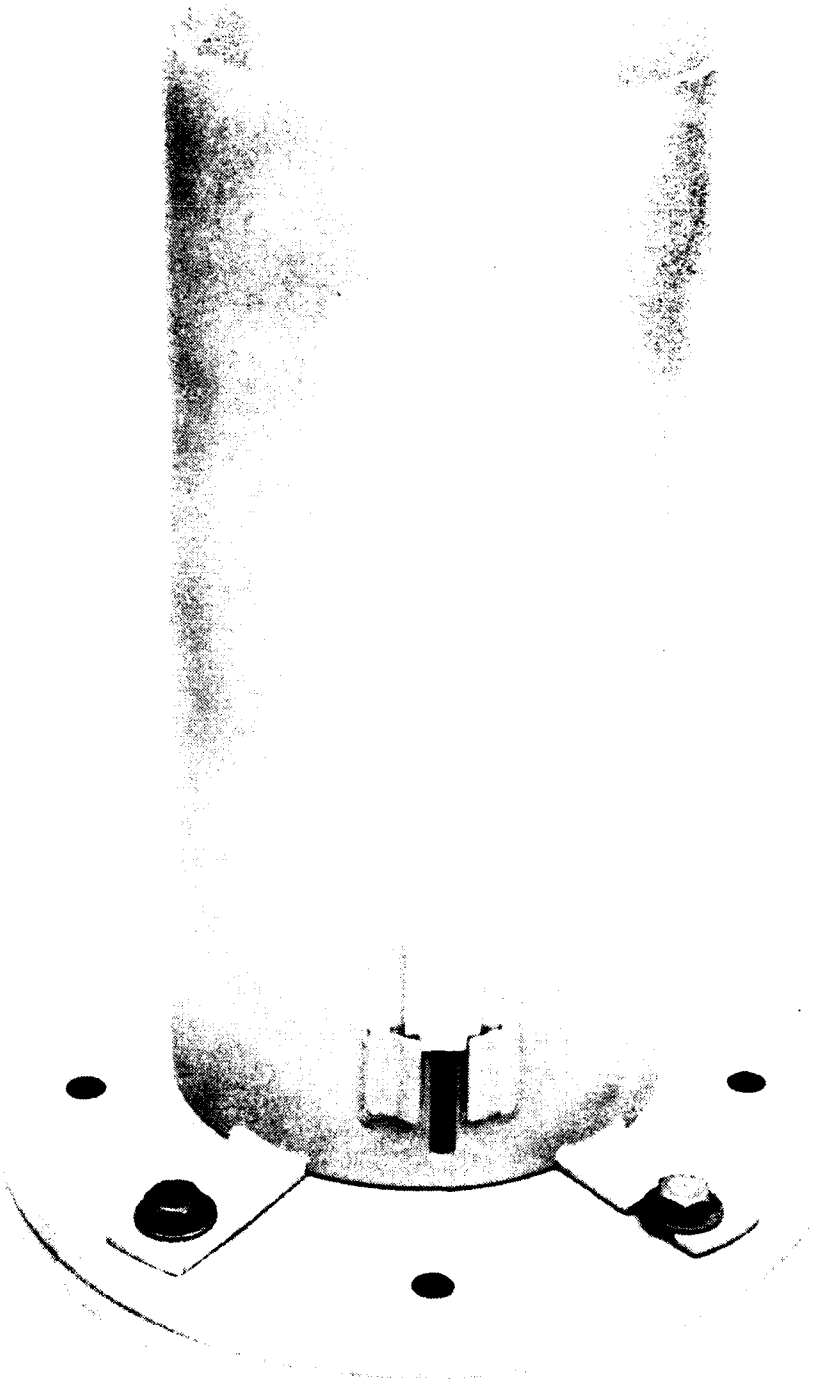

Figure 10. Shroud Fixture With Viewing Slot

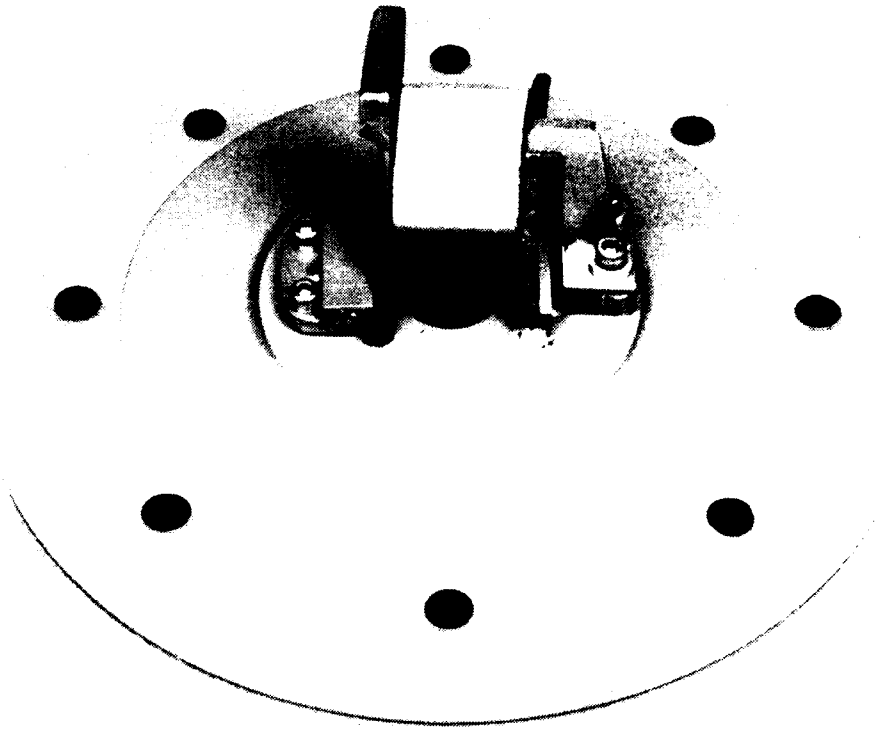

Figure 11. Single-Vane Nozzle Located at Exit Nozzle of Combustor Plate - System 1

Typical test parameters for both high and low flow conditions are reported in Table 1. Note that during the 10-minute low-temperature period, the fuel flow was reduced 33 percent while the air was significantly increased, thus raising the air-to-fuel ratio to levels typically found in gas turbines. The products of combustion, as calculated from the total consumption of fuel and air, are listed in Table 2.

2.4 DIAGNOSTIC TECHNIQUES

Metallography was employed routinely throughout the program to monitor microstructural changes as a result of exposure to the various test regimes. The main difficulty encountered in preparing metallographic mounts was that the NS-4 coating itself was brittle and polished differently from the C129Y substrate alloy and produced less than satisfactory photomicrographs. For specimens that were to be examined by scanning electron microscopy (SEM), a cerium oxide polishing compound was used instead of chromium oxide. Energy dispersive X-ray analysis (EDX) capabilities were available on the SEM and semi-quantitative and qualitative anayses were utilized when necessary to provide further insight into the phenomena of coating/substrate interaction and coating deposition.

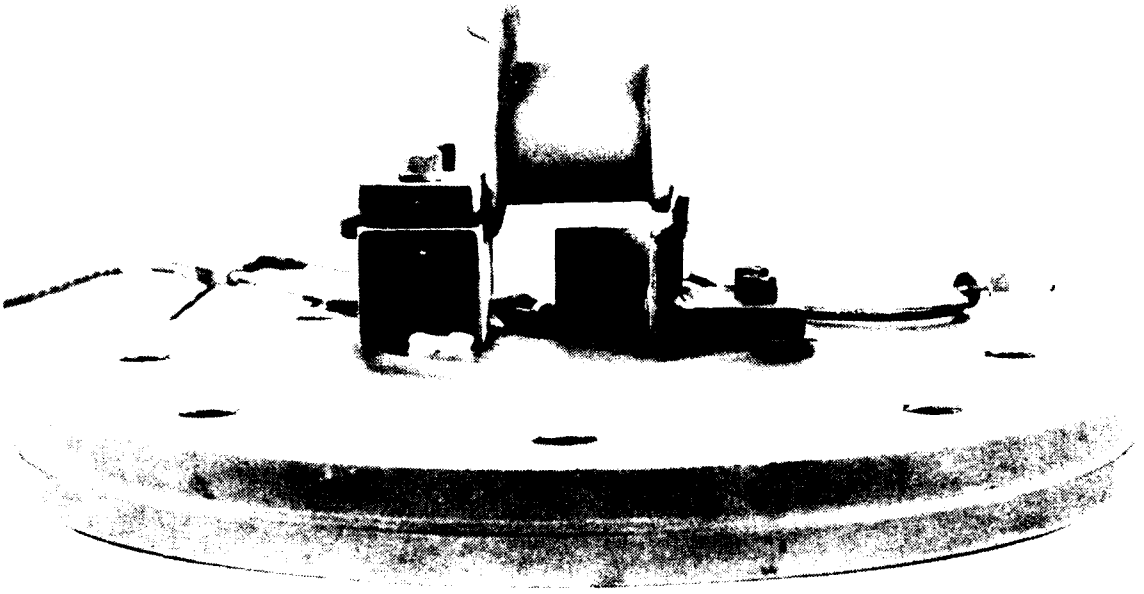

Figure 12. NS-4 Coated C129Y Nozzle Prepared for Burner Rig Testing - System 2

Table 1

Oxidation Burner Rig Test Parameters

	High Temperature	Low Temperature
Air flow	3.9 to 4.2 Kg/min.	4.8 to 6.3 Kg/min.
Fuel flow	0.15 to 0.16 Kg/min.	0.09 to 0.12 Kg/min.
Air-to-fuel ratio	24 to 28	40 to 70
Specimen leading edge temperature	1316 $\pm$ 30°C	<816°C
Flame temperature	~1540°C	~860°C
Incoming air temperature	~192°C	112°C
Mach number	0.87	1.07
Air velocity	690 m/sec.	645 m/sec.

Table 2

Combustion Products Calculated From Fuel and Air Consumption

Fuel/ Air Ratio	Air/ Fuel Ratio	Percent Volume				
		H_2O	CO_2	O_2	N_2	Argon
0.040	25	8.67	7.95	8.18	74.27	0.93
0.033	30	7.44	6.67	10.21	74.75	0.94
0.025	40	5.87	5.04	12.79	75.36	0.95
0.014	70	3.82	2.91	16.16	76.15	0.96

3

PHASE I - CASTING DEVELOPMENT

3.1 CASTING PROCESS DEVELOPMENT

3.1.1 Alloy Selection

Columbium-base alloy C129Y was selected for production of the cast nozzle vanes based upon the mechanical properties of similar parts produced by REM Metals Corp. (Ref. 3). In order for columbium alloy nozzles to be competitive both with superalloy and ceramic parts, high tensile and creep strength is necessary at operating temperatures of 1204° to 1371°C, coupled with adequate room-temperature ductility. Of the four alloys evaluated in casting by REM, C129Y was second only to SU31 in high-temperature strength, significantly above either C103 or Cb752. Table 3 presents typical properties for four columbium-base alloys, together with those of the superalloy presently used for nozzle production, the point being that the columbium-base alloy should equal, at much higher temperatures, the properties of the superalloy at 871° to 927°C. While SU31 demonstrates higher strength at temperature, neither room-temperature nor elevated-temperature ductilities are adequate.

While the above-referenced report indicates some degree of difficulty in casting C129Y alloy, it was decided in conjunction with REM that the advantages of this alloy were worth pursuing. REM felt, initially, that the melting problems could be satisfactorily identified and resolved by variations in the consumable electrode arc melting procedure. Accordingly, 450 pounds (204 kgm) of 4 inch (100 mm) diameter electrode and 50 pounds (23 kgm) of starter stock chips were ordered in C129Y alloy from Wah Chang, Albany, Oregon. Crystal grade hafnium was specified to minimize oxygen and nitrogen content of the composition which was specified as per Wah Chang TWCA-CB-MS-1 (Appendix C).

Analysis of the material supplied indicated it to have much less than the required yttrium content. Analyses are seen in Table 4. This circumstance presumably is due to failure to compensate for evaporation in vacuum melting. (Yttrium content of the C129Y alloy castings previously poured by REM, Ref. 3, was about 0.07%.) It was determined in conference with REM and Wah Chang that remelting the alloy to add yttrium could raise the interstitial levels beyond acceptable levels; and secondly, that the requisite delay in melting and forging of new ingots would seriously jeopardize the conclusion of the program. As such, the decision was made to proceed with the material as

Table 3

Typical Physical and Mechanical Properties of Columbium and Cobalt Alloys

Designation	Major Alloying	Coefficient of Thermal Conductivity (Btu/hr/ft^2/°F/ft)	Melting Point (°F)	0.2 Percent Tensile Yield Strength (ksi)		Tensile Elongation (%)		Modulus of Elasticity (psi x 10^6)	Comments
				70°F	Elevated Temperature	70°F	Elevated Temperature		
C103									
Wrought	10Hf, 1Ti	25.8	4260	88.0	20.0 (2000°F) 10.5 (2500°F)	>30.0	>50.0 (2200°F)	12.6	Highest ductility Most widely used in Cb investment coatings
Cast				46.0	24.5 (2200°F)	17.8	9.2 (2200°F)	13.1	
CB752									
Wrought	10W, 2.5Zr	--	4400	85.0	30.0 (2200°F)	--		15.0	Poor weldability
Cast				56.0	20.0 (2200°F)	5.8	4.5 (2200°F)	15.0	
SU-31									
Wrought	17W, 3.5Hf	--	5020	77.0	40.0 (2000°F) 38.0 (2200°F) 24.0 (2500°F)	25.0- 28.0	18.0 (2200°F)	18.0- 19.0	Probable susceptibility to embrittlement by interstitial contamination
Cast				75.0	35.0 (2200°F)	1.5	3.5 (2200°F)	18.5	
C129Y									
Wrought	10W, 10Hf	44.4	4350	102.0	40.0 (2000°F) 20.0 (2500°F)	--	>45.0 (2200°F)	16.0	Good weldability
Cast				66.0	35.0 (2200°F)	7.5	8.5 (2200°F)	16.3	
X-45M									
Cast	10Ni, 25Cr, 8W	12.8	2450	64.5	25.0 (1600°F)	9.0	22.0 (1700°F)	29.0	Cobalt-base alloy used in Solar Centaur 1st-stage nozzle vane at 1600°F

Note: Compilation of data from:

1. "Mechanical Properties of Columbium Alloy SU-31", A.A. Tavassoli, private communication, KBI.
2. Materials Selector, 1975, Reinhold Publications.
3. Product Data, Columbium Alloy SU-31, Kawecki Berylco, 1975.
4. "Precision Casting of Columbium-Based Alloys for Turbine Applications", DAAG46-75-C-0007, REM Metals, 1975.
5. Solar data
6. "Columbium (Niobium) Alloys for Structural Applications", A.A. Tavassoli, SAMPE Journal, Vol. II, No. 1, 1975.

Table 4

Chemical Analyses of Electrode Stock

Element	Requirement TWCA-CB-MS-1	Prior Work Ref. 3		Percent by Weight			
		Top	Bottom	Top	Bottom	Top	Bottom
				Heat 572122		Heat 572123	
Hf	9.0-11.0	9.0	8.5	10.7	9.9	10.1	8.8
W	9.0-11.0	9.6	9.7	9.9	10.2	10.0	9.6
Y	0.05-0.3	0.067	0.074	0.0200	0.0200	<0.0050	<0.0200
C	0.015 max	0.0060	0.0060	0.0110	0.0060	0.0070	0.0070
H	0.0015 max	<0.0005	<0.0005	0.0006	0.0009	0.0006	0.0005
N	0.0100 max	0.0040	0.0035	0.0065	0.0072	0.0060	0.0056
O	0.0225 max	0.0050	0.0050	0.0220	0.0210	0.0100	0.0120
Ta	-	-	-	0.4390	0.4460	0.4700	0.4365
Zr	-	-	-	0.4120	0.3490	0.3050	0.2650
Cb	-	-	-	Balance	Balance	Balance	Balance

Element	Top	Bottom	Top	Bottom	Top	Bottom	Top	Bottom
	Heat 572124		Heat 572125		Heat 572126		Heat 572127	
Hf	9.7	9.4	9.3	9.5	10.1	9.3	9.9	9.4
W	10.2	10.4	9.8	10.5	9.8	10.3	10.2	10.3
Y	0.0140	0.0230	0.0100	0.0190	0.0270	0.0200	0.0190	0.0220
C	0.0080	0.0090	0.0090	0.0100	0.0080	0.0070	0.0060	0.0070
H	<0.0005	0.0006	0.0025	0.0006	<0.0005	0.0007	<0.0005	0.0014
N	0.0076	0.0084	0.0074	0.0084	0.0094	0.0088	0.0047	0.0053
O	0.0060	0.0110	0.0070	0.0110	0.0140	0.0130	0.0090	0.0080
Ta	0.4850	0.4700	0.4270	0.4320	0.3940	0.4350	0.4640	0.4700
Zr	0.2860	0.2920	0.3990	0.3450	0.3840	0.3380	0.3430	0.3220
Cb	Balance	Balance	Balance	Balance	Balance	Balance	Balance	Balance

supplied and to attempt to add yttrium to the casting melt in elemental form. None of the castings produced in three foundry melts, however, had more than 0.011 percent yttrium, a fact which may have contributed to the observed poor fluidity of the alloy in all three pours.

3.1.2 Foundry Practice

REM Metals Corp. was selected as the foundry source of columbium alloy castings for this program. The decision was based mainly upon their greater experience in investment casting of columbium, as demonstrated in prior work (Ref. 3). Purchase orders were let for two sets of specimens to be used, first, in iterative development of casting processes, and second, in production of optimized specimens. The reference nondestructive inspection standard was specified as ASTM-E-155, Grade C, and provision was made for weld repair to this quality level.

REM employs a proprietary tungsten face mold system in production of reactive metal castings, columbium- or titanium-base. Wax patterns are fabricated by injection molding in steel dies and are assembled with gates and risers to form a pattern tree such as seen in Figure 13. This is then coated with a series of

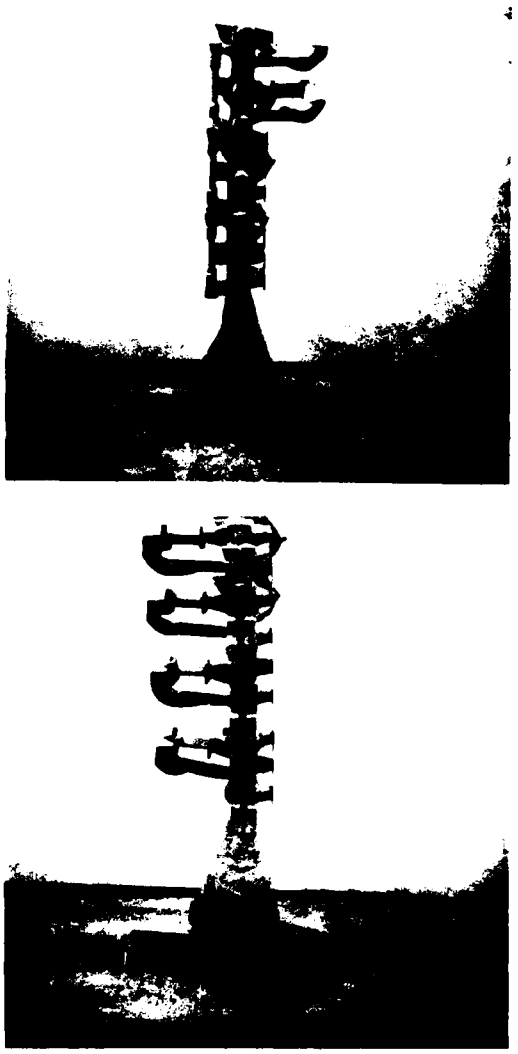

Figure 13. Side and Front Views of Assembled "Tree" of Molds Used in Investment Casting

refractory compound dips, the first of which is a tungsten compound, to form a shell mold. As the mold is fired, the wax melts away leaving a void in the shape of the nozzle and test specimens. The wax patterns and consequently the voids are slightly larger than the final castings, compensating for metal solidification shrinkage and providing material for chemical machining of the surfaces. REM skull melts a consumable columbium electrode, in vacuum, dumping the molten metal directly from the water cooled crucible into the preheated mold. The furnace is seen in Figure 14. The final step of the casting process is to break away the refractory mold material and to saw and snag the gates and risers from the castings. All casting surfaces are chemical machined 2 to 3 mils (0.05 to 0.08 mm) to remove the metal/mold reaction zone,and the castings are then nondestructively inspected by radiography, visual and penetrant methods.

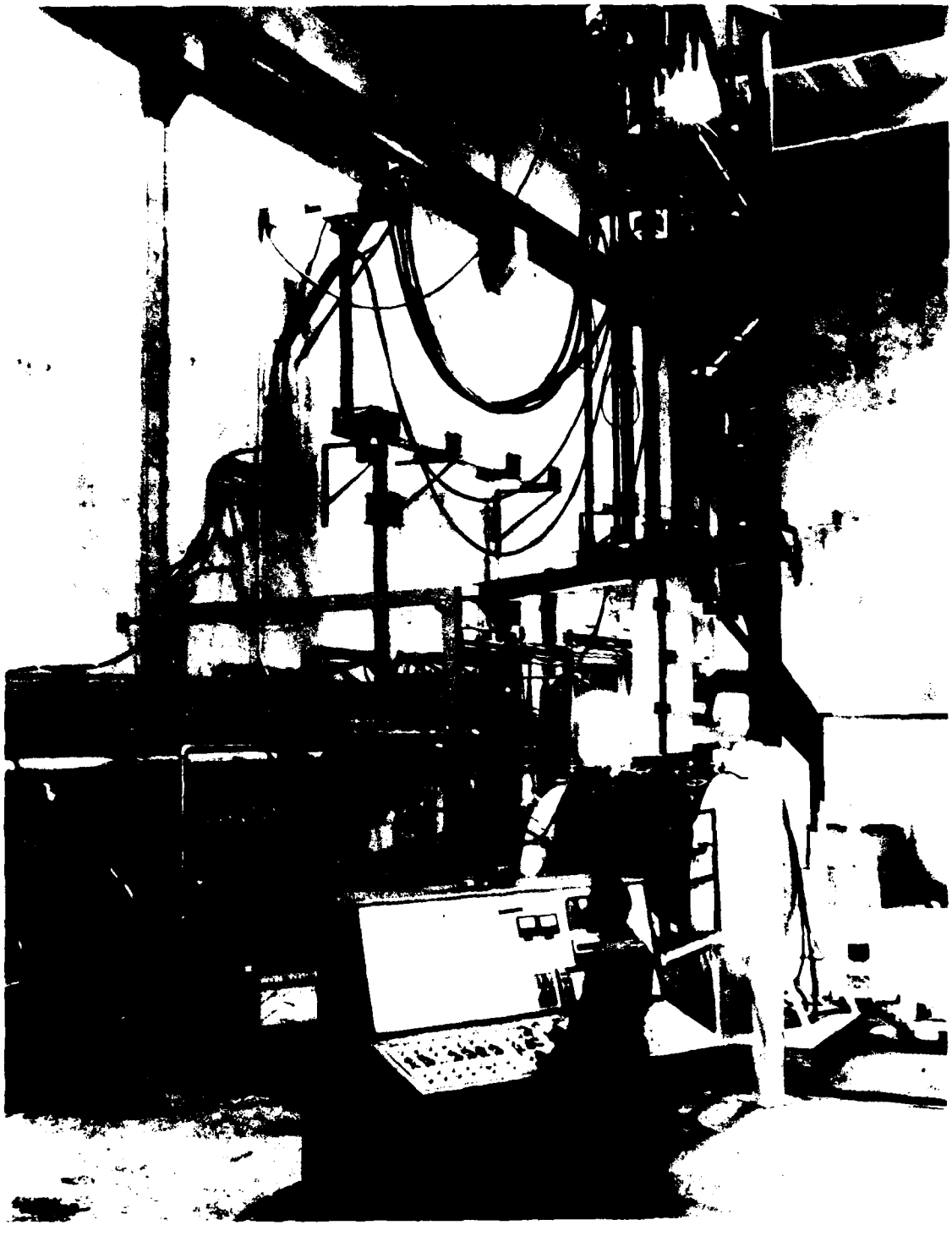

Figure 14. Consumable Electrode Arc Melting and Casting Vacuum Furnace; REM Metals, Albany, Oregon

The wax patterns for this program were ordered from Howmet Corp., LaPorte, Indiana, which is the foundry which currently produces the first-stage nozzle of the Centaur engine in cobalt-base X-45M. The total production included:

- Thirty-six (36) solid, single blade nozzles, Solar P/N 115893
- Thirty-six (36) hollow, single blade nozzles, Solar P/N 115893
- Forty-five (45) erosion test specimens, Howmet P/N 1807.

Engineering sketches for these castings, and for flat and round tensile specimens, which waxes were supplied by REM, are seen in Figures 15 through 19. The patterns were produced in McCaughin 2P31 wax, this being most compatible with REM's processing. Hollow nozzles are usually produced from patterns comprised of wax injected around a leachable ceramic core. This technique is not compatible with the higher melting and reactive columbium alloys, however, and it was necessary to fabricate a core pull, Figure 20, which could be removed from the center of the blade shape after wax injection, leaving the wax itself hollow.

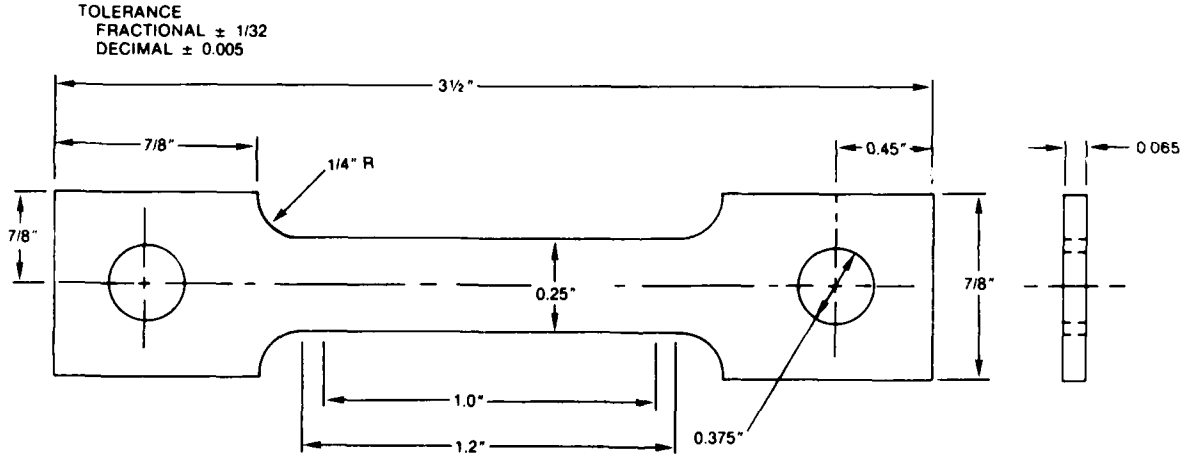

Figure 15. Flat Tensile Specimen - Pin Hole

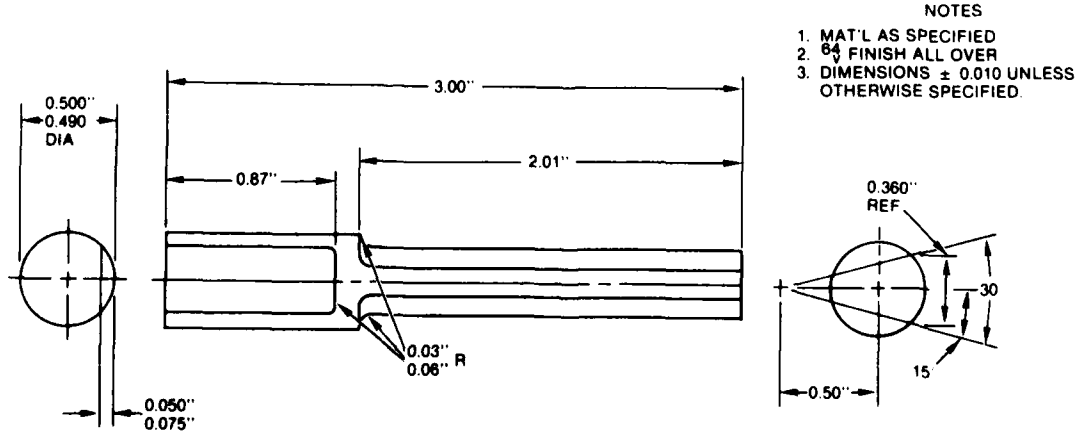

Figure 16. Erosion Bar Figure

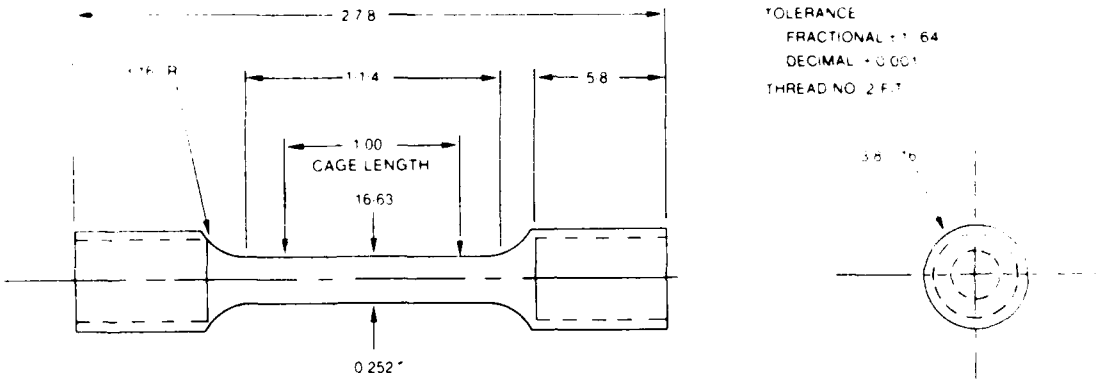

Figure 17. Threaded Tensile Specimen

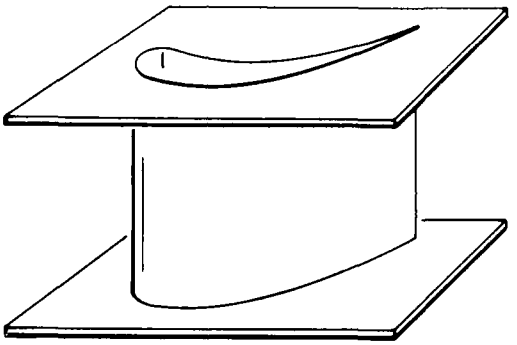

Figure 18. Hollow Vane Segment

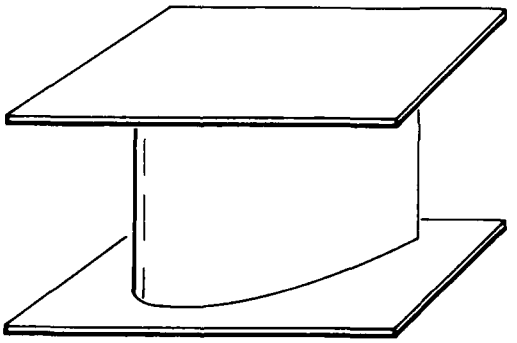

Figure 19. Solid Vane Segment

Figure 20.

Steel Core Pull For Investment of Hollow Wax Patterns (Shown Full Size)

3.1.3 Process Development

The initial task of casting development was intended as a three-stage iterative process, optimizing the techniques and parameters of investment casting in columbium alloys. Because of the delays occasioned by alloy procurement, it was decided that this task would proceed only with two iterative steps, each including half again as many specimens. Total requirement of the task was:

- Six (6) solid nozzles
- Six (6) hollow nozzles
- Twelve (12) round tensile bars
- Twelve (12) flat tensile bars

The first mold tree was prepared containing six of each of the flat and round tensile bars and the six solid nozzle sections. Three attempts at this first pour were made, spanning a time period of about two months. In the first attempt, the electrode melted at its welded connection to the attachment stub, falling into the crucible. In the second attempt, it was determined that the crucible had been damaged in the first try, and this attempt too was aborted. Subsequently, a series of difficuties ensued with the DC power supply and the vacuum system. The final pour of this series was successfully accomplished and filled five of six solid nozzle shapes and all six round tensile specimens. The flat tensile bars did not fill, nor did the nozzle platforms totally, owing to poor fluidity of the alloy in thin sections. The products of pour No. 1 are seen in Figure 21, together with their radiographs, Figures 22 and 23. As can be seen, all of the nozzles are flawed by what appears to be gas porosity. Three of the five which filled satisfy Class C radiographic requirements. There is no indication of microshrinkage either in the nozzles or platforms, the latter of which did not fill completely. The surface was excessively rough in the radii between the airfoil and platform, due to heat retention in that area. The round tensiles appeared to be free of all defects. Gating was revised for the flat specimens and nozzle platforms. The next pour was comprised of six each hollow nozzles, flat tensiles, and round tensiles. This pour, No. 2, proceeded without the difficulties experienced in the first. Again the flat specimens failed to fill properly, although they were much improved over those of the first pour. None of the hollow vane sections filled

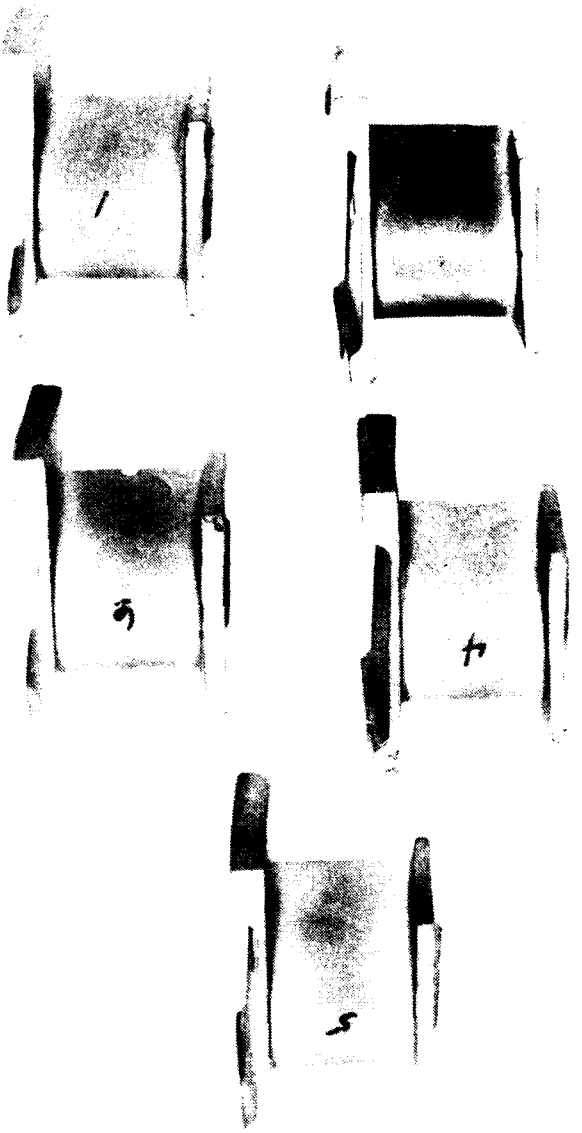

Figure 21. Cast Solid Nozzles of C129Y Alloy, Pour No. 1

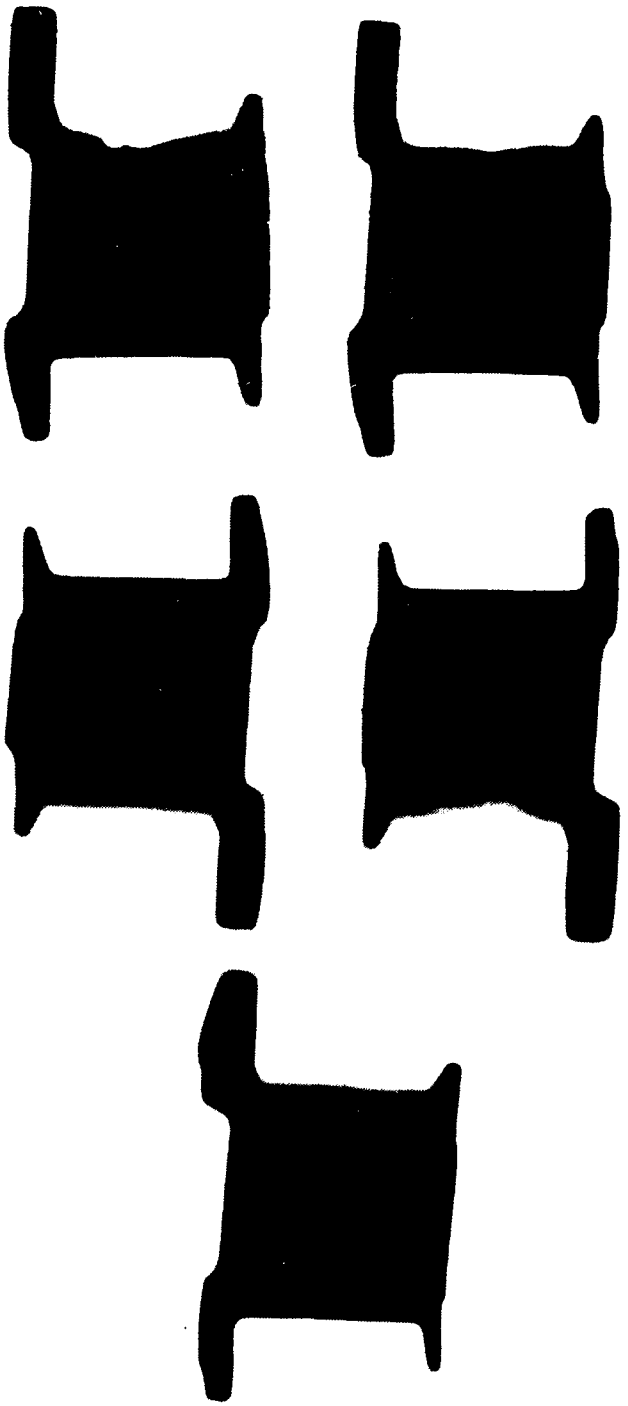

Figure 22. Radiograph of Solid Nozzles, Pour No. 1

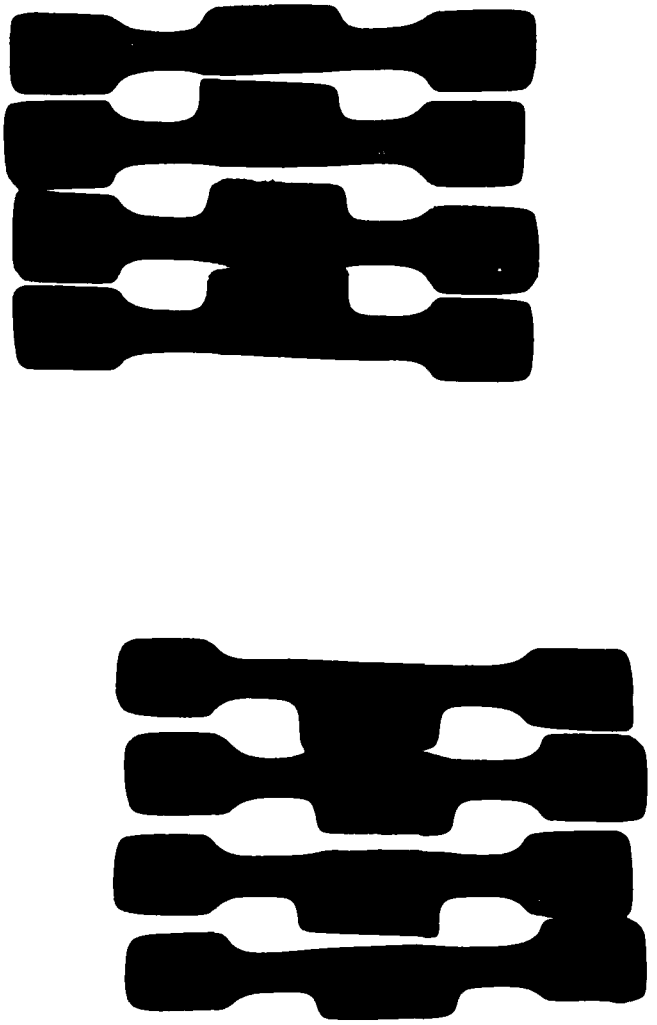

Figure 23. Radiograph of Round Test Bars, Pour No. 1

sections filled completely, attributable to lack of fluidity of the alloy. The products and radiographs of pour No. 2 are seen in Figures 24 through 27. Again the round tensiles appear to be sound. Subsequent tensile testing, however, disclosed serious gas porosity in at least two.

Figure 24. As-Cast Hollow Vanes, Pour No. 2

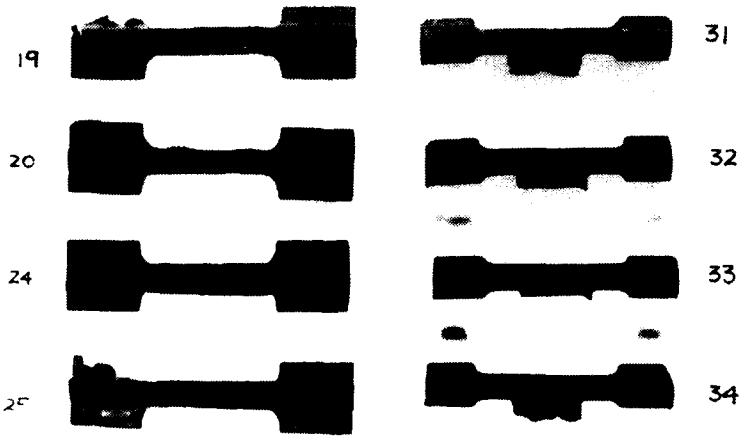

Figure 25. As-Cast Flat and Round Test Specimens, Pour No. 2

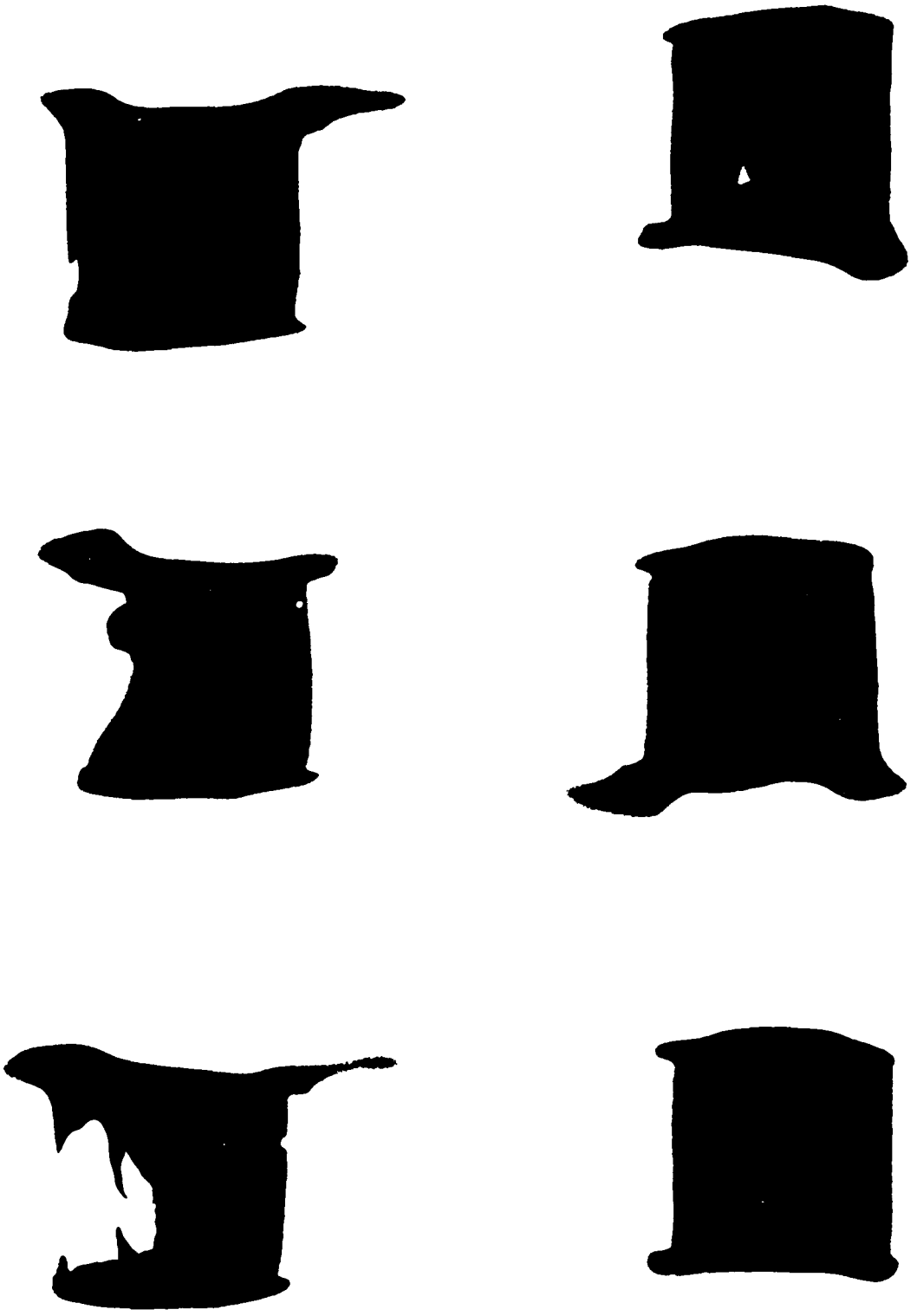

Figure 26. Radiograph of Hollow Vanes, Pour No. 2

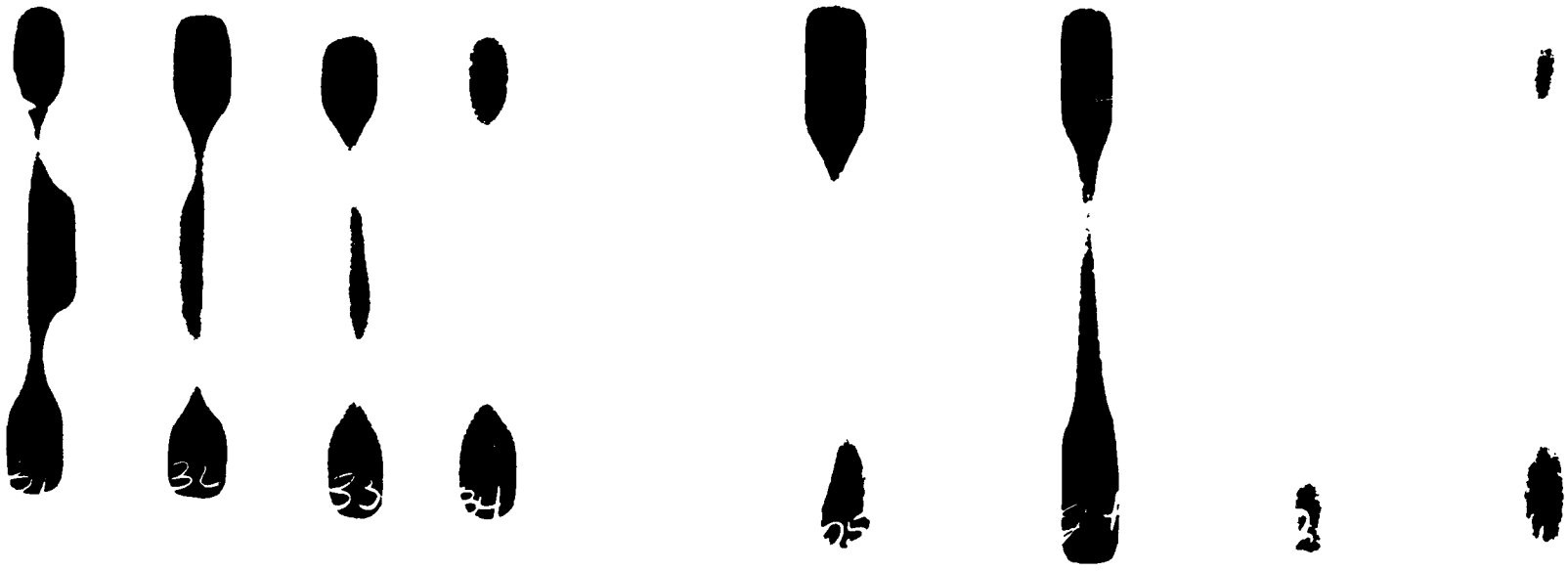

Figure 27. Radiograph of Flat and Round Test Specimens, Pour No. 3

Despite a lower melting point than several other cast columbium-base alloys, C 129Y appears to require much higher amperage to establish a molten pool in the crucible. Current in excess of 10,000 amps is required for C 129Y, in contrast to other alloys which typically melt in the range of 4000-5000 amps. The elements contained in C 129Y and in all other castable alloys display similar alloying behavior (in the range of interest), i.e., the formation of continuous solid solutions with columbium. Other castable alloys contain as much or more tungsten and hafnium as C 129Y, although not in the same combination. The behavior of yttrium is an exception to that of other elements in the alloy. Its solid solubility is limited to about 0.05 atomic percent and it is a monotectic system at 0.5 atomic percent yttrium. This behavior does not explain the melting difficulties and, even if salient, can be disregarded due to the almost complete lack of yttrium in the Wah Chang supplied material.

In summary, the behavior of C 129Y in melting remains unexplained and the poor reliability tends to discourage its near-term use in castings despite excellent ambient and elevated temperature properties.

3.1.4 Casting Properties

Tables 5 and 6 describe the results of REM and Solar mechanical property tests on the two development pours. Chemical analyses are seen in Table 7.

Only Solar conducted elevated-temperature tests of the castings, using an Instron model TTD tensile test machine, as described in Section 2. Both the ambient and elevated temperature results of casting pour No. 1 compare favorably with prior castings produced by REM (Ref. 3), which properties are included for reference in Tables 5 and 6. As noted, only the specimens from pour No. 1 were tested at elevated temperature. Of the two from pour No. 2 intended for elevated-temperature testing, one broke in machining and the second was seen to be seriously flawed by gas porosity, despite acceptable radiographic results.

No flat specimens were produced in pour No. 1; and the flat specimens from pour No. 2 which had been scheduled for mechanical property determination were largely unacceptble for this purpose due to extensive unfilled areas and shrinkage. They were instead sectioned into smaller pieces and used for coating and oxidation studies.

Regarding the round test specimens, a direct correlation is evident between the levels of interstitial element concentration in pours No. 1 and No. 2 and their relative ductility. Pour No. 1 was higher than REM's previous work (Ref. 3) in all interstitial elements but hydrogen. Despite this, the ambient and elevated temperature mechanical properties of Pour No. 1 castings were significantly improved over those of the previous program, suggesting that hydrogen contents, even below specification maximum, have a profound influence on ductility of this alloy. There is a very loose confirmation of this hypothesis in the behavior of Pour No. 2, which far exceeded maximum allowable hydrogen content of the specification and which displayed exceedingly low tensile ductility, both at room temperature and 2000°F. It should be noted that carbon, nitrogen, and oxygen contents of this pour were all marginal or slightly over allowable limits, as well.

Table 5

Tensile Properties of Cast C129Y Specimens (Pour No. 1)

	Temperature (°F)	Strain Rate (in./in./min.)	Offset (%)	Ultimate Tensile Strength (ksi)	Yield Strength (ksi)	Reduction in Area (%)	Elongation (%)
Solar	70	0.005(1)	0.2 0.6	96.9	80.1 83.6	18.8	19.7
Solar	70	0.005(1)	0.2 0.6	96.1	77.8 81.7	25.7	23.6
Solar	2000	0.003(2)	0.2	48.5	48.2	52.7	22.5
Solar	2000	0.003(2)	0.2	45.6	44.6	43.3	20.4
REM	RT	N.S.	0.2	98.3	76.8	36.4	24.0
Ref	RT	N.S.	0.2	82.7	65.6	11.0	10.5
Ref	2200	N.S.	0.2	37.3	28.3	9.0	8.5

(1) After 0.6 percent offset, 0.050 in./in./min to failure

(2) Calculated from crosshead speed of 0.050 in./in./min and Young's modulus of 15.7 x 10^6 at room temperature

N.S. = Not Specified

Table 6

Tensile Properties of Cast C129Y Specimens (Pour No. 2)

	Temperature (°F)	Strain Rate (in./in./min.)	Offset (%)	Ultimate Tensile Strength (ksi)	Yield Strength (ksi)	Reduction in Area (%)	Elongation (%)
Solar	70	0.005(1)	0.2 0.6	91.0	81.5 85.2	3.1	4.2
Solar	70	0.005(1)	0.2 0.6	81.8	79.1 Broke before 0.6%	0.75	1.3
Solar	2000	Broken in machining					
Solar	2000	Excessive porosity					
REM	RT	N.S.	0.2	85.1	79.9	2.0	2.5
Ref	RT	N.S.	0.2	82.7	65.6	11.0	10.5
Ref	2200	N.S.	0.2	37.3	28.3	9.0	8.5

(1) After 0.6 percent offset, 0.050 in./in./min to failure

N.S. = Not Specified

Table 7

Chemical Analyses of Casting Pours

Element	Requirement TWCA-CB-MS-1*	Percent by Weight		
		Pour No. 1 REM Analysis	Pour No. 2 REM Analysis	Prior Work (Ref. 3)
W	9.0-11.0	9.9	10.4	Not reported
Hf	9.0-11.0	9.7	11.9	" "
Y	0.05-0.3	0.011	0.0100	" "
C	0.015 max.	0.0060	0.0200	0.0040
H	0.0015 max.	0.0005	0.0042	0.0013
N	0.0100 max.	0.0080	0.0100	0.0038
O	0.0225 max.	0.0240	0.0250	0.0110
Zr	0.5000 max.	0.3790	0.3040	Not reported
Ta	0.5000 max.	Not reported	Not reported	" "

* Electrode specification

The addition of elemental yttrium to the foundry melt obviously did little to correct the alloying of the C129Y. The maximum percentage recorded (in Pour No. 1) is only about one-fifth of the minimum required by the material specification. A final yttrium content was not reported for the previous work, but it is noted that the analysis of the consumable electrode used for that melt was 2-1/2 to 15 times that of the present program, Table 4. The effect of yttrium dilution in the alloy is not noted in comparison of the tensile results of the two programs. The probable rationale for yttrium addition is as a scavenger for oxygen and a grain refiner. Lack of scavenging action may have had an adverse effect on the fluidity of the molten alloy, although evidence is scant either way.

3.2 PRODUCTION OF OPTIMIZED TEST SPECIMENS

3.2.1 Casting Production

On the basis of Task I iterative pours, it became apparent that thin-wall sections, e.g., flat test bars and hollow nozzle vanes, cannot be cast in C129Y alloy. A series of gates to the unfilled areas of the vanes might solve the filling difficulties, but the cast part would be far from net shape and would require extensive finishing of the airfoils to smooth the surface.

Since one goal of the program was to produce precision C129Y nozzle vane castings to near-net shape, the re-gating of the hollow vane nozzles was discarded and a decision made to proceed with the solid vane configuration only. This decision also obviated the need for flat tensile bars since their function was to evaluate the mechanical, metallurgical, and coating interaction properties of the thin wall hollow vanes.

Subsequent to this decision, REM proceeded with the preparation of mold trees to include:

- Thirty (30) thermal fatigue specimens (30° angle)
- Sixteen (16) solid vane nozzles
- Forty-eight (48) round test specimens.

The first pour of this series was accomplished without incident (except for the "unusually high" amperage required to effect melting) and resulted in filling 22 of the 24 round test specimens in one mold tree, Figure 28.

A second pour attempt was aborted due to the arc inadvertently penetrating the copper liner of the crucible. Two welding repair sequences were conducted to repair the damage but the pour was not completed.

Subsequently, the unavailability of a qualified vacuum casting operator forced a decision between REM, Solar and AMMRC to reduce the program scope to ensure that the coating and testing phases could be completed within a reasonable time frame. Accordingly, a revised program plan was developed and testing proceeded with the cast materials on hand:

- Five (5) solid vane nozzles - Task I, Pour 1
- Six (6) hollow vane nozzles - Task I, Pour 2
- Four (4) flat tensile specimens - Task I, Pour No. 2
- Twenty-two (22) round test bars - Task II, Pour No. 3.

3.2.2 Casting Properties

Chemical Analysis

Table 8 shows the analysis of pour No. 3, comprised of 22 round test bars. Again it is evident that addition of elemental yttrium did nothing to alloy the castings. The level of yttrium in these castings, 0.006 weight percent, is even less than that of the electrodes from which they were made.

Carbon and nitrogen levels of pour No. 3 are somewhat higher than those of the first two pours; the latter exceeding specification limits. Hydrogen, similarly, increased beyond the maximum limit, being four times that of pours No. 1 and 2;

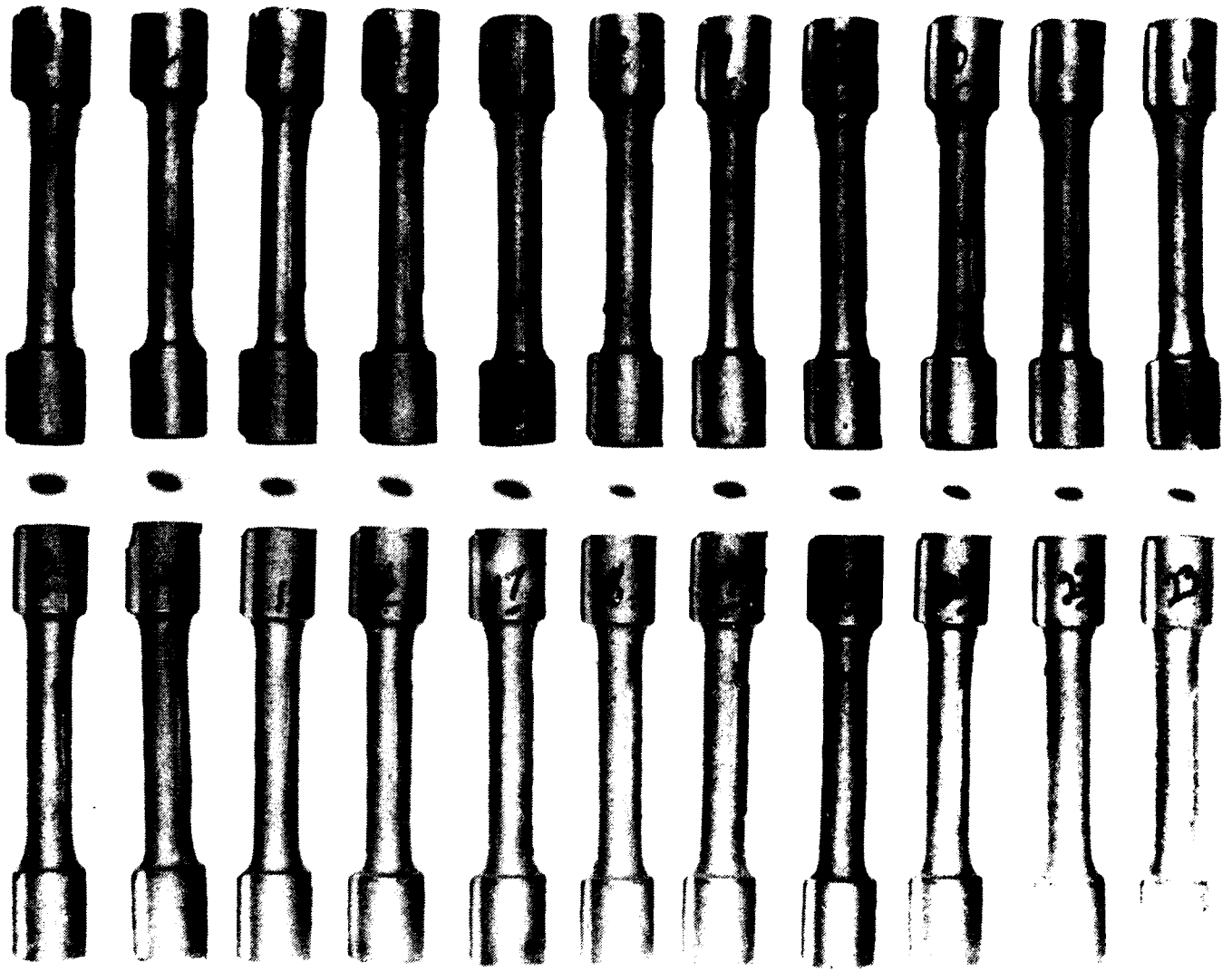

Figure 28. Cast Round Test Bars of C129Y Alloy

Table 8

Chemical Analyses of Casting Pours
(Percent by Weight)

Element	Requirement TWCA-CB-MS-1*	Percent by Weight	
		Pour No. 3 Koon-Hall Analysis	Prior Work (Ref. 3)
W	9.0-11.0	9.7	Not reported
Hf	9.0-11.0	9.5	" "
Y	0.05-0.3	0.0060	" "
C	0.015 max.	0.0080	0.0040
H	0.0015 max.	0.0021	0.0013
N	0.0100 max.	0.0130	0.0138
O	0.0225 max.	0.1330	0.0110
Zr	0.5000 max.	0.3960	Not reported
Ta	0.5000 max.	0.4000	" "

* Electrode specification

and oxygen increased to almost six times the allowable limit. The preponderance of hydrogen and oxygen in the analysis may indicate an air or water vapor leak in the vacuum system; however, the melting data shown in Table 9 do not suggest any anomolies.

Nondestructive Inspection

Radiographic inspection of pours indicated most specimens to be internally sound. A reproduction of this film is seen in Figure 29. Exceptions were:

Test Bar Number	Condition
9	Gas porosity, Grade A, ASTME 155
10	" " " B, " "
11	" " " C, " "
13	Crack
15	Gas porosity, Grade B, " "
17	" " " C, " "
19	" " " C, " "
20	" " " B, " "

Table 9

Vacuum Furnace Data Sheet

	Pour No. 1	Pour No. 2	Pour No. 3
Date:	5/13/77	7/22/77	12/9/77
Mold:	6 solid nozzle 6 round tensile 6 flat tensile	6 hollow nozzle 6 round tensile 4 flat tensile	24 round tensile
Electrode:			
Size	3 inch round	4 inch round	4 inch round
Weight: Before	64.5 lbs	78 lbs	73 lbs
After	32.5 lbs	38 lbs	N.R.
Skull	Old	Old	Old
Weight: Before	23 lbs	26 lbs	21.4 lbs
After	26.5 lbs	21 lbs	33 lbs
Pot Size (Ti)	50 lbs	50 lbs	50 lbs
Base	5 lbs chips	None	1.5 lbs chips
Mold Weight: In	N.R.	N.R.	19 lbs
Out	67 lbs	N.R.	47.5 lbs
Vacuum at start	12 microns	13 microns	10 microns
Vacuum rise, melting	180 microns	90 microns	115 microns
Furnace leak rate, Hot:			
(Vac. rise) Start	11 microns	10 microns	4 microns
1st min	18 microns	26 microns	18 microns
2nd min	25 microns	36 microns	22 microns
Arc voltage, max	34	35.5	39-40
Amps, start	4000	4000	4000
Amps, max	13,000	13,000	10,500-11,000
Melt time	10 min	N.R.	10.6 min
Pour speed	70%	70%	80%
Pour time	3.2 sec	3.1 sec	2.8 sec
Mold temperature	N.R.	950°F	1000°F

Penetrant inspection revealed two pieces with one or two cracks initiating from the ends of center gates (on the gage length) which were scrapped. The balance of the pieces showed occasional shallow indications which, REM indicated, were typical of columbium alloy castings.

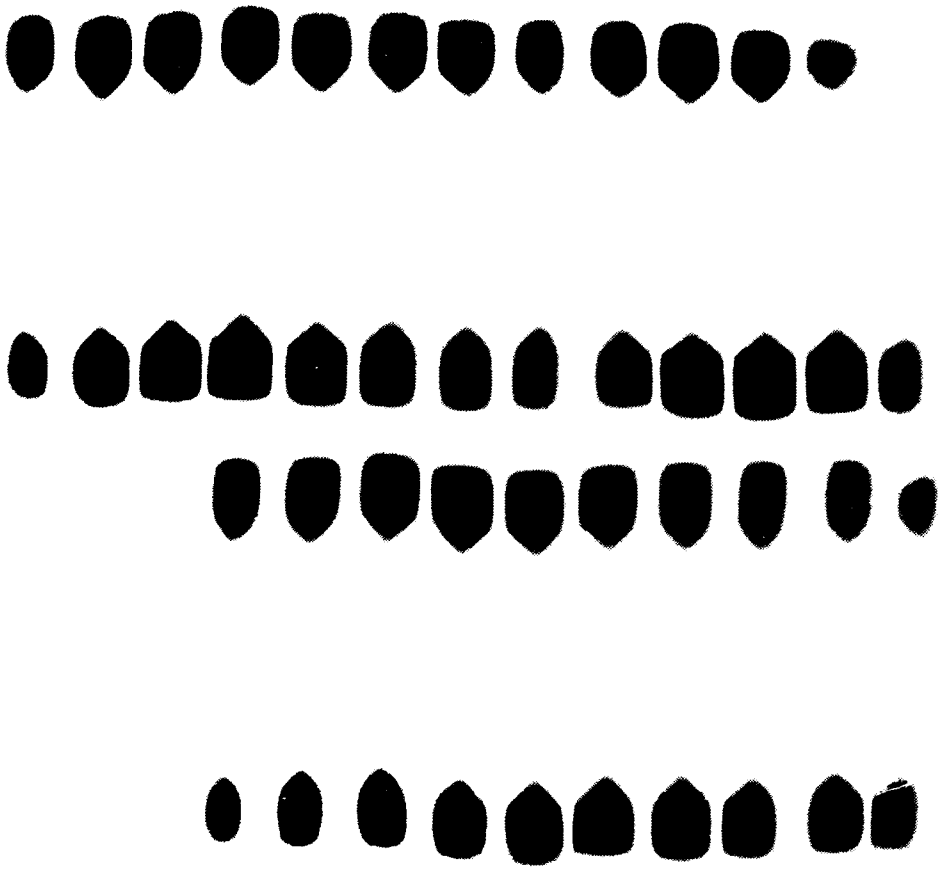

Figure 29. Radiograph of Round Test Bars

Mechanical Properties

Results of tensile and stress rupture testing of castings are presented and discussed here. For additional mechanical property data on coated castings, reference should be made to sections 4.3.1 and 4.3.2.

Tensile Testing. Tensile testing of cast specimens were performed at room temperature, 1093°C (2000°F) and 1204°C (2200°F). Results are reported in Table 10. Due to the scarcity of available test pieces, only a limited number of tests were run. Room temperature results were inconclusive since specimen No. 11 was badly flawed by gas porosity (see Sec. 3.2.2) probably explaining its lack of ductility and failure to reach 0.2 percent offset yield strength. This was the only as-cast specimen tested at ambient temperature and it is not possible to determine what effect the high level of interstitials had

Table 10

Tensile Test Data of C129Y Cast Specimens

Specimen Number	Coating	Temperature (°F)	Temperature (°C)	Ultimate Tensile Strength (ksi)	Ultimate Tensile Strength (MPa)	Yield Strength (ksi)	Yield Strength (MPa)	Reduction in Area (%)	Elongation (%)
11	No	77	25	81.0	558	-	-	0.6	-
18	No*	74	23	78.7	542	77.2	532	0.2	1.4
15	No	2000	1093	47.6	328	39.7	274	45.0	27.9
12	No	2200	1204	40.5	279	33.1	228	22.6	18.5
14	No	2200	1204	41.2	284	33.4	230	7.4	22.2

* Specimen was subjected to the coating cycle heat treatment

on mechanical properties. The relatively poor ductility of specimen 18, which was submitted to the coating heat cycle treatment but not actually coated, is not explained by radiographs or penetrant inspection results. Metallographic examination of the broken specimen indicates an extremely brittle, nondeformed fracture path with extensive secondary cracking in many areas of the specimen, including the non-reduced diameter. Figure 30 is a typical example. Also noted was one area of shrinkage porosity in the gage length which was exposed to the surface by machining, Figure 31. Peculiarly, no fracture was noted to have extended from this defect. The extensive surface cracking observed in this sample suggests that premature failure and low ductility may have been the result of defects generated in the simulated coating cycle and/or machining of the specimen.

Figure 32 is a graph based upon the averages of data in Table 10 and (Table 21 in Section 4.3.1) and upon manufacturer's literature for X-45M cobalt-base alloy showing an approximate comparison of their tensile and yield strengths. C129Y columbium alloy demonstrates at 2000 and 2200°F tensile strength ductility equivalent to the 1600°F properties of the cobalt-base X-45M from which the Solar Centaur first-stage nozzle is presently cast. Room temperature ductility of C129Y, pour No. 3, is suspect but was demonstrated in pour No. 1 (Table 5) to be the equal of the cobalt-base alloy.

Stress Rupture Testing. Stress rupture life of as-cast C129Y specimens are given in Table 11. The poor showing of specinem No. 5 (uncoated) at 1093°C (2000°F) is explained, correctly, by SoRI as atmospheric contamination of the test chamber. Specimen No. 1, which was tested immediately prior to No. 5, can similarly be explained in terms of contamination. The fracture surface was seen to be covered with a white, fibrous residue, Figure 33, which in energy dispersive X-ray analysis proved to be oxides of columbium, hafnium and tungsten. The spectrum, seen in Figure 34, also shows traces of iron, silver and aluminum which are explained as extraneous indications from the scanning electron

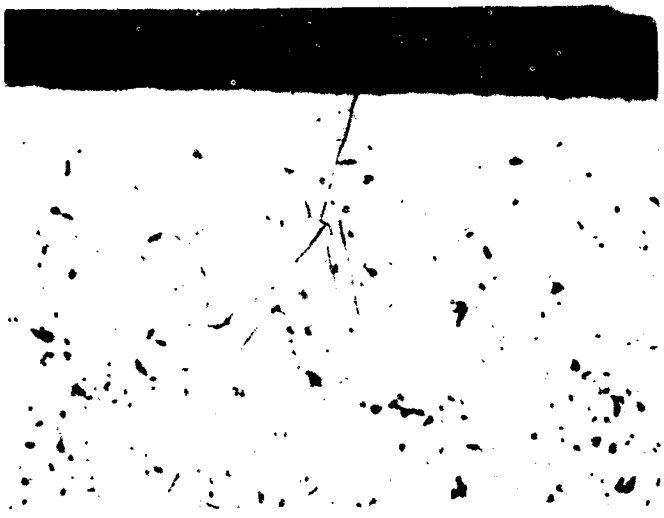

Figure 30.

Brittle Secondary Cracking in Tensile Sample No. 18

Hf-HNO^3 Etch

Magnification: 250X

Figure 31.

Shrinkage Porosity n Tensile Sample No. 18

Hf-HNO_3 Etch

Magnification: 250X

microscope used in the analysis. The fibrous residue became highly charged during the analysis, typical of oxide behavior, and the relative absence of other elements in the specimen suggests that contamination of the test chamber is responsible for the reduced ductility and strength of this specimen. At 2200°F the premature fracture of specimen No. 13 is explained by a radiographic anomoly, appearing to be a crack or possibly a cold shut.

In general, the material displays significantly better creep resistance at 2200°F than was noted by prior investigators (Refs. 3, 8). Creep-rupture strength demonstrated for the test specimens at 2200°F was, at 20 ksi, 10 to 100 hours greater than comparable tests of FS-85, Cb752 or C129Y alloys in the wrought condition. Only alloy SU-31 exceeded the time to rupture of the present cast C129Y test results.

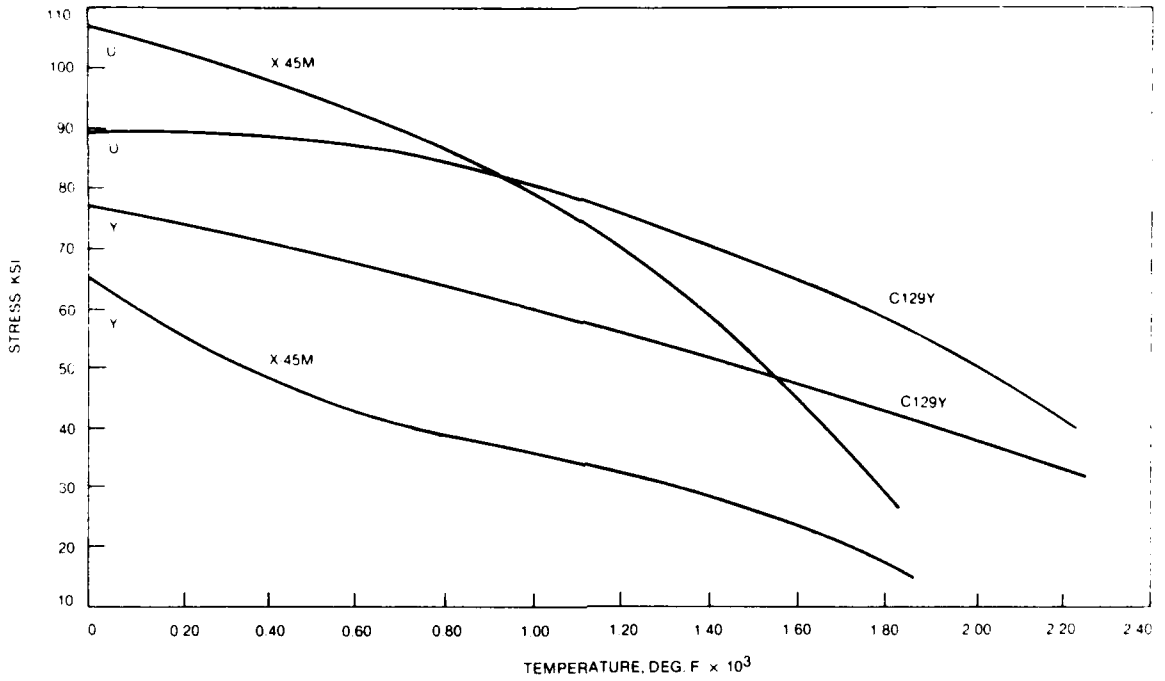

Figure 32. Tensile, Ultimate and 0.2 Percent Yield Strengths of C129Y and X-45M Alloys at Ambient and Elevated Temperature

Table 11

Stress-Rupture Life of C129Y Castings

Specimen Number	Test Temperature °C (°F)	Test Stress MPa (ksi)	Total Hours to Failure
1	1093 (2000)	103 (15) to 138 (20)	~35.0
5	1093 (2000)	103 (15)	~15.0
13	1204 (2200)	138 (20)	35.3
22	1204 (2200)	138 (20)	60.0

The cast C129Y test bars demonstrate significantly higher rupture strength than does X-45M cobalt-base superalloy from which the nozzles are presently fabricated. This superalloy has a 100-hour rupture limit of about 13,000 psi at 1600°F. Figure 35 presents relative Larson-Miller plots of stress-rupture life based upon these limited data showing the significant temperature increase available

Figure 33.

Scanning Electron Micrograph of Residue on Fracture Surface and Gage Length of Stress-Rupture Specimen No. 1

Magnification: 24X

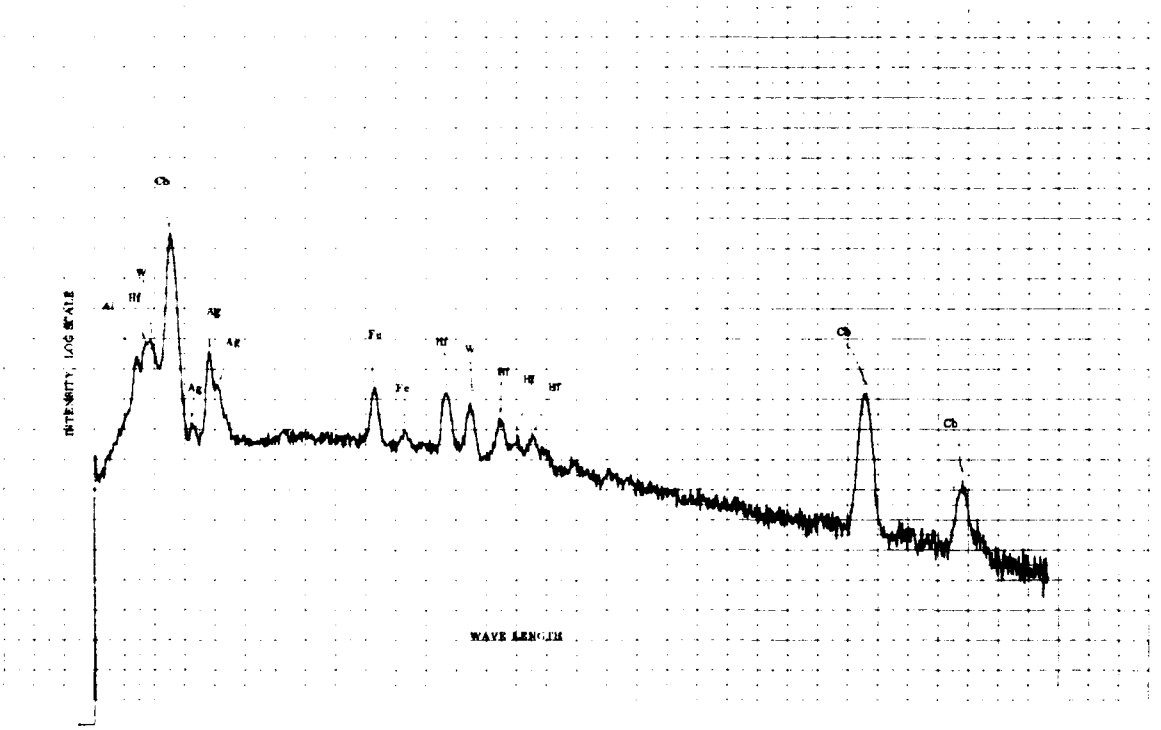

Figure 34. Energy Dispersive X-ray Analysis Spectrum of White Residue on Stress-Rupture Specimen No. 1

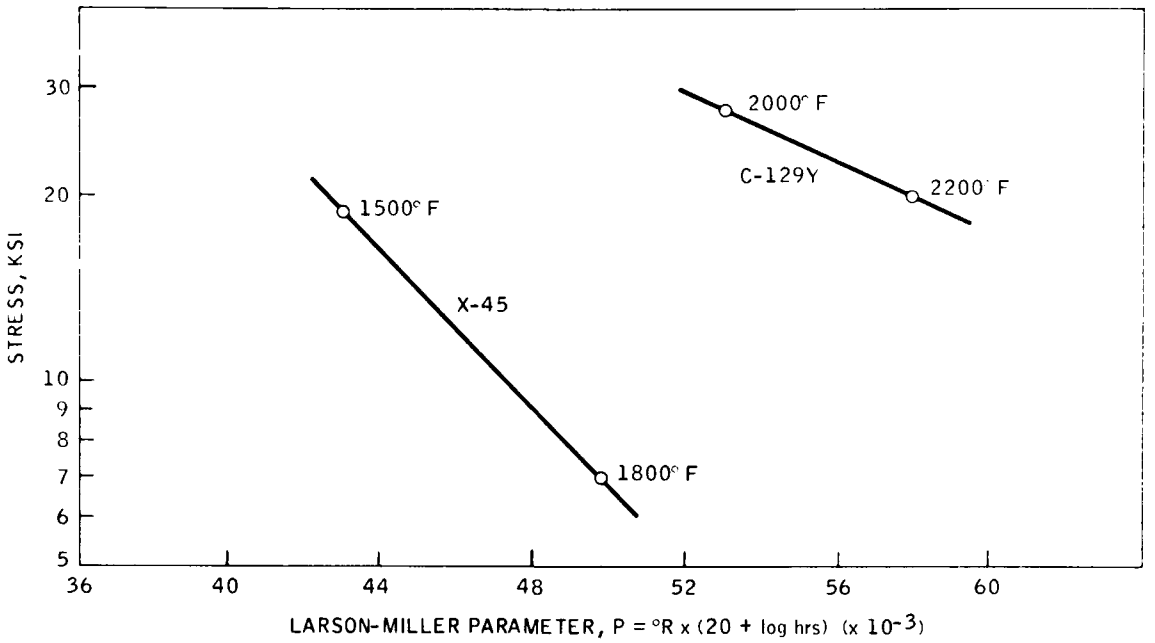

Figure 35. Larson-Miller Plots of Stress-Rupture Life

with coated C129Y. The upper data point (2000°F) represents run No. 4 of specimen No. 2, 26.1 hours at 27,500 psi, and actually should be farther to the right as the specimen has already sustained over 150 hours at lower stresses. The lower data point (2200°F) is an average of all five 2200°F runs. Alloy X-45M data points are from the manufacturers' literature.

Producers' literature for C129Y wrought alloy indicates a 10-hour rupture life at 15,000 psi and 2000°F. The properties developed in stress-rupture testing of casting pour No. 3 exceed this value by wide margins. Figure 36, extrapolated slightly, shows the value to be closer to 30,000 psi stress for 10-hour life at 2000°F.

In summary, creep-rupture properties of C129Y specimens cast in pour No. 3 of this program are significantly higher than those of the previous cast columbium alloy work (Ref. 3); higher than those of wrought columbium alloys, except SU-31, tested by KBI (Ref. 8); and superior to published data for X-45M cobalt-base alloy castings, comparing the alloys at 2000-2200°F versus 1600°F, which strength advantage was a minor goal of this program.

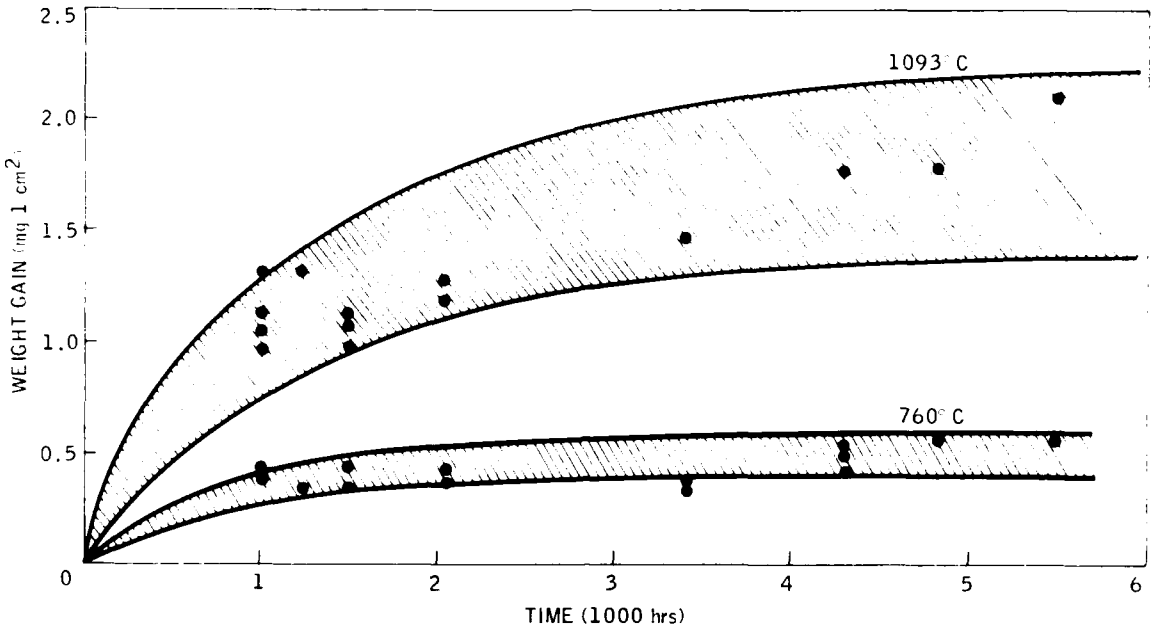

Figure 36. Weight Change Versus Time of Oxidation Specimens

4

PHASE II - COATING AND TESTING OF COMPONENTS

Phase II of the program was concerned with process development and process optimization for coating application to the relatively complex shapes of solid and cored airfoils and evaluation of coating/substrate interaction by various mechanical property and environmental tests. This phase was divided into three tasks, as follows:

Task I - Optimization of Coating Application

Task II - Coating of Components

Task III - Property Evaluation

All Phase II activity was completed in the early months of the program. As casting difficulties developed in Phase I and program scope changes were initiated to allow for the reduced number of cast specimens available from the casting subcontractor, Tasks II and III were also modified. With hollow nozzle vanes eliminated from the program, the need for processing both internal and external surfaces of hollow vanes was also eliminated. However, process optimization will be discussed in full in this section even though all program specimens were coated using the conventional slurry spray technique.

4.1 TASK I - OPTIMIZATION OF COATING APPLICATION

The reaction sintered concept as applied to the NS-4 coating consists of three major steps:

1. Application of modifier bisque to prepared surface (50W-20Mo-15VH_2-15TiH_2) typically in order of 50-125 m.

2. Vacuum sintering of modifier at $<10^{-4}$ Torr at 1516°C (2760°F) for three hours.

3. Pack siliciding of sintered modifier to form disilicides (W, Mo)Si_2 at 1149°C (2100°F) for eight hours.

The standard procedure for application of modifier is by slurry spraying which has proved to be excellent for imparting momentum to the modifier particles, thus producing a dense, well packed bisque. During the vacuum sintering step, much of the vanadium and titanium are volatilized, leaving behind sufficient amounts to lower glass softening temperature at 538-816°C. The final

siliciding step results in approximately 150 percent volume growth as the refractory elements are converted to the disilicide form, thus creating a reserve of silicides to replenish surface oxides which are, in effect, the true oxidation barrier.

The hollow cast and columbium coated nozzle vane configuration was originally conceived of having the advantages of both high-temperature durability and increased thrust-to-weight ratio. However, this implies that the particular coating must be applied to all internal and external surfaces. The approach taken in this program was to use the slurry dip technique for the internal surfaces followed by standard spray techniques for the external airfoil. While dipping is by no means a new process, it is very much dependent on the process variables which vary with configuration. The following investigation is presented under the following process variables:

- Specimen configuration
- Dip application apparatus
- Slurry dip coating slip formulation
- Slurry dip coating slip characterization
- Specimen orientation during dripping
- Rate of withdrawal
- Dip/spray overlap
- Multiple dipping
- Sintering and siliciding.

4.1.1 Specimen Configuration

Due to the high cost and exceedingly long lead time involved in procurement of columbium alloy castings, process optimization and development was conducted utilizing specimens fabricated from either 310 stainless steel or columbium metal. Several configurations were used, each increasing in degree of geometrical complexity in order to study different aspects of the dipping process. Stainless specimens were used primarily for dipping only, while columbium specimens were used for full process treatment, sintering and siliciding.

Initially, coupons such as shown in Figure 37 were cut from sheet metal of both stainless steel and recrystallized columbium as the fundamental and simplest form. A second specimen configuration was fabricated stainless steel tubing and rolled and welded columbium, see Figure 38, with the wall thickness approximating that typically found in cooled airfoils. The radius was chosen to simulate the internal radius at th trailing edge. The next level in specimen configuration is shown in Figure 39 which was fabricated from columbium sheet

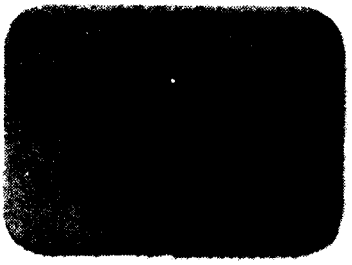

Figure 37.

Columbium Metal Coupon Specimen

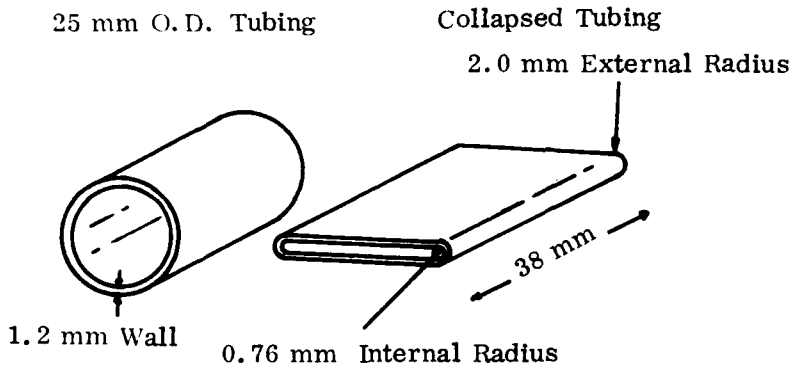

Figure 38. Coating Development Specimen

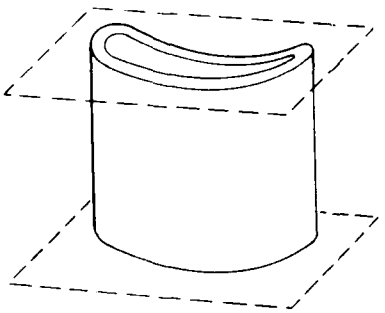

Figure 39.

Simulated Airfoil Specimen Fabricated From Columbium Metal

metal formed and cold worked around a dye made in the shape of the core of an airfoil. By fitting two flanges over the ends of the airfoil, as shown in Figure 39, the specimen was made to closely resemble the actual vane segment. Each of the above specimen configurations was utilized for a specific purpose and for establishing empirical values between critical parameters involved in the slurry dip process.

4.1.2 Dip Application Apparatus

The apparatus used for dip application studies is shown in Figure 40. The setup consisted of a Bodine Electric motor and a Minarek speed control box, both of which were rigged and calibrated such that the rate at which a specimen was withdrawn from a slurry dip was readily controlled. Figure 41 shows a similar arrangement with the addition of an ultrasonic bath to aid in agitation of the slip during withdrawal. Various alligator clips and clamps were used to fasten the specimens. Clamp marks were subsequently repaired by hand.

4.1.3 Slurry Dip Coating Slip Formation

The composition of the slurry dip used in this dipping study was 50W-20Mo-30Ti. The vanadium had been deliberately left out due to its high cost factor. Therefore, this experimental slip was designated NS-4X.

Five batches of powder were prepared by milling the appropriate quantities of <44 μm tungsten, molybdenum and TiH_2 into a ball mill for different lengths of time. The first batch was milled for 24 hours in an E-4 vehicle (ethyl cellulose binder in xylene) and subsequent batches have either xylene or cellulose vehicles only, which were more readily removed by drying than E-4. The characteristics of batches 2 to 5 are shown in Table 12.

The specific gravities of the powder mixture were verified using the measured densities of the constituents given in Table 13. The calculated value of the NS-4X composition is 7.88 g/ml. This value was quite close to the measured values reported in Table 11 and the small differences noted were probably due to entrapped air bubbles in the powder during measurement.

In Reference 6 the particle size of the powders was maintained at <3 μm and it was believed that small particle sizes improve the suspension characteristics and thereby the quality of the coating. The particle size versus milling time of batches 2 to 5 are plotted in Figure 42. It can be seen that milling times of 40 hours or more are required to produce particles with an average size of <3 μm. However, it was found that with batches 3 and 4, i.e., particle size <3 μm, the bisques obtained were unacceptable due to streaking on the flat surfaces of the coupon specimen. From a visual aspect, batches 1, 2 and 5 were satisfactory. For all subsequent work, a milling time of 24 hours was employed.

Reference 6 reported that the NS-4 coating slip was milled in E-4 followed by drying and suspension of the fine powders in equal portions of acetone and Rohm and Hass acryloid B-7. This process was reproduced here and, using flattened stainless steel tubing specimens, a number of specimens were dip coated. The results are given in Table 14. (The effects of withdrawal rates will be discussed in a later paragraph.) Bisque thicknesses varied from 0.03 mm to as high as 0.20 mm. The major drawback to the use of this vehicle system was the fact that the bisque could not be readily duplicated because of the significant loss of acetone through evaporation, thus in effect, the specific gravity of the slip was slowly changing even as the specimens were drawn up.

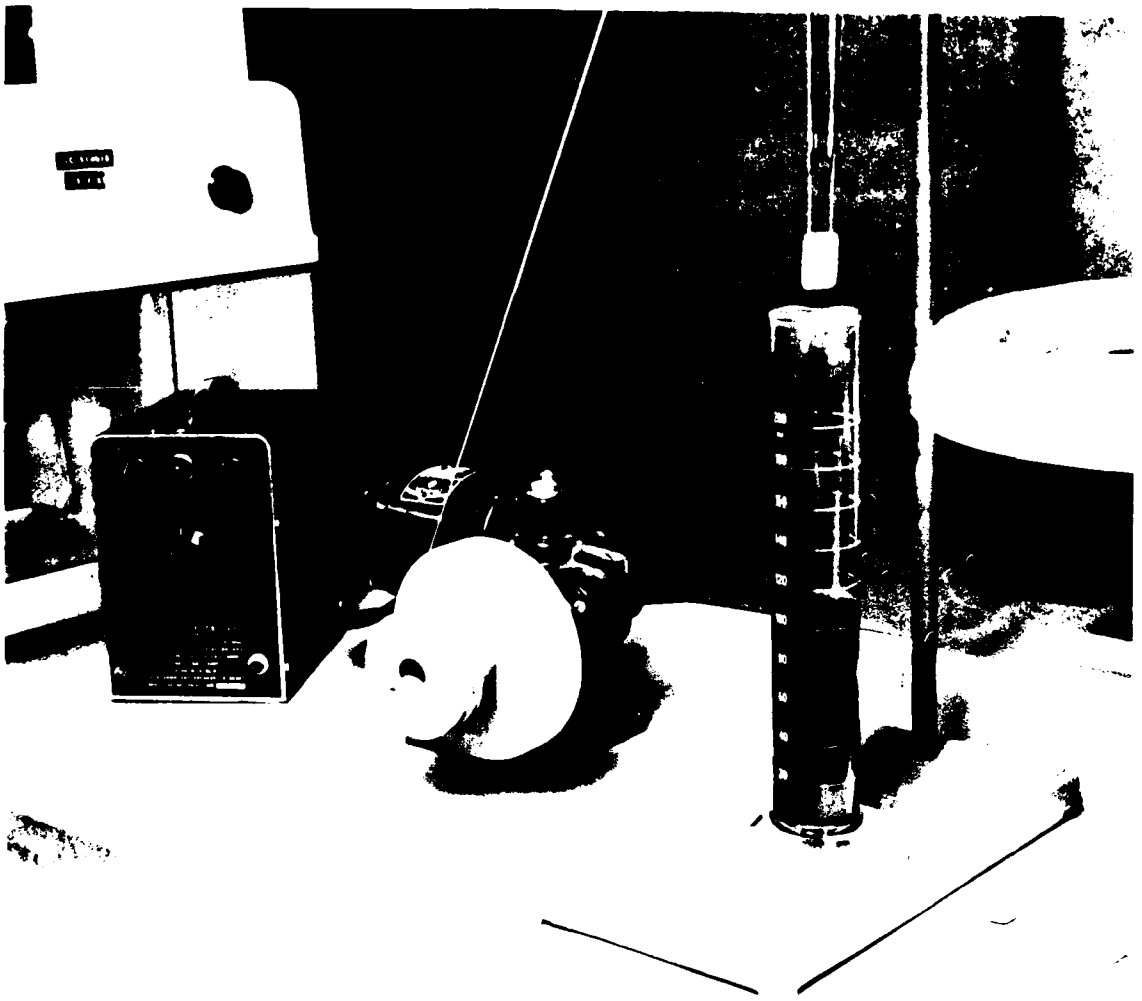

Figure 40. Test Setup for Dip Application of Development Coating

Furthermore, the rapid drying of the slip prevented the formation of usually acceptable coatings as the bisque tended to "cake" and form agglomerates as the acetone vaporized. Since the surface tension of a liquid is a factor in determining the degree of wetting, the addition of petroleum ether, a liquid of lower surface tension than acetone, to the slip was investigated. Once again, the high vapor pressure of this solvent resulted in less than satisfactory bisques due to premature drying. The high evaporation rates of acetone and petroleum ether were somewhat minimized by conducting the dipping operation in an equilibrium vapor over a pool of the solvent. While additions of surface active compounds such as petroleum ether did not alleviate the non-uniform coating problem, the use of a pool of acetone surrounding the dipping operation has led to a more uniform, albiet thinner, coating.

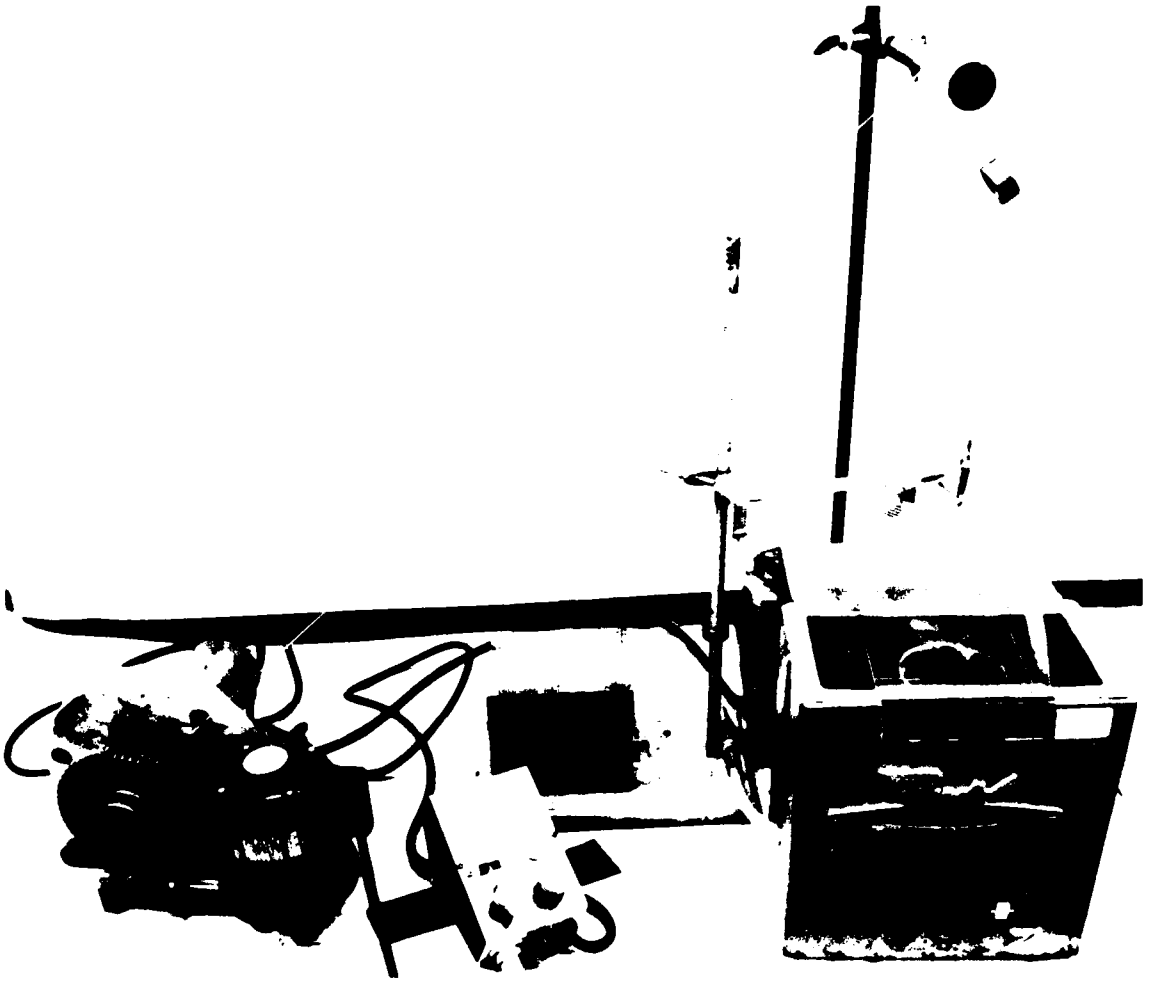

Figure 41. Test Setup for Dip Application With Ultrasonic Path

One other investigation in slip solvent was conducted using only ethylene dichloride to make the slip. When this was ultrasonically agitated, stratification of the slip occurred and therefore efforts to employ a one solvent slip was abandoned.

The above work indicated the need for a more suitable vehicle and this was realized in Cellosolve, a glycol ether commercially available from Union Carbide. The viscosity of the vehicle is 2.1 cps at 20°C and combined with Romn and Hass Acryloid B-7, the bisque produced was very satisfactory and reproducible. The good suspension characteristics of this slip is probably due to the fact that the structured cellulose can hydrogen bond to the surface of the metallic particles to form micellar species that remain in suspension. In addition, the higher boiling point (136°C) minimized evaporation and handling problems. The cellosolve and acryloid slip was selected for further investigation of dipping parameters.

Table 12

Characteristics of Development Coating Batches

Batch Number	Mill Time (Hours)	Specific Gravity 25°C (Note 1)	Fraction Less Than 10 µm (Note 2 - %)	Average Particle Size (µm) (Note 3)
2	30	7.86	28	3.85
3	45	7.85	49	2.69
4	45	--	62	2.12
5	23	7.84	55	4.1

Notes: 1. Measured by a pycnometric method employing condensed xylene as the pycnometric fluid.

2. This fraction was measured by noting the weight percent of material passing a 10 µm screen.

3. Average particle size measured by ASTM method B330-65.

Table 13

Density of Developmental Coating Constituents

Constituent	Literature[1]	Measured (25°C)
Tungsten	19.35 (20°C)	18.79
Molybdenum	10.2	9.97
Titanium Hydride	3.9 (92°C)	3.74
Xylene[2]	0.8642 (20°C)	0.8597

Notes: 1. Handbook of Chemistry and Physics, Robert C. Weast ed., CRC, Cleveland, OH 56 ed. (1975).

2. Pycnometric Fluid.

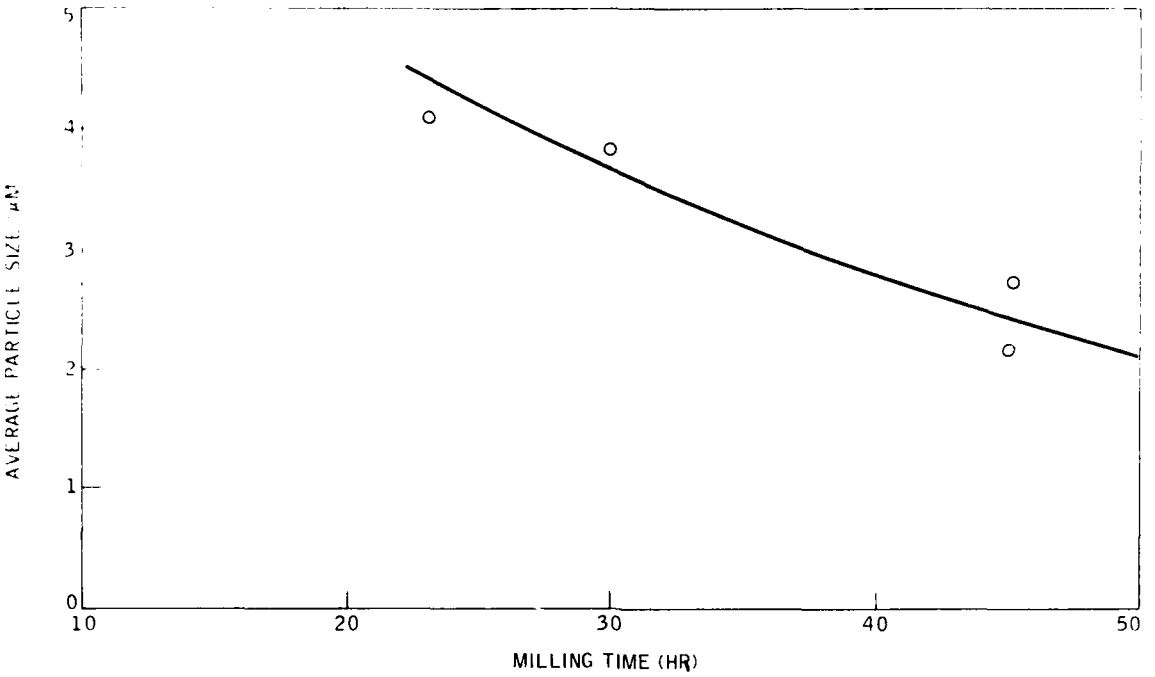

Figure 42. Average Particle Size Versus Milling Time

Table 14

Conditions and Results of Dip Application of Development Coating

Specimen Number	Withdrawal Rate (mm/min.)	Weight of Coating Applied (gms)	Ultrasonic Stirring of Slip	Coating Thickness		
				Inside Flat mm	Bottom Edge mm	Inside Radius mm
2	3.3	1.05	No	0.041-0.061	0.061-0.20	0.20
3	6.6	0.75	Yes	0.030-0.051	0.10-0.14	0.10
5	3.3	1.06	Yes	0.051	0.071-0.12	0.11
6	2.5	0.82	Yes	0.051-0.10	0.051-0.061	0.15

Note 1. Slip mixture 445 gm of Batch No. 2 of developmental coating suspended in 50 ml of acetone and 50 mls of B-7 acryloid, Specific gravity 3.31.

2. Specimens used are flattened SS tubing as shown in Figure 31

4.1.4 Slurry Dip Coating Slip Characterization

Slip characterization was established to monitor [illegible] composition as a result of solvent evaporation and unequivocal losses [illegible] drying or caking of powder in handling. The following techniques were investigated:

- Specific gravity
- Deposition on standard specimens under specified conditions
- Rotational viscometry
- Settling or 'set' property.

The latter two techniques were dismissed as unsuitable for the following reasons.

Rotational viscometry is commonly employed to measure viscosities of enamel slips and has the advantage of making the measurements at consistent rates of shear and can be adapted to estimate such properties as thixotropy and dilatancy. The operating principle is based on the fact that an object rotated a given speed develops a torque which is directy proportional to the viscosity of the fluid in which it is immersed. However, the setting tendency of the coating slip was such that significant error resulted from the change in viscosities in the time required to take a reading due to settling of the metal powder which was not compensated for by the rotational agitation of the spindle.

Another method of monitoring the slip is to allow a standard aliquot of sample to stand undisturbed for a fixed period of time during which particle size, range and solvent viscosity determines the rate at which the particles can move to the bottom and settle out. The amount of clear solvent formed at the top in the fixed period of time was used as an indication of composition. In the case of the NS-4X modifier slip (acryloid/cellosolve), the time required for this phenomenon to occur was prohibitively long, in the order of hours, and thus render this method impractical.

The two methods chosen for characterization of slip were specific gravity (pycnometry) and the use of a stainless steel flattened tubing specimens (see Fig. 38) dip coated under specified conditions. The reproducibility of the two methods are noted below and both were used when needed to monitor and maintain the desired slip characteristics.

Method	Trial 1	Trial 2	Average
Specific gravity	3.67 g/ml	3.66 g/ml	3.67 g/ml
Coating weight	0.70 g	0.74 g	0.72 g

(Withdrawal rate = 3.81 mm/min.)

4.1.5 Specimen Orientation During Dipping

A problem encountered during dipping studies was that of beading, i.e., the excessive buildup of bisque at that part of the specimen which was withdrawn last from the slip. This buildup caused major spalling at the edges where it was often found. Fortunately, this can be minimized by orienting the specimen such that the last part of the specimen to leave the slip was a point or tip of an edge and the beading effect was confined to a smaller area which was subsequently repaired by hand. The flattened tubing configuration was successfully coated with an orientation angle of about 30 degrees from the normal.

On withdrawal of a specimen from the slip, a flow field is established within the non-Newtonian fluid around the object. This flow field is dependent on the configuration of the object and controls to varying degrees the slip drainage. The presence of flanges, a relatively large surface area on the plane perpendicular to the direction of withdrawal, was found to result in increased deposition on the internal surfaces of the simulated airfoil specimens. A reasonable explanation was that as the flanged specimen was moved upward in the slip, the area immediately below the flange area underwent pressure reduction. The net effect of this was to cause adjustments of the flow field such that the slip drained down the inside of the airfoil at a rate greater than expected with the rate of withdrawal. This was compensated for by adjusting the withdrawal rate to achieve the desired bisque thickness.

4.1.6 Rate of Withdrawal

A sixth development batch of NS-4X was prepared by milling in xylene for 24 hours followed by removal of xylene and adding acryloid/cellosolve to a specific gravity of 3.44 g/ml. Using this slip, and the flattened stainless steel tubing specimens, the correlation between withdrawal rate and internal bisque weight was obtained. The results are shown in Table 15 and plotted in Figure 43. The internal weight was determined by carefully removing the bisque from the outer surfaces. From Figure 44, it can be seen that there appears to be an almost linear relationship between bisque weight and withdrawal rate. Once established for the particular specimen configuration, this proportionality can serve as the basis for selection of optimum withdrawal conditions for dipping application.

Another experiment monitored the bisque weight deposited on both external and internal surfaces of the airfoil specimen. The results, Table 16 and Figure 44, show that bisque deposition on any surface appears to be primarily a function of withdrawal.

Table 15

Weight of Internal Coating Versus Rate of Withdrawal

Number	Rate (mm/min)	Internal Weight (g)
6A	6.2	0.35
2	8.2	0.30
1	12.4	0.34
6	17.3	0.48
3	22.6	0.48
4	29.5	0.61
7	46.2	0.83
5	59.2	0.88

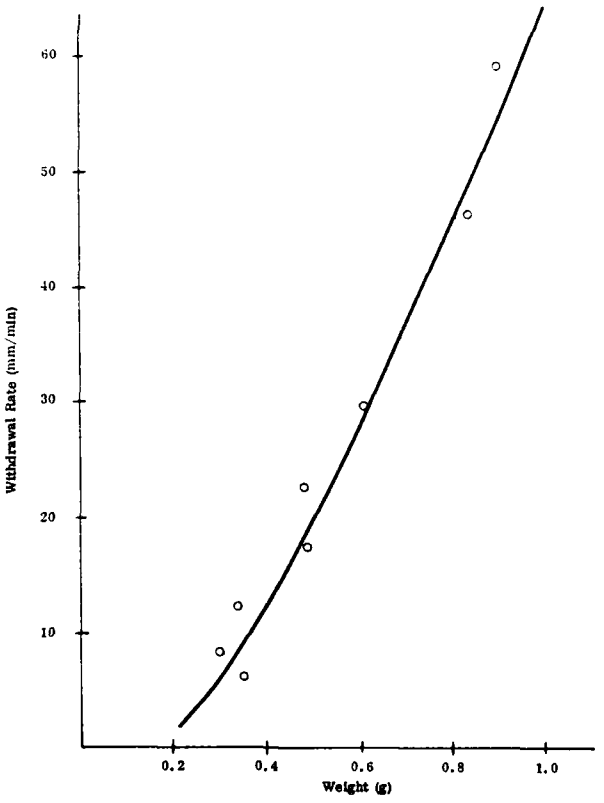

Figure 43. Correlation of Coating Weight Deposited on Simulated Airfoil and Withdrawal Rate

Table 16

Correlation of Weight of Coating and Rate of Withdrawal

Withdrawal Rate (mm/min.)	A Total Wt. (g)	B Int. Wt. (g)	C Ext. Wt. (g)	D Total Wt. (g)
3.81	0.644	0.276	0.368	0.520
4.70	0.764	0.319	0.445	--
6.22	--	--	--	0.630
9.65	1.040	0.447	0.593	0.859
12.45	1.342	0.576	0.966	1.043

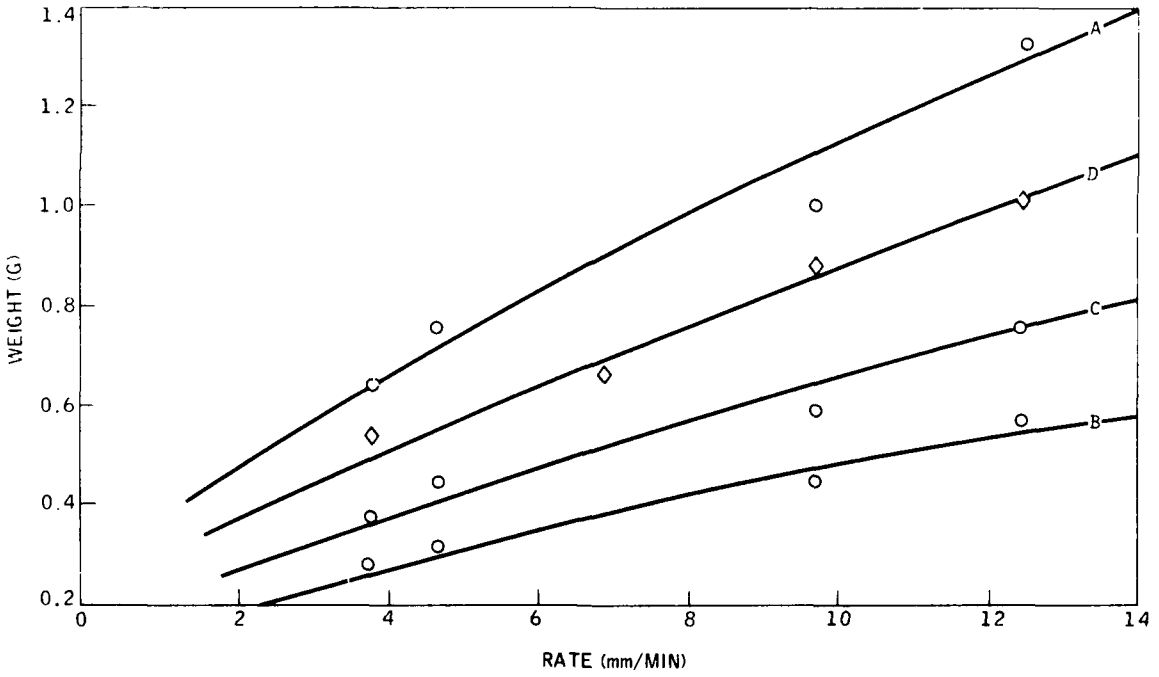

Figure 44. Weight of Coating Versus Rate of Withdrawal

4.1.7 Dip/Spray Overlap

An important aspect of this study was to evaluate the overlap at the rim of the hollow airfoil where the dipped bisque overlaps the spray bisque. The goal was to achieve a uniform, well feathered and continuous coating at the overlap region. By careful manipulation and orientation of both dipping and spraying processes this was achieved, as illustrated in Figure 45.

Figure 45.

Dip/Spray Interface

Magnification: 250X

4.1.8 Multiple Dipping

Another approach to bisque application control is the multiple dip coating. This was demonstrated using two recrystallized columbium speciens which were first dipped and withdrawn at 3.81 mm/min and 12.45 mm/min. They were then sintered at 1516°F for three hours, cooled to room temperature and dipped again under identical conditions. The weight gains are reported in Table 17. Note that the second dipping operation essentially deposited equivalent amounts of bisque on the part. The microstructure of the specimen withdrawn at 3.80 mm/min after dip/sinter/dip operation is shown in Figure 46. There appeared to be some diffusion across the substrate/coating boundary (light gray) and no discernible demarcation was noted between the two coats. Therefore, this represented an alternative, albiet more time consuming, route to achieving desired coating thickness.

Table 17

Developmental Coating Thickness With Two Dip Applications

Rate (mm/min.)	1st Coat (mm)	2nd Coat (mm)	Total (mm)
3.80	0.030	0.051	0.081
12.45	0.0609	0.069	0.129

Figure 46.

Microstructure of Dipped/ Sintered/Dipped Specimen

Magnification: 250X

4.1.9 Sintering and Siliciding

A seventh powder batch was prepared using the correct composition for NS-4. The characteristics of this mill are reported in Table 18. An acryloid/ cellusolve slip was prepared and a total of 16 specimens were coated.

A deviation from previous experimental dip studies was the elimination of ultrasonic agitation during dipping. It was established by X-ray fluorescent analysis of dipped bisques that due to the disparity of atomic weights of titanium, vanadium, molybdenum and tungsten, stratification within the ultrasonically agitated slurry occurred during dipping, thus resulting in low molybdenum and tungsten levels in the coating bisque. Consequently, instead of ultrasonic agitation, the slip was thoroughly stirred between each dip application to ensure homogeneity.

Table 18

Weights of NS-4 Coated Specimens

	Number	A Average Weight As-Coated (mg/cm^2)	Weight (mg/cm^2)			B Average Weight Gain After Siliciding (mg/cm^2)	
			As-Dipped	As-Sintered(3)	As-Silicided(4)	Experimental	Calculated
L/S 1.5(1)	1A		45.85	-	-	-	-
	1B		53.44	47.78	-	-	-
	1C	52.0	47.40	42.17	71.38	30.0	26.0
	1D		54.32	48.66	79.86		
	1E		54.68	48.85	80.31		
L/S 2.0(2)	2A		27.22	-	-	-	-
	2B		16.15	13.35	-	-	-
	2C	28.0	28.86	24.53	47.53	23.0	12.0
	2D		25.61	21.71	43.74		
	2E		29.18	24.70	47.61		
E4 Vehicle	3A		47.62	42.92	71.68		
	3B	46.0	45.52	40.88	68.88	28.0	23.0
	3C		43.93	39.06	66.62		
Acryloid/Cellosolve Vehicle	4A		34.61	29.84	54.49		
	4B	32.0	33.59	28.93	53.08	24.0	15.0
	4C		28.92	24.87	47.74		

Notes:
1. Rate of withdrawal = 0.96 mm/min.
2. Rate of withdrawal = 29.5 mm/min.
3. 1516°C, 3 hours.
4. 1149°C, 8 hours.

In Table 18, two liquid-to-solid (L/S) ratios were studied, 1.5 and 2.0, and the rates of withdrawal for each dip slurry were 0.96 and 29.5 mm/min, respectively. Baseline specimens were prepared by spraying NS-4 with both E4 and acryloid/cellusolve vehicles. Figure 47 shows the microstructures of the 1.5 L/S slip, No. 1A, 1B and 1C. The as-dipped bisque No. 1A appeared to be very porous; this is in fact an artifact resulting from handling of the soft, unfired bisque. The polishing process pulled out the unsintered particles from the bisque which was only held together by a cold epoxy compound. After sintering, the specimen showed good bonding to the substrate although porosity was still a distinguishing feature. Specimen No. 1C, having undergone both sintering and siliciding, showed a wide interface which contained some silicon. Note the cracks in the coating induced by thermal mismatch.

Figure 48 is a plot of the as-dipped bisque weight versus weight due to silicon pickup. Note that while both calculated and experimental curves appear to be almost linear, there is significant displacement indicating that not only is silicon consumed to form disilicides with the coating elements, but some silicon penetration probably occurred in the columbium substrate itself.

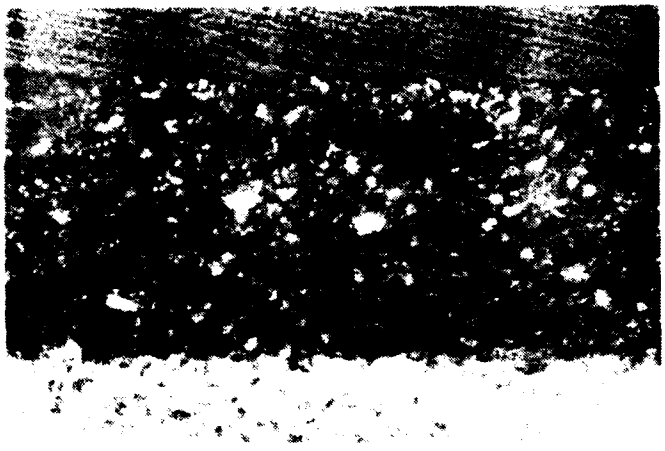

As-Dipped - No. 1A

Magnification: 250X

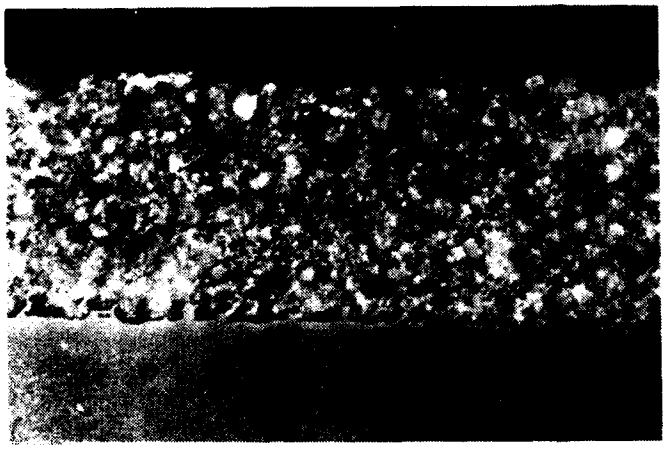

As-Sintered - No. 1B

Magnification: 250X

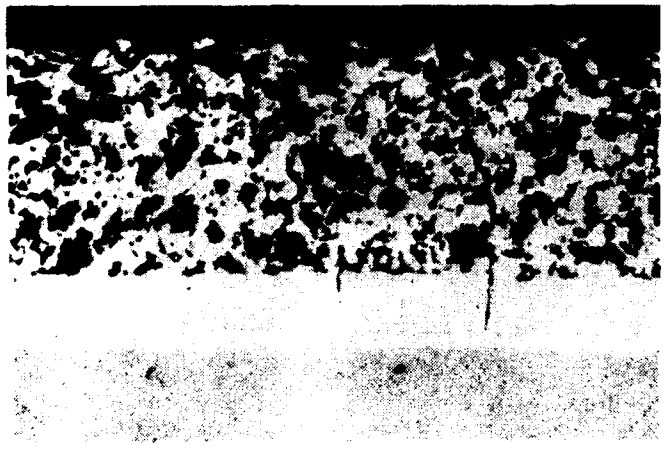

As-Silicided - No. 1C

Magnification: 250X

Figure 47. Microstructures of NS-4 Coating Formation

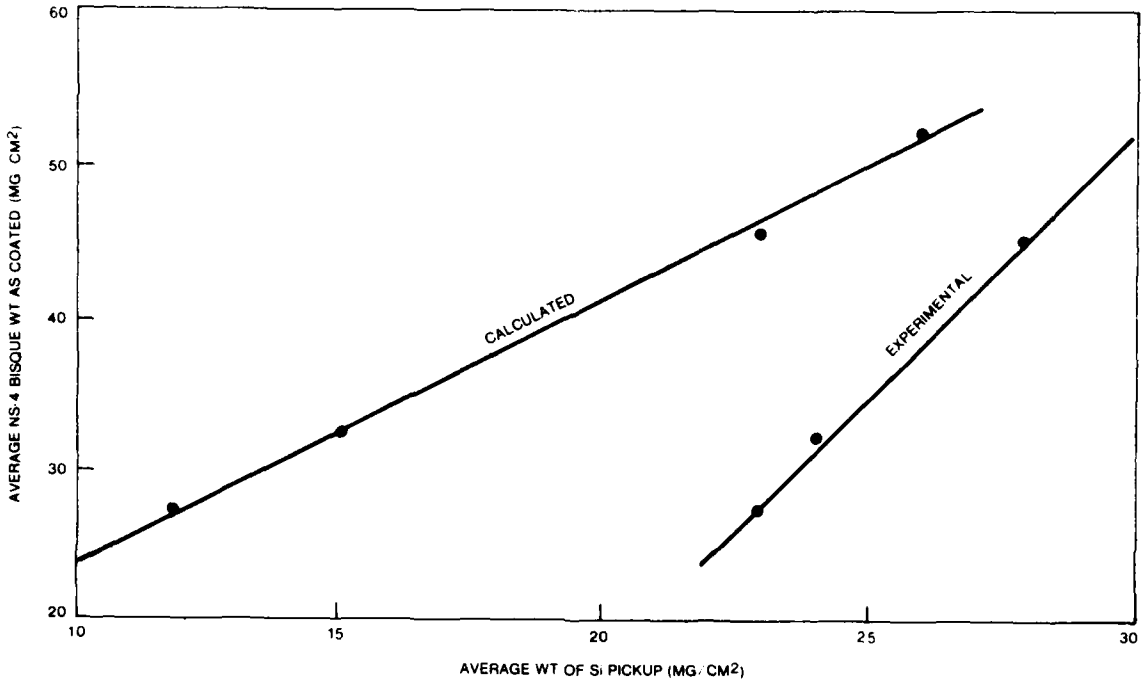

Figure 48. NS-4 Bisque Weight Versus Silicon Pickup Weight

Figure 49 shows the sprayed NS-4 coating using the two vehicle systems. The E-4 bisque exhibited lower porosity than the acryloid/cellusolve system.

4.1.10 Summary of Task I

The end point of the process development study was coating of the simulated airfoil specimen. Lacking the cast columbium vane segment to bring the study to its final point, the findings of this study were extrapolated in order to prepare process specifications for the cored vane segments. Complete specifications are incuded as Appendix D.

4.2 COATING OF COMPONENTS

As a result of the change in scope of the program, only external surfaces of test specimens and solid airfoils required coating; consequently only the slurry spray technique was used, as described in Appendix D. The actual coating weights are reported in Table 19. Since the test bars were threaded, the NS-4 modifier was applied to the reduced gage section only (see Figs. 50 and 51), although the subsequent siliciding operation resulted in the formation of silicides on all surfaces. The final pre-oxidation treatment involved a 1-hour exposure in air at 1371°C.

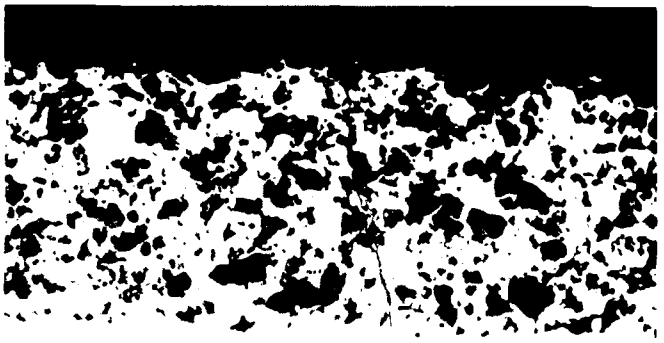

A. As-Silicided - No. 3C

Sprayed in E-4 Vehicle

Magnification: 250X

B. As-Silicided - No. 4B

Sprayed in Acryloid/
Cellosolve Vehicle

Magnification: 250X

Figure 49. Microstructures of Sprayed Specimens

Table 19

NS-4 Coated C129Y Alloy Specimens

Specimen Number	Area (cm^2)	Weight Bisque		Weight Sintered		Weight Silicided		Weight Pre-Oxidized	
		(g)	(mg/cm^2)	(g)	(mg/cm^2)	(g)	(mg/cm^2)	(g)	(mg/cm^2)
Coupons									
1	5.58	0.1845	33.1	0.1750	31.4	0.3022	54.2	0.3128	56.1
2	4.78	0.1714	5.9	0.1625	34.0	0.2717	56.8	0.2861	59.9
3	4.92	0.2092	42.5	0.1996	40.6	0.3305	67.2	0.3412	69.4
4	4.24	0.1525	36.0	0.1452	34.3	0.2465	58.1	0.2547	60.1
5	4.69	0.1685	35.9	0.1604	34.2	0.2716	57.9	0.2813	60.0
6	4.80	0.2199	45.8	0.2100	43.8	0.3405	70.9	0.3525	73.4
7	4.47	0.1966	44.0	0.1879	42.0	0.3068	68.6	0.3177	71.1
8	2.75	0.1203	43.8	0.1131	41.1	0.1925	70.0	0.1990	72.4
Bars (Solar)									
4	2.82	0.1818	64.5	0.1810	64.2	0.5592		0.5760	
6	2.82	0.1567	55.6	0.1550	55.0	0.4853		0.5003	
7	3.65	0.2064	56.6	0.2032	55.7	0.5937		0.6097	
10	3.44	0.1653	48.1	0.1631	47.4	0.5502		0.5665	
Bars (SRI)									
2	6.64	0.2520	38.0	0.2490	37.5	0.6680		0.6889	
9	6.83	0.2662	39.0	0.2614	38.3	0.6949		0.7192	
16	6.80	0.2092	30.8	0.2039	30.0	0.6213		0.6445	
23	6.81	0.2149	31.6	0.2120	31.1	0.6385		0.6619	

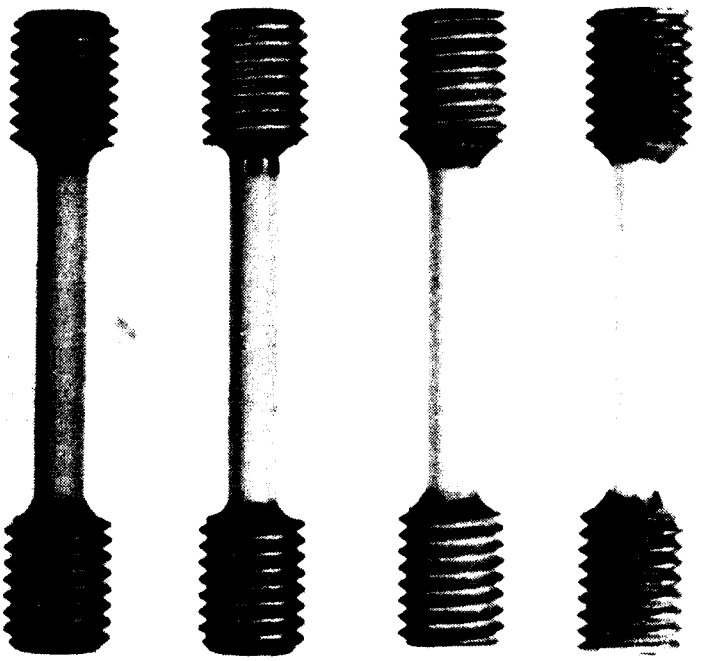

Figure 50. NS-4 Coated Stress-Rupture Bars in As-Coated Condition

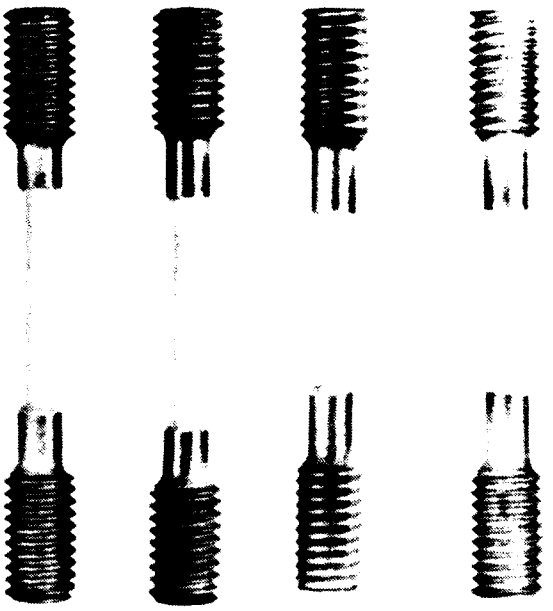

Figure 51. NS-4 Coated Tensile Bars in As-Coated Condition

From the weight change data derived from coating test coupons, the relationship between modifier bisque to silicon pickup is shown in Figure 52. The data points appeared to be best fitted by a second order polynomial. This non-linear function would imply that under the imposed limits of 8 hours in a siliciding pack at 1149°C, the amount of silicon deposited in the coating would gradually taper off as the coating becomes excessively thick.

Table 20 shows similar coating weight changes for the four solid cast columbium vanes processed similarly.

4.3 PROPERTIES OF COATED SPECIMENS

4.3.1 Tensile Properties

This section presents both the as-cast and as-coated properties of test bars from pour No. 3. Data are seen in Table 21. At room temperature, specimen No. 4 exhibited excellent strength and ductility compared to the two uncoated bars, Nos. 11 and 18. Since No. 18 was also subjected to the same thermal cycles used in coating processing, it should be compared to No. 4. The difference in tensile and yield strengths can be attributed to scatter in data points but some embrittlement was noted in the low values in elongation and area reduction in No. 18.

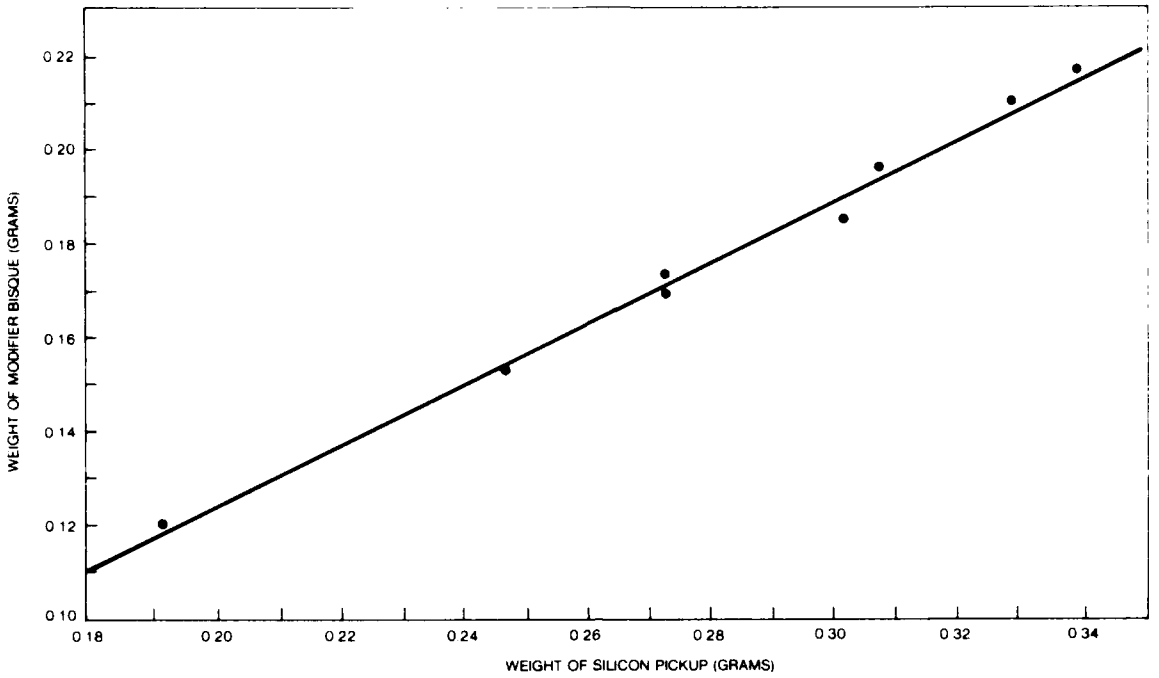

Figure 52. Correlation of Bisque Weight With Silicon Pickup Computer Fit to Equation: $Y = 0.165X^2 + 0.580X + 0.0003$ Where Y is Weight and X is Weight of Silicon

Table 20

Coating Weight Gain of Cast Columbium Nozzle Vanes

Specimen Number	Weight of Bisque (g)	Weight After Sintering (g)	Weight After Siliciding (g)	Weight After Pre-Oxidating (g)
6-2	3.54	3.30	5.71	-
1-3	4.40	4.07	6.83	7.17
5,3*	3.79	3.42	5.89	6.17
3,4*	4.03	3.55	6.07	6.34

* Sintering cycle was 8 hours instead of 3 hours.

Table 21

Tensile Test Data of C129Y Alloy

Specimen Number	Coating	Temperature (°F)	Temperature (°C)	Ultimate Tensile Strength (ksi)	Ultimate Tensile Strength (MPa)	Yield Strength (ksi)	Yield Strength (MPa)	Reduction in Area (%)	Elongation (%)
11	No	77	25	81.0	558	-	-	0.6	-
18	No*	74	23	78.7	542	77.2	532	0.2	1.4
4	Yes	77	25	89.7	618	75.8	522	23.8	9.7
15	No	2000	1093	47.6	328	39.7	274	45.0	27.9
7	Yes	2000	1093	51.5	355	37.2	256	35.3	23.9
10	Yes	2000	1093	49.6	342	37.4	244	23.2	13.0
12	No	2200	1204	40.5	279	33.1	228	22.6	18.5
14	No	2200	1204	41.2	284	33.4	230	7.4	22.2
6	Yes	2200	1204	41.8	288	31.8	219	10.8	18.3
17	Yes	2200	1204	40.8	274	30.4	209	27.1	20.4

* Specimen was subjected to the coating cycle heat treatment

Results of the 2000 and 2200°F tests are uniformly good. There is no significant difference between as-cast and coated properties, verifying the viability of the system. Specimens No. 15, 10 and 17 display adequate strength and ductility although slightly flawed with gas porosity.

4.3.2 Stress-Rupture Testing

Stress-rupture test results as reported by Southern Research Institute are shown in Table 22. Creep rates are plotted in Figures 53 and 54 for 2000°F and 2200°F, respectively.

Specimen No. 2 was tested at 2000°F after modification of the test chamber to eliminate leakage and contamination of the inert environment. The stress level for this specimen was increased from 13 ksi to 34 ksi as creep rate was extremely low. At 100 hours, the thermocouple failed but the specimen had only increased by <1 percent. The stress was increased subsequently, which led to sudden onset of third-stage creep followed by failure at 81 hours, or 181 hours total.

Of the specimens at 2200°F, No. 9 was found to be flawed with gas porosity, detectable in the radiograph, but in this case no adverse effects were seen in the creep results, the sample demonstrating adequate ductility to relieve the stress concentration effect of the flaw. The remaining specimens appeared, in radiographic inspection, to be sound and, as such, the creep results may be viewed as valid. Specimen No. 23 did not fracture. It elongated such that the laoding arm activated the furnace cutoff switch which normally happened only upon failure.

Table 22

Test Results on C129Y Alloy

Specimen Number	Run Number	Specimen Condition	Test Temp. (°F)	Test Stress (ksi)	Total Hours at Failure	Specimen Gage Diameter (inch) Coated/Uncoated	Specimen Gage Length (l) (inch)	Total Change in Length (Δl) (inch)	$\Delta l/l$ (in./in.)	Reduction in Area (%)	Remarks
1	1	Uncoated	2000	15 and 20	35.0	0.7047	1.1170	0.0064	0.00573	--	
3	2	Uncoated	2000	15	15.0	0.205	0.6741	0.00265	0.00303	--	
2	3	Coated	2000	13 and 35	100.6[1]	0.2287 / 0.2184	0.5901	0.00437	0.00735	--	T/C failed but specimen was still intact.
2	4	Coated	2000	20, 22.5 and 27.5	80.9	0.2287 / 0.2184	0.7489	0.14120	0.18854	16.9	Spec. 12 reran at 20,000 psi after 4.7 hrs increased stress to 22,500 psi. After 49.1 hrs increased stress to 27,500 psi.
9	5	Coated	2200	20	57.5	0.2360 / 0.2247	0.7779	0.2168	0.2787	21.6	
16	6	Coated	2200	20	25.8	0.2236	0.6791	0.0419	0.0617	--	
13	7	Uncoated	2200	20	35.3	0.205	0.6692	0.0205	0.0306	None	
22	8	Uncoated	2200	20	60.0	0.206	0.6828	0.1203	0.1762	17.5	
23	9	Coated	2200	20	30.0[2]	0.2240	0.7241	0.1825	0.2520	14.3	Did not fail specimen length - 3.010 inches. Final specimen length - 3.342 inches.

1 - Did not fail at 100 hours.

2 - Did not fail.

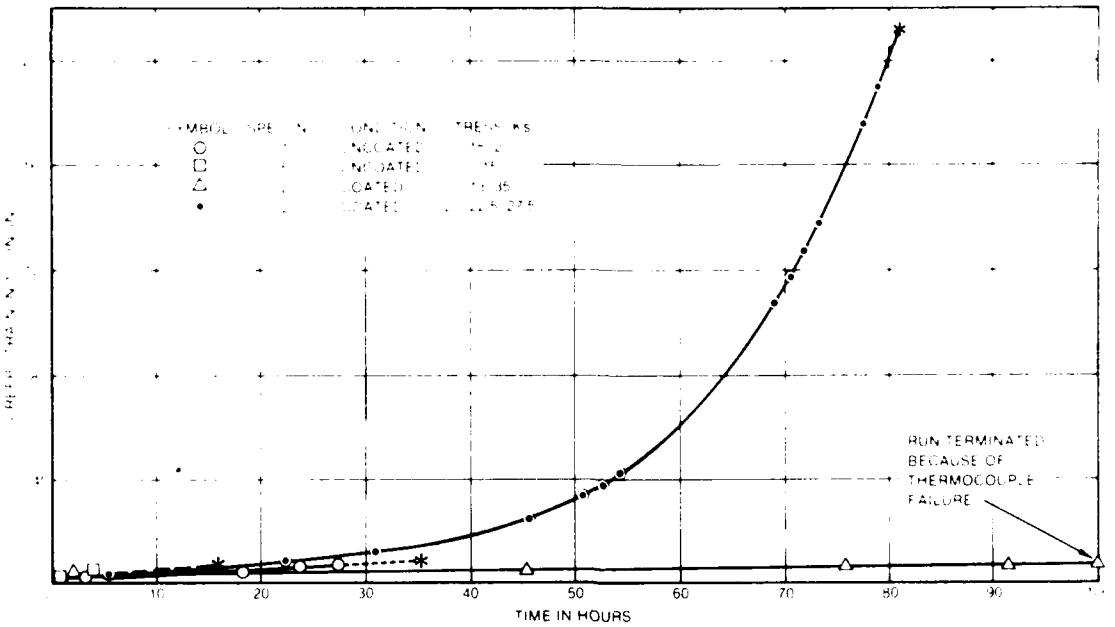

Figure 53. Creep Rates of C129Y Specimens at 2000°F

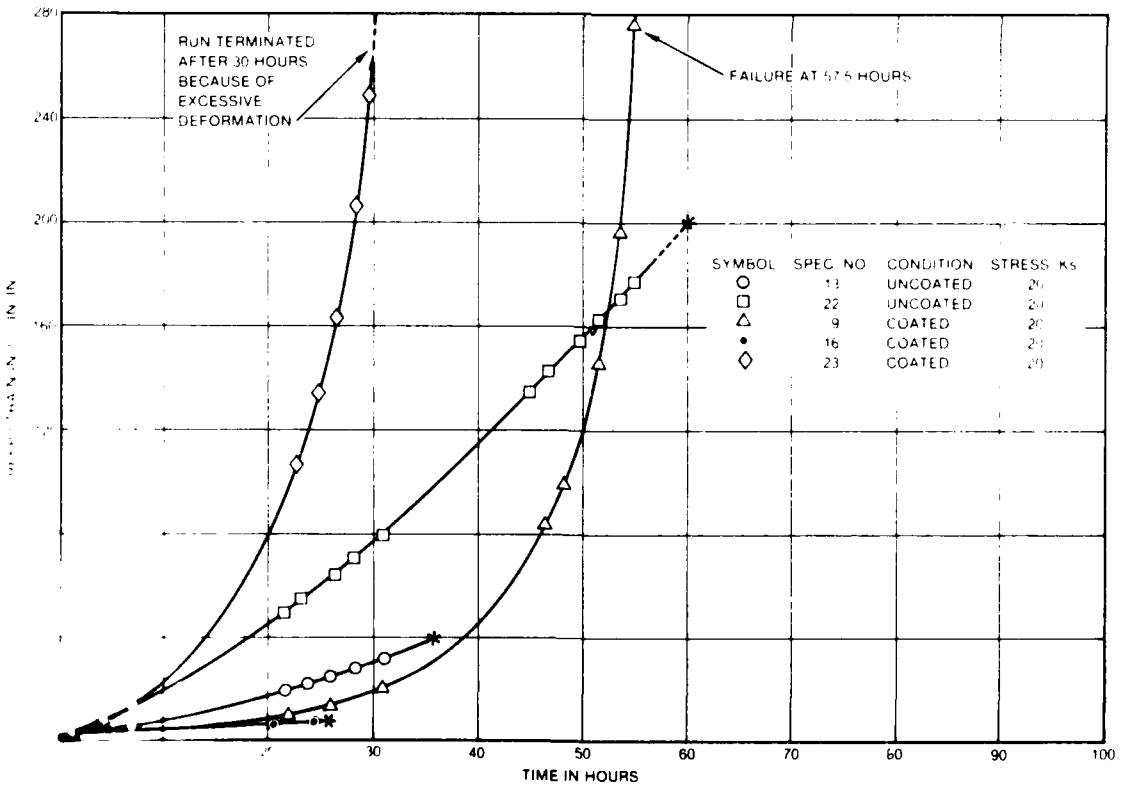

Figure 54. Creep Rates of C129Y Specimens at 2200°F

The curves in Figure 54 seem to be almost linear for uncoated bars while the creep rates changed from second- to third-stage before failure occurred. The scatter in stress-rupture life suggests an inhomogeneity in the base metal. However, in spite of the scatter, results did demonstrate equivalency in stress-rupture lives for both coated and uncoated specimens.

4.3.3 Furnace Oxidation Testing

Eight coated specimens were prepared for static oxidation testing at furnace temperatures of 760 and 1093°C (1400 and 2000°F). Weight changes monitored are reported in Table 23. Specimens 1 through 4, which were exposed to air at 760°C, typically exhibited weight gains of less than 1 mg/cm^2 while the specimens tested at 1093°C, Nos. 5 through 8, gained up to 2 mg/cm^2 during the 5500-hour test. The data points are plotted in Figure 36 and generally, two trends can be detected. The 760°C specimens fall in an envelope which appear to level off around 0.5 mg/cm^2. The upper band represents the 1093°C specimens which have a greater spread. The kinetics of chemical reaction and transport (diffusion) phenomena are dependent on temperature and, therefore, proceed at a greater rate at the higher temperature. At elevated temperature, it is believed that oxidation proceeds in a parabolic manner while at lower temperature, the trend tends to be exponential (Ref. 9). In this case, the stabillity and crystal structure of the SiO_2 scale formed at each temperature will determine the rate of oxidation as lattice defects will promote diffusion and enhance the rate of oxidation. Under the nominally static conditions (minimal thermal cycling), the NS-4 coating at 760°C appeared to be highly protective with no evidence of "pesting" previously noted. This could be indicative of relatively slower formation of SiO_2 resulting in a dense, adherent scale, impervious to O_2 diffusion during the long uninterrupted time periods between weighing.

Table 23

Weight Change Data for Furnace Oxidation Test Specimens

Specimen Number	Temperature (°C)	Weight Change at Inspection (mg/cm^2)							
		1015 Hours	1259 Hours	1491 Hours	2132 Hours	3402 Hours	4314 Hours	4841 Hours	5561 Hours
1	760	0.39	-	0.41	0.41	0.36	0.43	-	0.56*
2	760	0.40	-	0.33	0.38	0.36	0.50	0.56*	-
3	760	0.39	-	0.43	0.41	0.39	0.51**	-	-
4	760	0.42	0.33*	-	-	-	-	-	-
5	1093	0.98	-	1.00	1.17	1.47	1.73	-	2.07*
6	1092	1.35	1.35*	-	-	-	-	-	-
7	1093	1.12	-	1.07	1.16	1.48	1.74	1.74*	-
8	1093	1.05	-	1.09	1.27**	-	-	-	-

* Removed for metallography
** Damage in handling

Figures 55 and 56 show the physical appearance of coated specimens. Note that no surface penetration was observed and no evidence of coating failure was found at any time. The excellent appearance after 5561 hours at both temperatures is indicative of the remarkable durability of this coating under static isothermal conditions.

A total of six specimens taken at various times from the test were prepared for metallographic analyses. Typical microstructures are shown in Figures 57 and 58 with baseline microstructures of an as-coated specimen shown in Figure 59. The as-coated specimen exhibited a narrow interface region; with thermal expansion, especially at the higher temperature, the interfacial band increased noticeably. (The lateral cracks observed in the interface are probably caused by stresses induced during cutting.) The cracking in the coating, normal to the plane of the surface, is typically found in this coating as a result of thermal mismatch.

Comparison of coating microstructures reveal that with increasing exposure, porosity in the coating also increases. Close examination shows that in the porous outer portions of the coatings, two phases can be noted - a light grey phase and a darker, mottled grey phase. Energy dispersive X-ray analysis indicated the presence of columbium in the latter dark grey phase together with greater quantities of vanadium and titanium. The lighter grey phase had an X-ray energy spectrum very similar to the standard NS-4 coating. Therefore, it can be assumed that with thermal exposure, columbium diffused outward from the substrate into the coating and concentrated around coating porosity, probably contributing to oxide formation and thus reducing the effectiveness of the SiO_2 scale.

The primary difference between the two sets of microstructures (Figs. 57 and 58) is the slightly narrower interfacial band (as a result of lower reaction rates) and the relatively greater areas of the light grey coating phase on the 760°C specimens.

In order to study the compositional changes in the coating during oxidation exposure, a series of EDX elemental line scans were performed. The six sets of profiles are shown in Figures 60 through 65. The vertical axes shown are only indicative of the increasing trend in concentration. No attempt was made to directly quantitize the concentration of each element. Molybdenum was not shown because of the >50 percent overlap of the molybdenum L-lines with columbium, and since columbium had the stronger signals, L-lines of molybdenum were completely masked.

The elemental profiles for test specimens at 760°C show that, initially, silicon was found throughout the coating, and at the end of 5561 hours, a definite gradient can be noted as silicon was consumed to form surface oxides and also by diffusion into the substrate. In the case of titanium and vanadium, there was little noticeable difference in concentration distribution across the coating. the columbium scan showed a trend opposite to the of silicon; with increasing exposure times, columbium diffused into the coating, as did hafnium. However, after 5561 hours, the retention of hafnium in the coating appeared to have leveled off. Tungsten was initially randomly

As-Coated (No. 1) | 1015 Hours (No. 1) | 4841 Hours (No. 2) | 5561 Hours (No. 1)

Figure 55. Surface Appearance of NS-4 Coated Oxidation Specimens After Various Exposure Times at 760°C

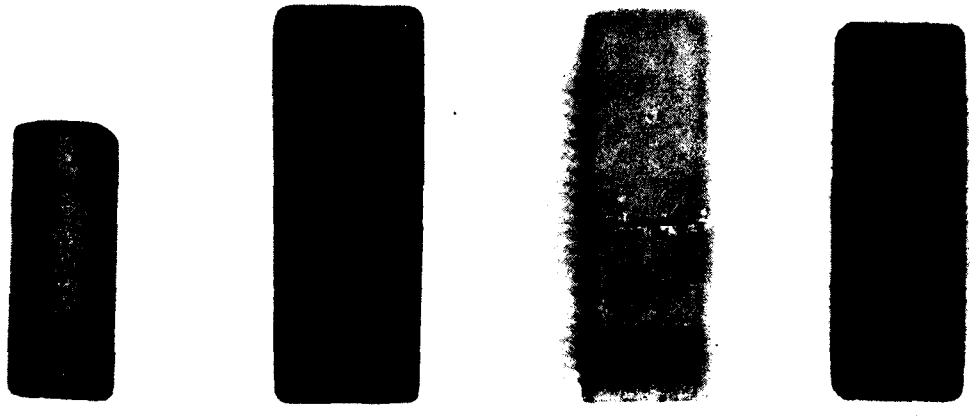

As-Coated (No. 8) | 1015 Hours (No. 7) | 4841 Hours (No. 7) | 5561 Hours (No. 5)

Figure 56. Surface Appearance of NS-4 Coated Oxidation Specimens After Various Exposure Times at 1093°C

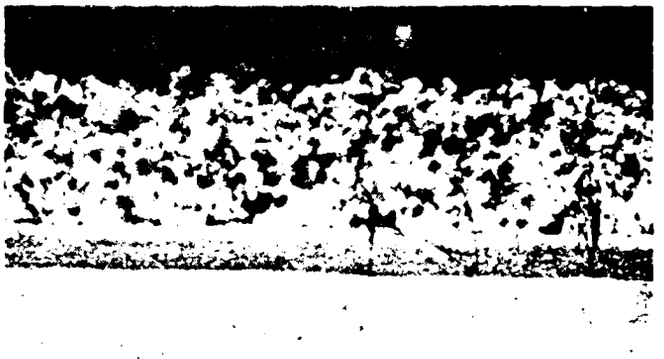

A. Specimen No. 4 After 1259 Hours

Magnification: 200X

B. Specimen No. 2 After 4841 Hours

Magnification: 250X

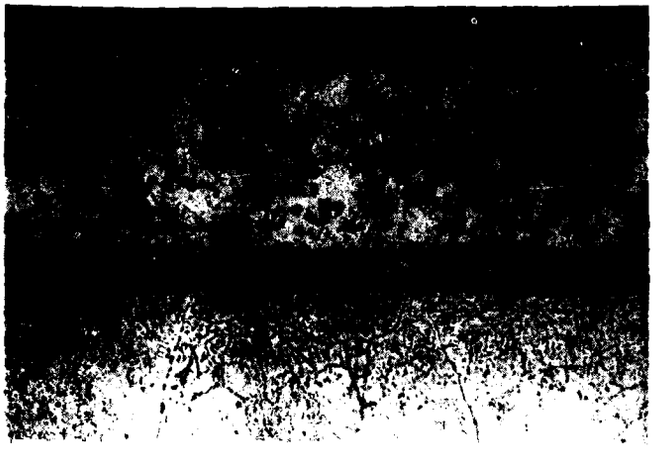

C. Specimen No. 1 After 5561 Hours

Magnification: 250X

Figure 57. Microstructures of NS-4 Coated C129Y Specimens After Oxidation Testing at 760°C; Hf-HNO_3-Lactic Etch

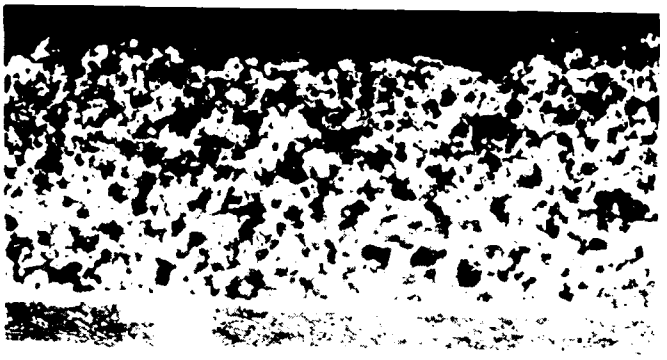

A. Specimen No. 6 After 1259 Hours

Magnification: 200X

B. Specimen No. 7 After 4841 Hours

Magnification: 250X

C. Specimen No. 5 After 5561 Hours

Magnification: 250X

Figure 58. Microstructures of NS-4 Coated C129Y Specimens After Oxidation Testing at 1093°C; Hf-HNO_3-Lactic Etch

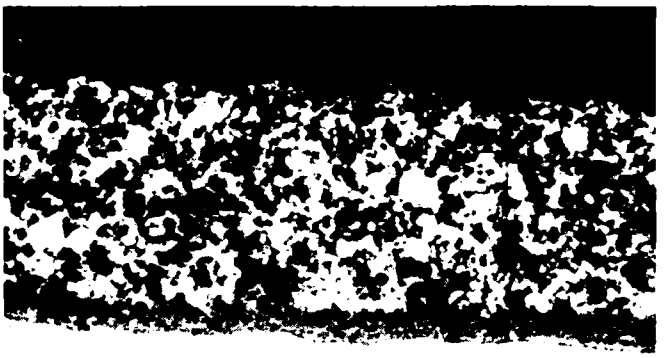

As-Coated

Hf-HNO_3-Lactic Etch

Magnification: 250X

Figure 59. NS-4 Coated C129Y Specimen in As-Coated Condition; With Pre-Oxidation

distributed in the coating but in time, there appeared to be a definite concentration near the coating surface, indicating a possible role in stabilizing the oxide scale.

A similar study of the X-ray line scans for the 1093°C specimens (Figs. 63-65) revealed characteristics of the elemental distribution that correspond to the 760°C specimens. An interesting feature can be noted in the hafnium substrate scan region where theundulating concentration can be related to the presence of hafnium-rich 'nodules' in the alloy grain boundary. Figure 66 is a high magnification SEM photo of the grain boundary typically found in all test specimens regardless of test parameters. Referring to the SEM photomicrographs in Figures 60 through 65, the same light intergranular markings of hafnium can also be distinguished. Since hafnium formes a series of continuous solid solution with columbium, a possible explanation of this discrete hafnium precipitate is that during casting, insufficient heat was provided to produce the super heated alloy melt and, therefore, hafnium could have been precipitated.

Further evidence of hafnium was found in specimen No. 2 (Fig. 67) which had two large agglomerations of hafnium, with a substrate matrix studded with dark grey hafnium precipitates. Alongside the hafnium agglomerate was also found shrinkage porosity. It is not clear from the photomicrograph as to the effect of the porosity and hafnium on coating/substrate integrity, but since no coating failure was noted in the test, the effects could not be significant in an isothermal situation.

Finally, microhardness measurements (100g load) were taken and the results show (Table 24) that the interface was an extremely hard and brittle layer and some hardening of the substrate next to the coating was noted. The C129Y alloy itself tends to be somewhat less brittle with increasing exposure.

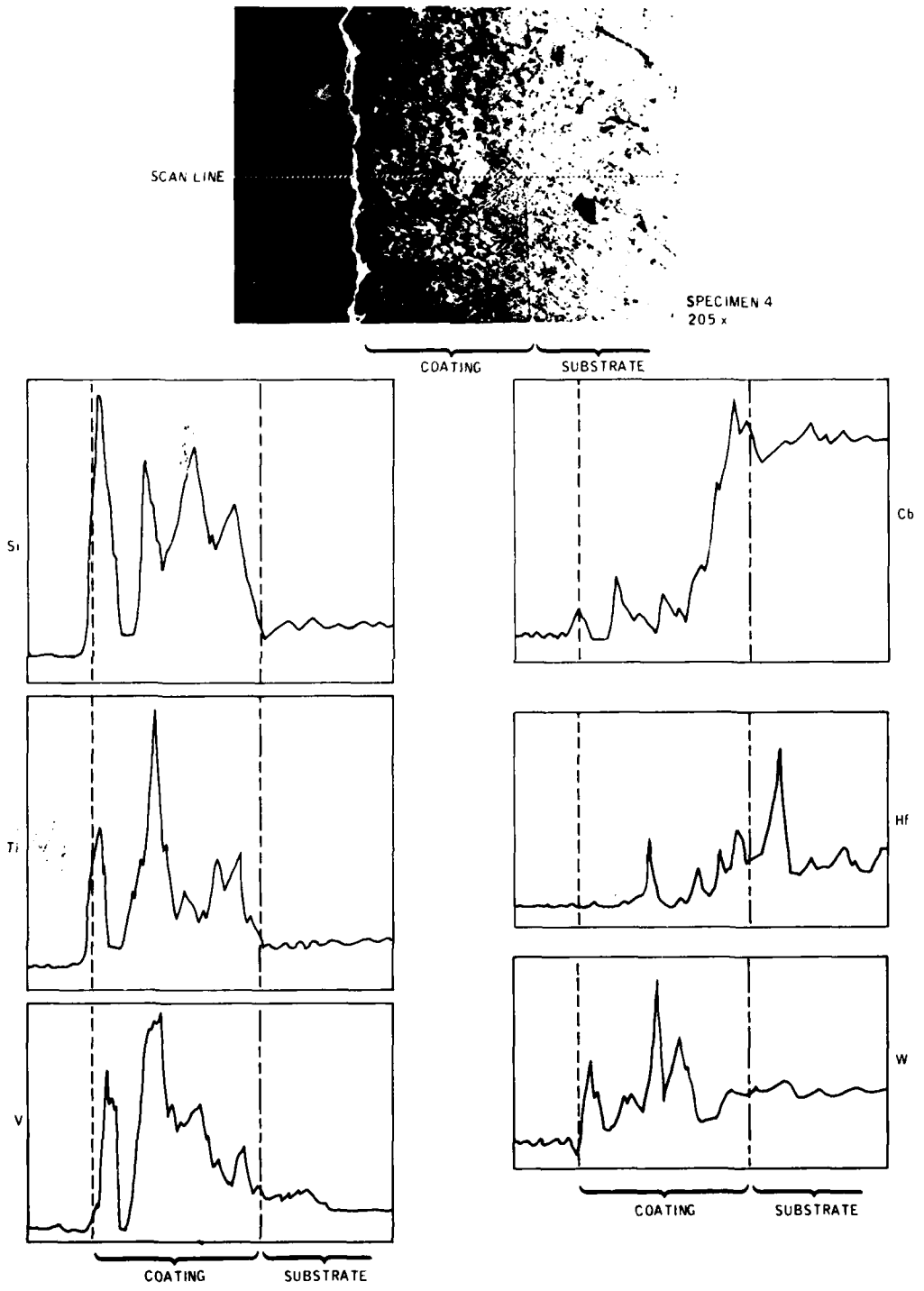

Figure 60. EDX Elemental Line Scan of Oxidation Specimen No. 4 After 1259 Hours at 760°C; Magnification: 205X

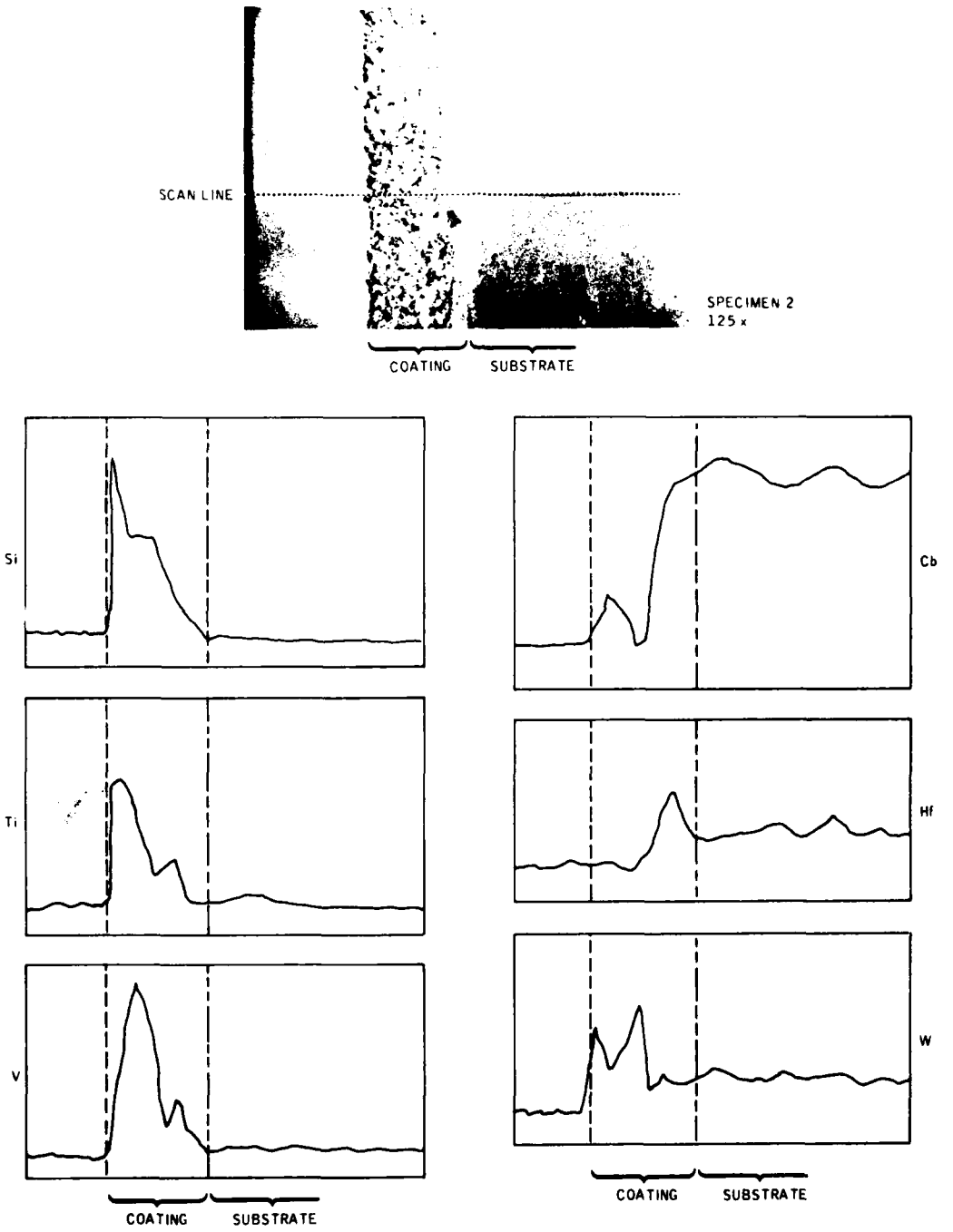

Figure 61. EDX Elemental Line Scan of Oxidation Specimen No. 2 After 4841 Hours at 760°C; Magnification: 115X

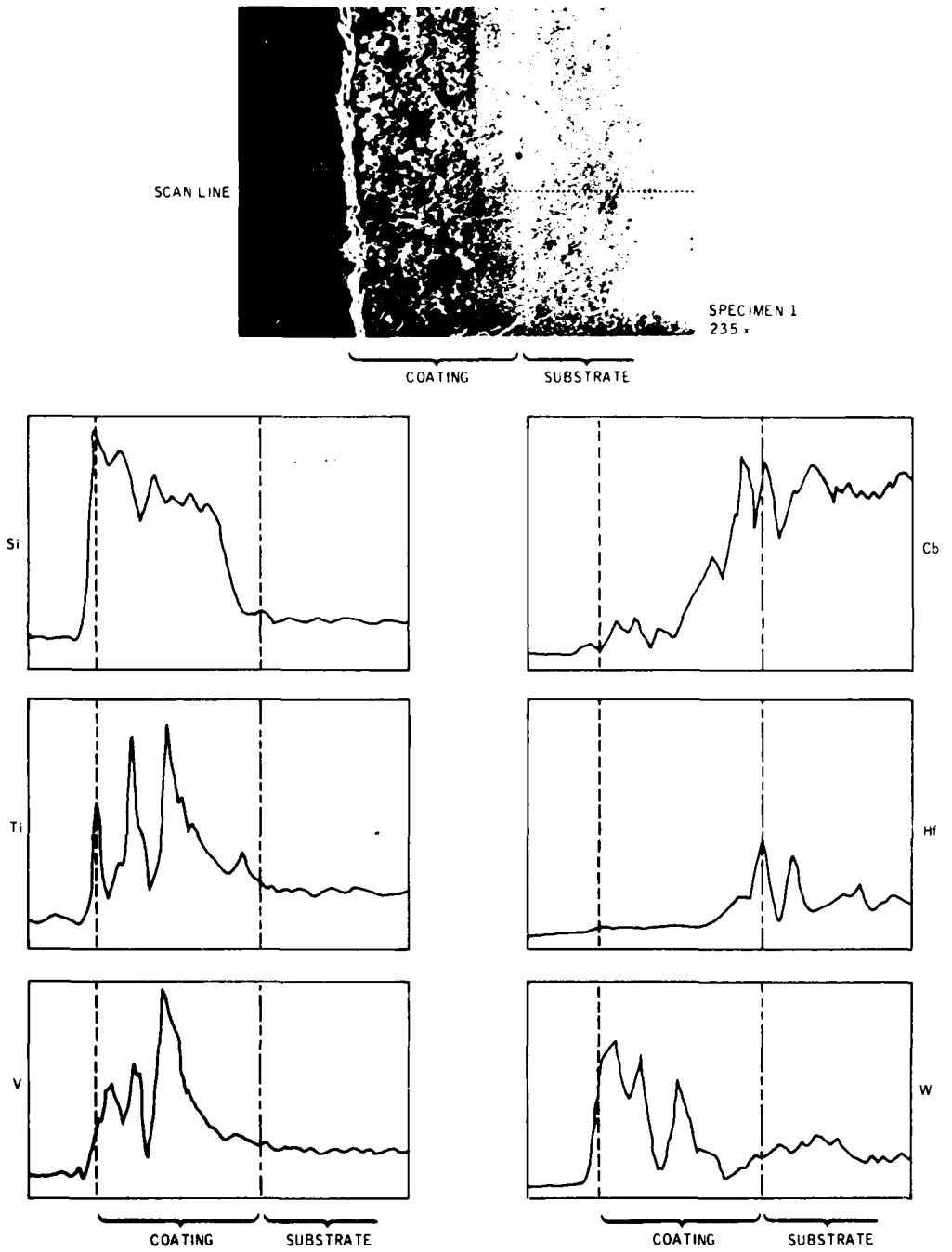

Figure 62. EDX Elemental Line Scan of Oxidation Specimen No. 1 After 5561 Hours at 760°C; Magnification: 235X

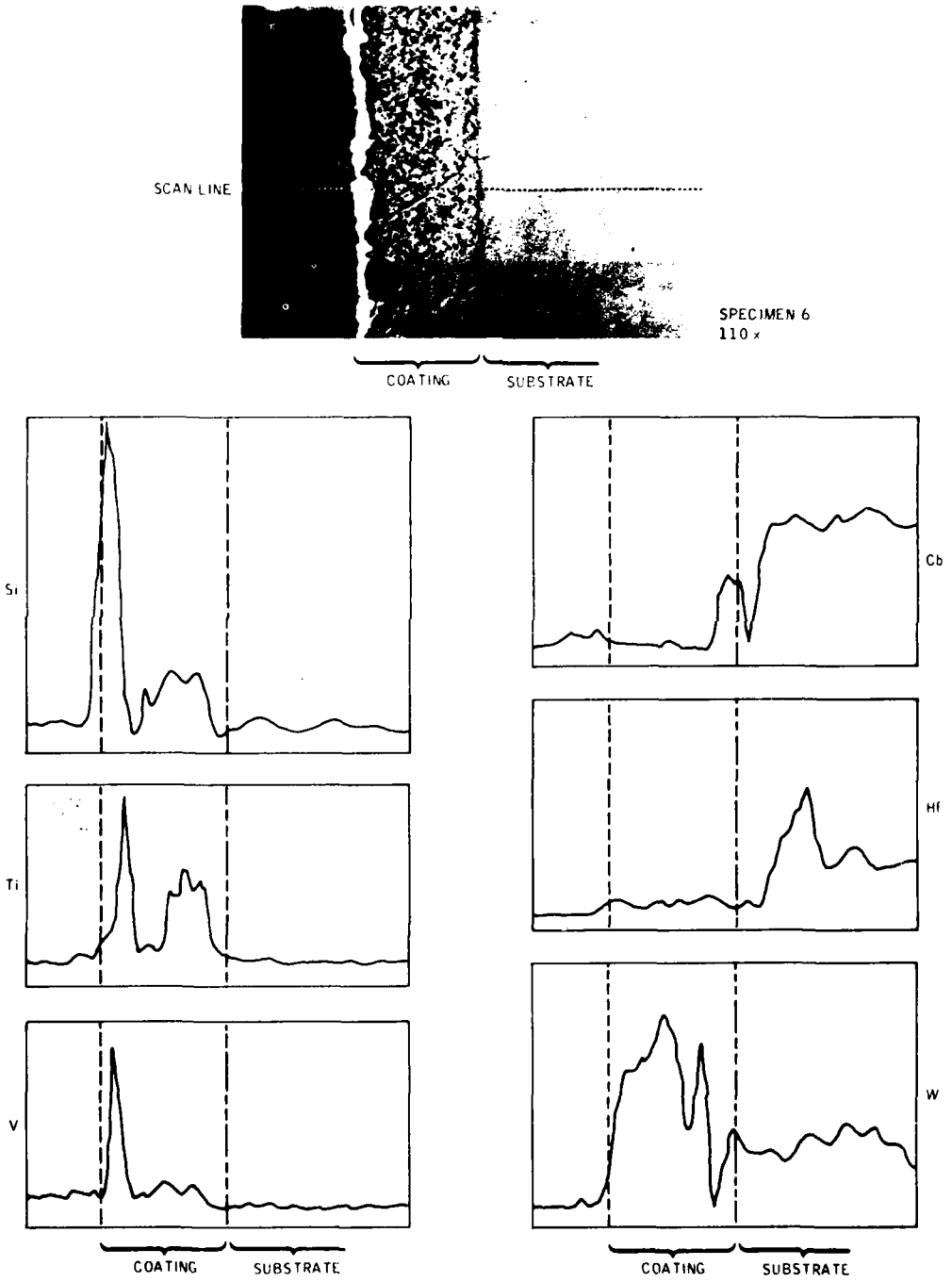

Figure 63. EDX Elemental Scan of Oxidation Specimen No. 6 After 1259 Hours at 1093°C; Magnification: 110X

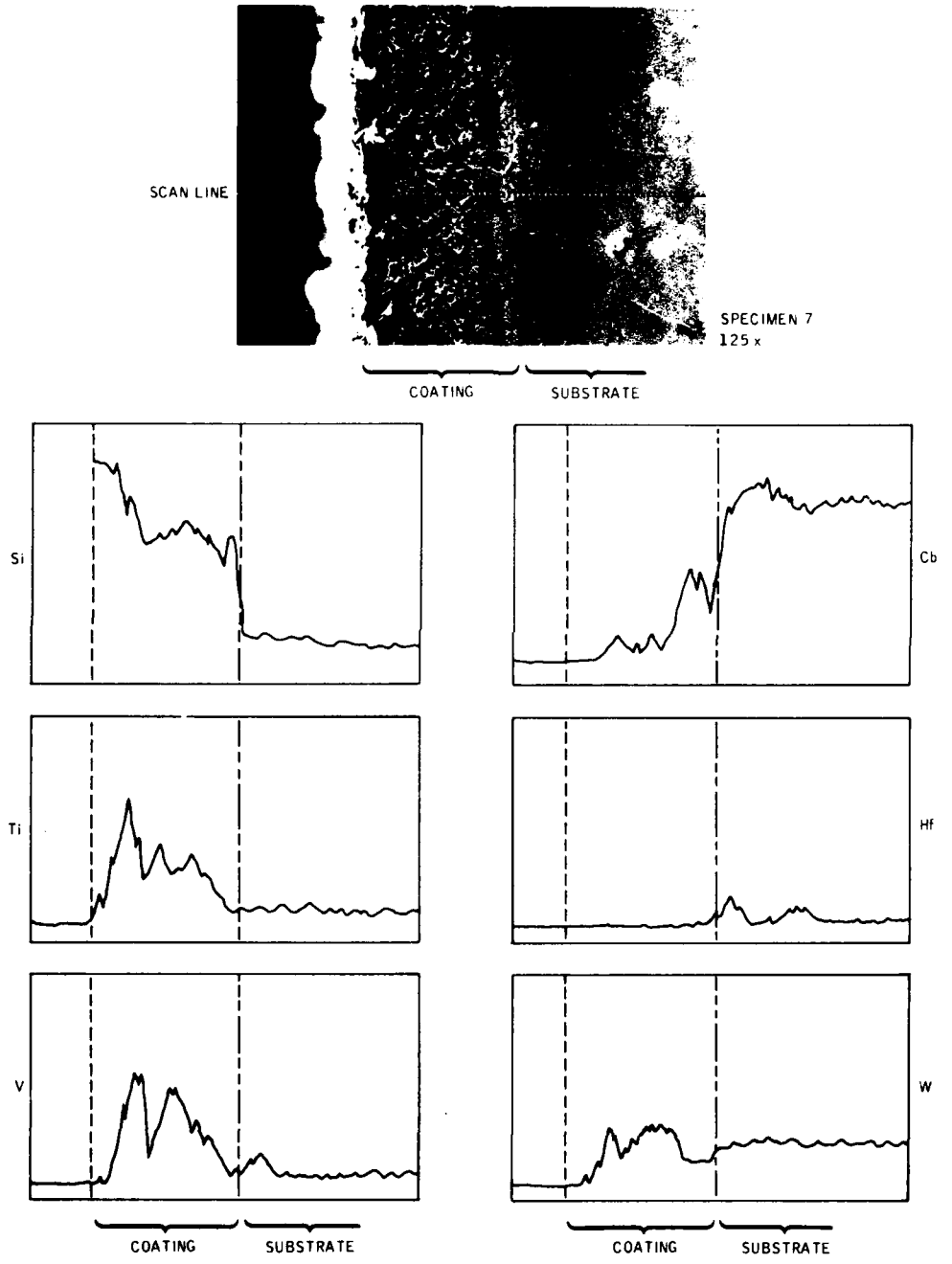

Figure 64. EDX Elemental Line Scan of Oxidation Specimen No. 7 After 4841 Hours at 1093°C; Magnification: 125X

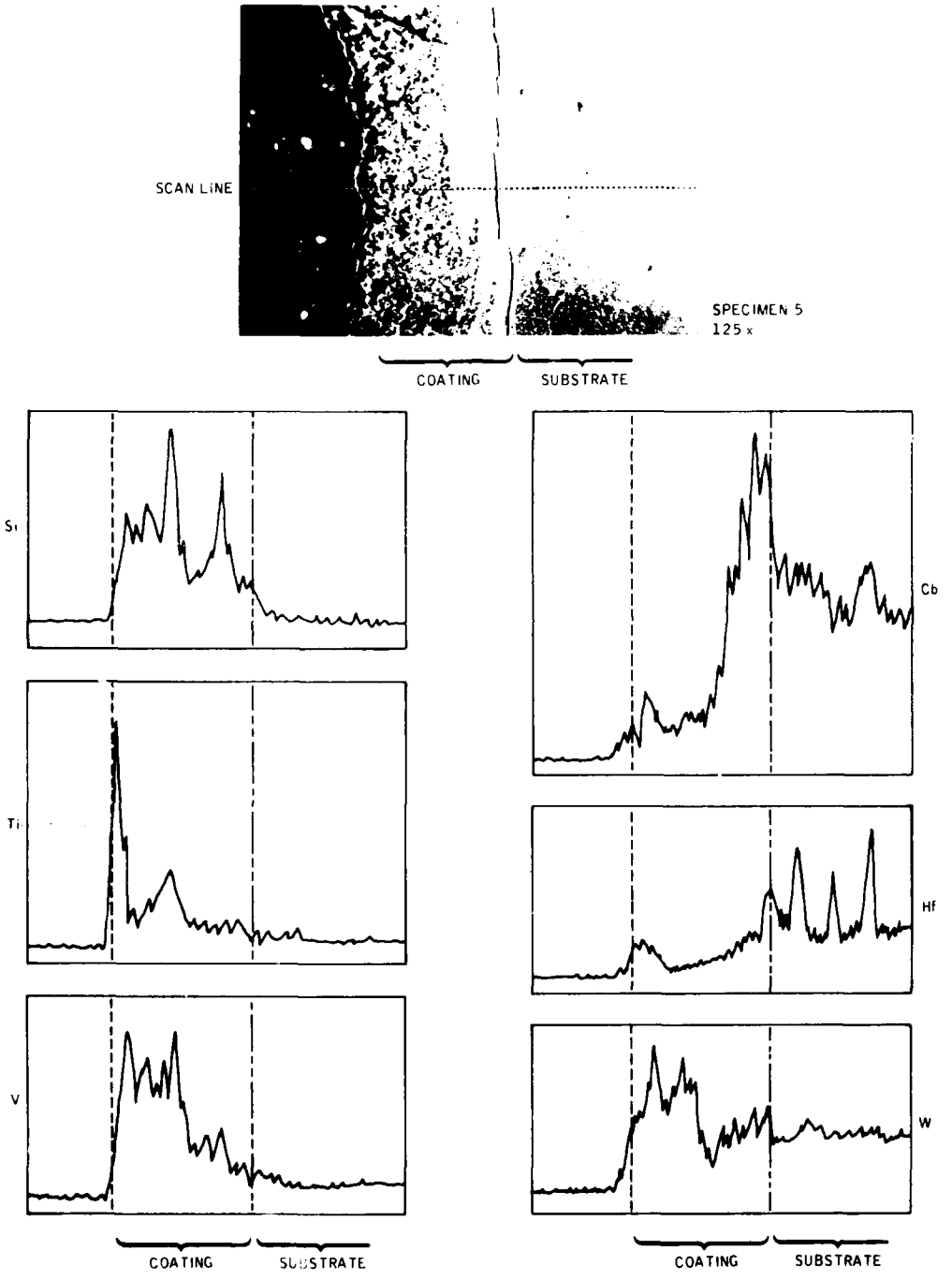

Figure 65. EDX Elemental Line Scan of Oxidation Specimen No. 5 After 5561 Hours at 1093°C; Magnification: 125X

Specimen No. 4

Magnification: 4500X

Figure 66. Hafnium-Rich Areas in the Alloy Grain Boundary

Table 24

Microhardness(KHN-100g Load) Measurements of C129Y Oxidation Specimens

Specimen Number	Exposure (hrs)	Temperature (°C)	Microhardness (KHN)		
			Interface	Substrate Near Interface	Alloy
4	1259	760	1350	280	260
2	4841	760	1230	280	230
1	5561	760	1390	250	250
6	1259	1093	1500	270	270
7	4841	1093	1540	230	250
5	5561	1093	950	230	210

AD-A086 128 SOLAR TURBINES INTERNATIONAL SAN DIEGO CA F/G 11/6
COMPLEX, PRECISION CAST COLUMBIUM ALLOY GAS TURBINE ENGINE NOZZ--ETC(U)
APR 80 L HSU, W G STEVENS, A R STETSON DAAG46-76-C-0053
UNCLASSIFIED SR80-R-4444-25 USAAVRADCOM-TR-80-F-2 NL

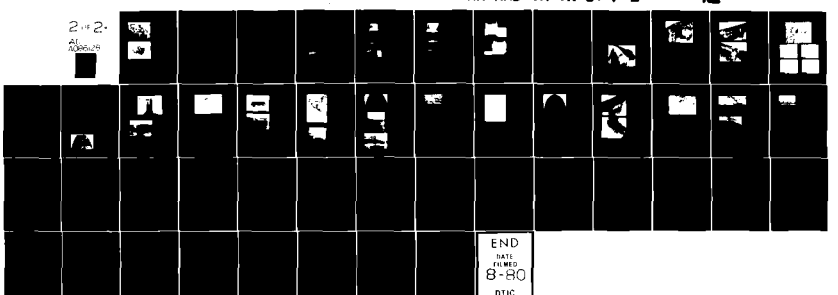

A. Light Microscopy

Magnification: 250X

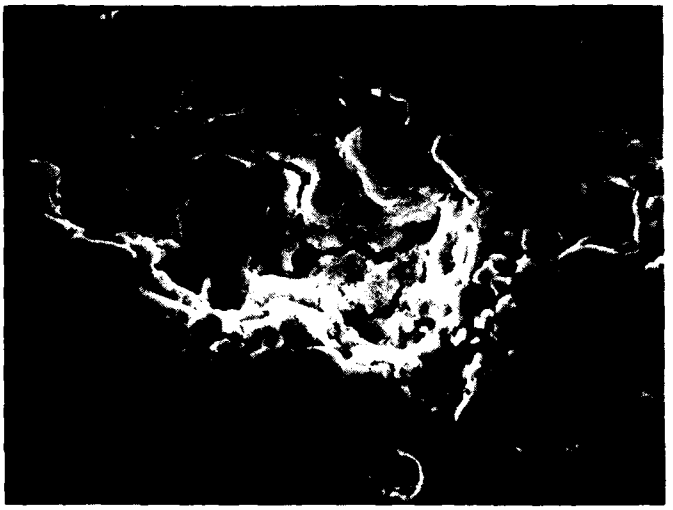

B. Shrinkage Porosity

Magnification: 1050X

Figure 67. SEM Photomicrographs of Inhomogeneous Substrate Areas on Specimen No. 2 Showing Hafnium Agglomeration and Porosity; 4841 Hours at 760°C

4.3.4 Dynamic Oxidation Burner Rig Testing

The objective of the burner rig oxidation test was to subject the NS-4 coated C129Y single vane segment to the hot combustion gases such that the leading edge temperature was at 1315°C (2400°F). The thermal cycle of 50 minutes at temperature followed by 10 minutes rapid cooldown induced thermal stresses that can severely tax the coefficient of thermal expansion mismatch between the NS-4 coating and the substrate. Since the combustor nozzle is only 2.5 cm in diameter, only the center of the leading edge was maintained at the desired test temperature while the rest of the airfoil and the side walls were cycled through different thermal cycles, depending on the mass, distance from the flame and radiation heat losses. The varying temperatures throughout the specimen were not monitored due to poor visibility through the viewing slit, excepting the mid airfoil and trailing edge temperatures which were visible to the radiation pyrometer. Measurements taken indicate that the 1315°C leading edge temperature produced temperatures of approximately 1200 and 1090°C at the mid-chord and trailing edges, respectively.

Results

A total of four specimens were tested with the results shown in Table 25. Specimens 6-2 and 1-3 were processed conventionally (1515°C/3 hours sinter, 1149°C/8 hours siliciding) while the last two, specimens 5-3 and 3-4, had the eight-hour sintering cycle. The first specimen tested, No. 6-2, was cycled for 10 hours before the specimen fixture failed and caused the airfoil to be carried upward by the high-velocity gas stream and thrown against the walls of the exhaust stack. The airfoil itself sustained minimal visual damage but this test was terminated. Figure 68 showed that the leading edge was still sound, although some coating breakthrough was noted at the sidewalls.

A second specimen, No. 1-3, was installed in a modified fixture assembly which necessitated the attachment of an "appendage" to the sidewall, as shown in Figure 69. Specimen 1-3 survived 57 hours of testing before leading edge failure was obtained. Upon removal from the nozzle plate, several areas of coating penetration were found on the side wall and "appendage" areas. The "appendage" failures were disregarded as they were caused by high loading levels imparted by the fixture screws to ensure secure installation. Optical examination of the leading edge failure revealed streaking of what appeared to be a liquid phase product down both convex and concave sides of the leading edge. This observation led to a decision to increase vacuum sintering time for subsequent specimens in order to minimize the lower melting, higher vapor pressure elements such as vanadium and titanium.

Specimens No. 5-3 and 3-4 were tested and survived 66 and 132 hours, respectively. The visual appearances are shown in Figures 70 and 71. Leading edge failure on specimen No. 5-3 was significant and areas on the side walls also suffered slight damage. Specimen No. 3-4 showed minimal damage at the leading edge and coating spallation on the affixed appendage areas with the side wall attack also noted on other vanes (Fig. 71).

Table 25

1315°C Burner Rig Test Results

Specimen Number	Number of Hours Exposed	Failed Area
6-2	10	Side walls
1-3	57	Leading edge and side walls
5-3*	66	Leading edge and sidewalls
3-4*	132	Discoloration at leading edge and side wall failure

* Sintering cycle was 8 hours instead of 3 hours at temperature

Before proceeding to a discussion of metallographic, SEM and EDX analyses of the specimens, some thought should be given to the repeated side wall failure found in all specimens. These side wall failures were invariably found on the corners of both inboard and outboard walls. Close scrutiny of the convex sides of all four specimens show failure on the outboard corner (<90°angle) adjacent to the leading edge. Another location highly susceptible to coating spallation and failure was found on the inboard corner (>90° angle) near the trailing edge.

It is not possible without additional information to explain fully the cause of these coating failures. However, two factors which may have contributed to the failures are mentioned here:

1. Configuration Factor - Previous work with NS-4 (and other thick overlay coatings) has shown that specimen edges are much more prone to spallation due to configuration aggravated trailing edge mismatch during thermal transients, as illustrated in Figure 70. The oxide layer formed at the coating surface is strained similarly, resulting in rapid oxide spallation and consumption of the coating to replenish the surface oxides.

A. Concave Surface

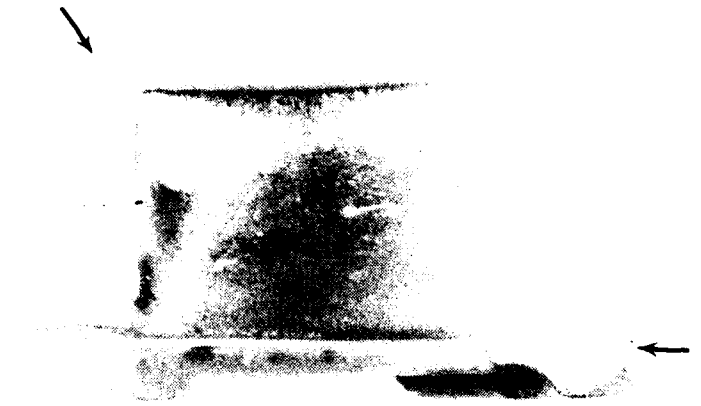

B. Convex Surface

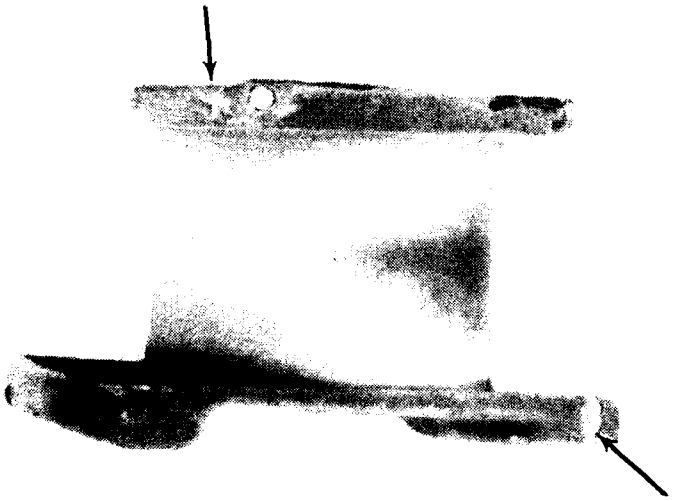

Figure 68. NS-4 Coated Test Specimen No. 6-2 After 10 Hours of Burner Rig Testing (Arrows Show Failed Areas)

A. Concave Surface

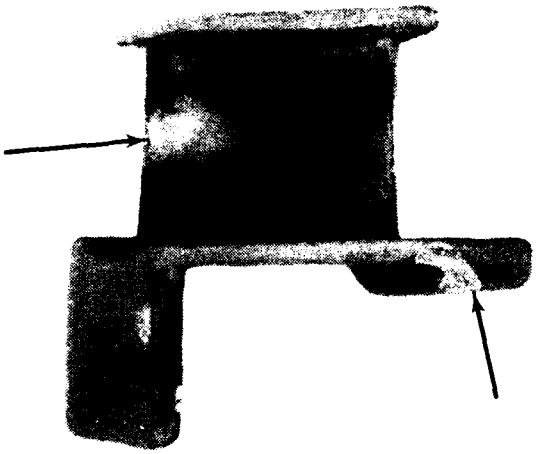

B. Convex Surface

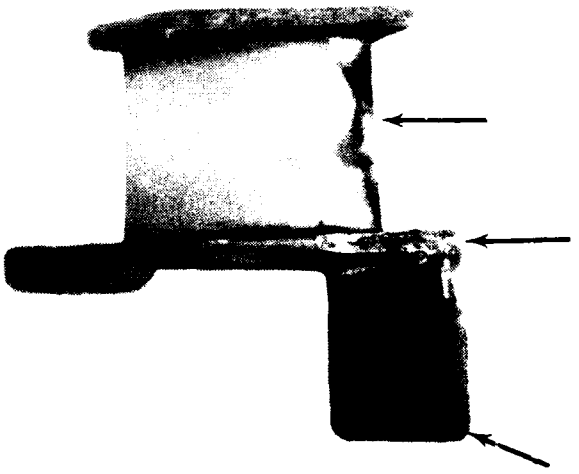

Figure 69. NS-4 Coated Test Specimen No. 1-3 After 57 Hours of Burner Rig Testing (Arrows Show Failed Areas)

A. Concave Surface

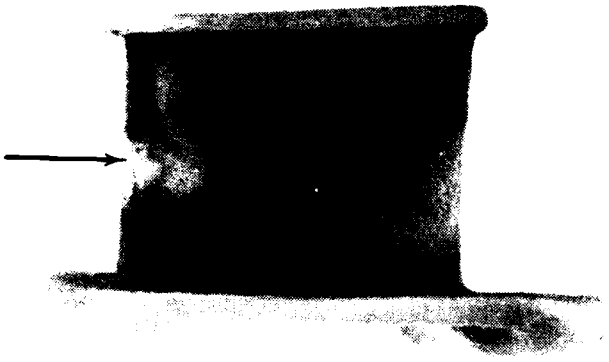

B. ConveX Surface

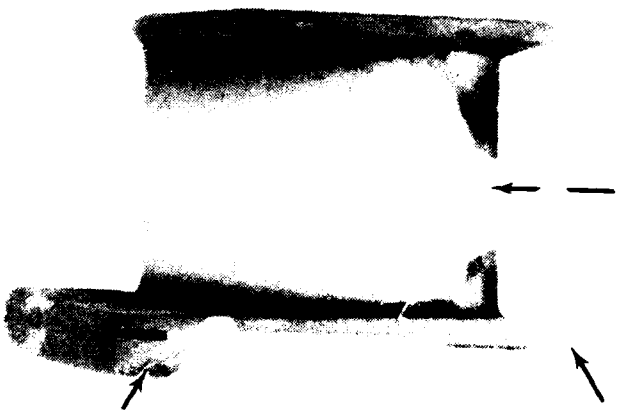

Figure 70. NS-4 Coated Test Specimen No. 5-3 After 66 Hours of Burner Rig Testing (Arrows Show Failed Areas)

A. Concave Surface

B. Convex Surface

Figure 71. NS-4 Coated Test Specimen No. 3-4 After 132 Hours of Burner Rig Testing (Arrows Show Failed Areas)

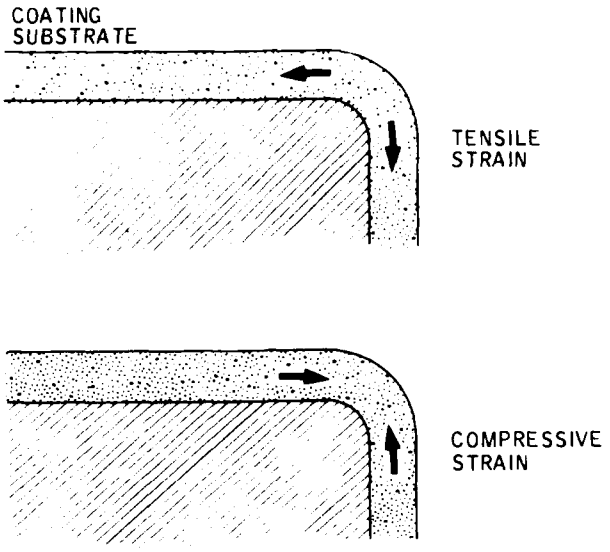

Figure 72. Schematic of Tensile and Compression Strains Induced at a Specimen Edge During Thermal Cycling

2. Equilibrium Temperature Factor - Radiation convection heat losses from areas not directly exposed to the hot gas stream may have imposed considerable temperature gradients at the side walls. As previously mentioned, no measurements were taken of temperature in these cooler areas but visual sightings through the viewing slit during testing revealed that the trailing edge corners were below the infrared emittance level while the corner near the leading edge end on the outboard side was highly emittive. Based on visual inspection, a thermal profile, such as in Figure 73, may have been in effect. Other than the "pest" temperatures of 649°C (1200°F) to 760°C (1400°F), little is known about the low temperature (<645°C) performance of the coating. Therefore, since the NS-4 coating was optimized for high temperature use and not for cooler temperatures, it may have failed rapidly at the cooler locations.

Specimen No. 6-2 (10 Hours)

This specimen was exposed to only 10 hours of testing and little useful information can be gleaned from the part. The most interesting item noted was the small circular failure noted at the outboard corner, see Figure 67(B). The oxidation process had just initiated and a 45X picture taken on the SEM shows a pit at the very tip of the corner, Figure 74. Energy dispersive analysis, Figure 75, indicated that light colored areas A at the bottom of the pit was a final remnant of coating in the alloy matrix. B marks the "walls" of the pit and the exposed C129Y alloy. Near the 'rim' of the pit, marked by C, are fibrous stringers which were found to be mostly silicon

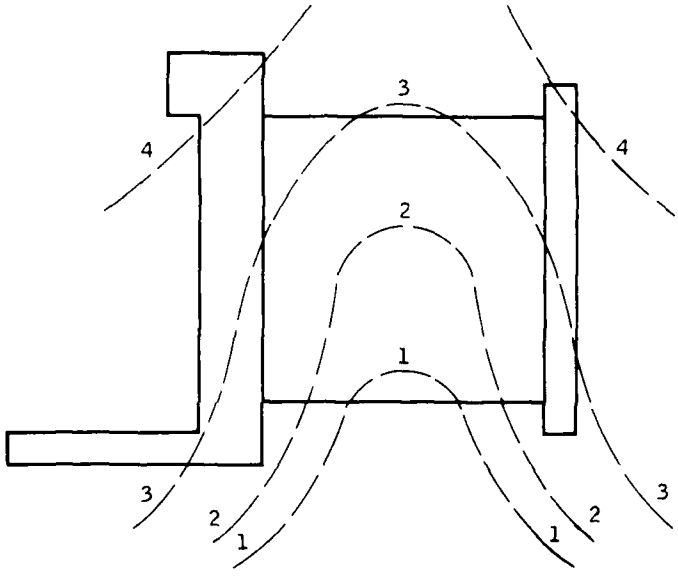

Figure 73.

Sketch of Hypothetical Isotherms Showing Thermal Profile of Vane During Rig Testing

1 = HOT TEST ISOTHERM
4 = COOLEST ISOTHERM

Figure 74. Low Magnification (17X) of SEM Photo of Failed Area on Specimen No. 6-2

(probably SiO_2) with some titanium. The area indicated by D is silicided substrate exposed to the environment and E points to the dark gray coating surface (in contrast to coating surfaces further away which are lighter in color) which has notable amounts of hafnium and columbium in the energy spectrum typical of NS-4.

Figure 75. High Magnification (45X) SEM Photograph of Failed Area of Specimen No. 6-2

To summarize the morphology of coating failure, as seen above, the pit is primarily exposed substrate with traces of coating entrapped at the bottom. Moving up the side of the 'pit', which is still exposed C129Y alloy, fibers of SiO_2 are found. As the 'rim' is approached, the alloy changes to silicided C129Y. Past the 'rim', there is a ring of darkened coating which is columbium and hafnium contaminated NS-4. Beyond that,the NS-4 coating is unaffected.

Specimen No. 1-3 (57 Hours)

The failed leading edge was viewed on both concave and convex sides as shown in Figure 76. Note that dark streak were found on both sides which appear to be liquid phase swept past the leading edge by the high-velocity gases. A closeup picture of the streaking is shown in Figure 77. Electron dot mapping of this particular region is also shown for the elements columbium, silicon, titanium and molybdenum. The electron images indicate that the dark areas contain columbium and molybdenum with a little silicon. The possibility of liquid phase formation at 1315°C or lesser could be attributed to eutectics of oxides such as MoO_3-WO_3 and Nb_2O_5-WO_3. The binary phase diagrams are shown in Figures 78 and 79 (Ref. 6). Molybdenum oxide is a oxide is a low-melting compound and the presence of up to 2 mole percent WO_3 depresses the melting point even further to 770°C. The Nb_2O_5-WO_3 is a much higher melting system but the eutectic formed at 1340°C could also produce localized liquid phase in WO_3-rich areas in the presence of Cb_2O_3.

A. Concave View

Magnification: 12X

B. Convex View

Magnification: 12X

Figure 76. SEM Photomicrograph of Leading Edge Failure of Specimen No. 1-3

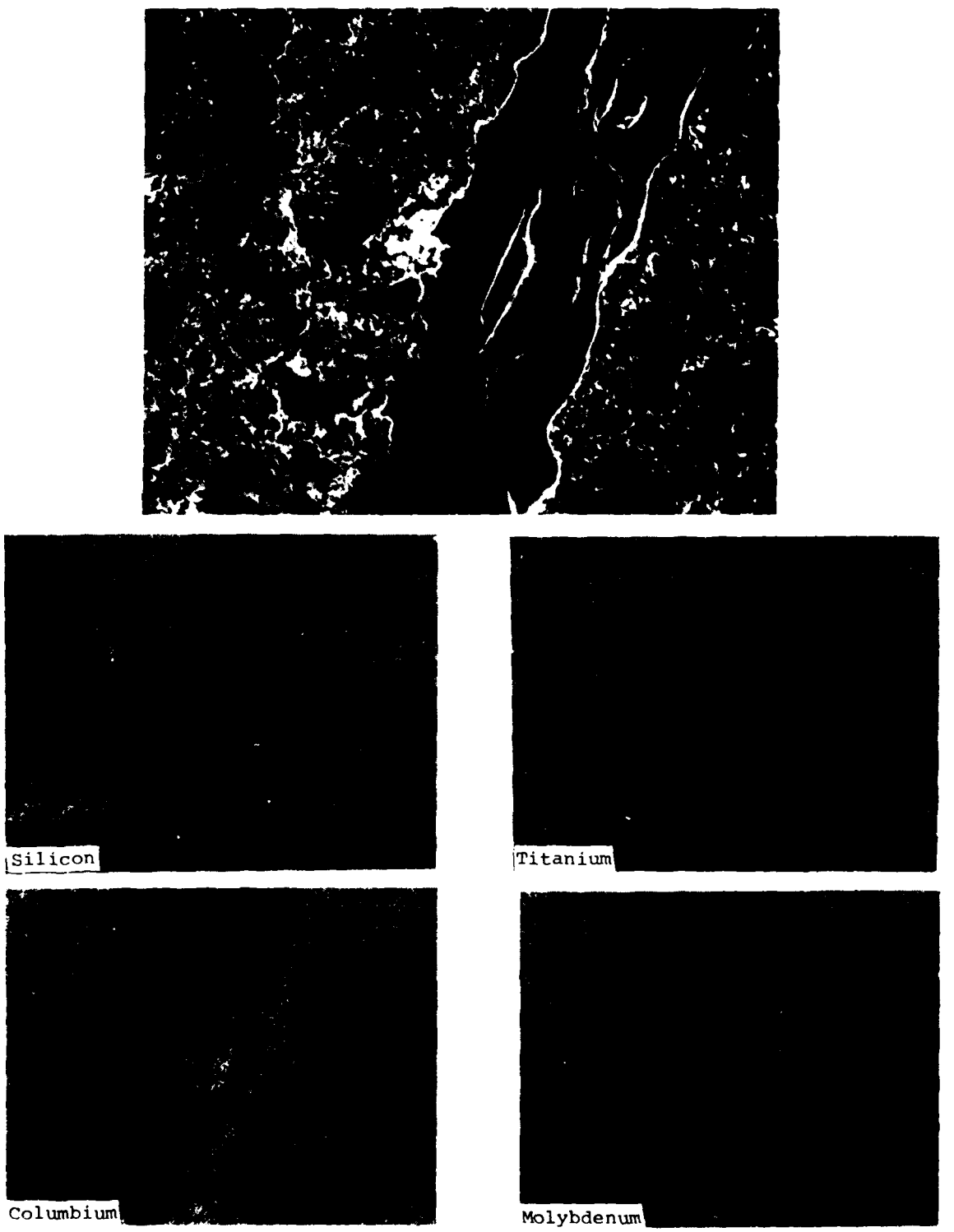

Figure 77. Dark Streaking on Convex Side of Leading Edge of Specimen No. 1-3

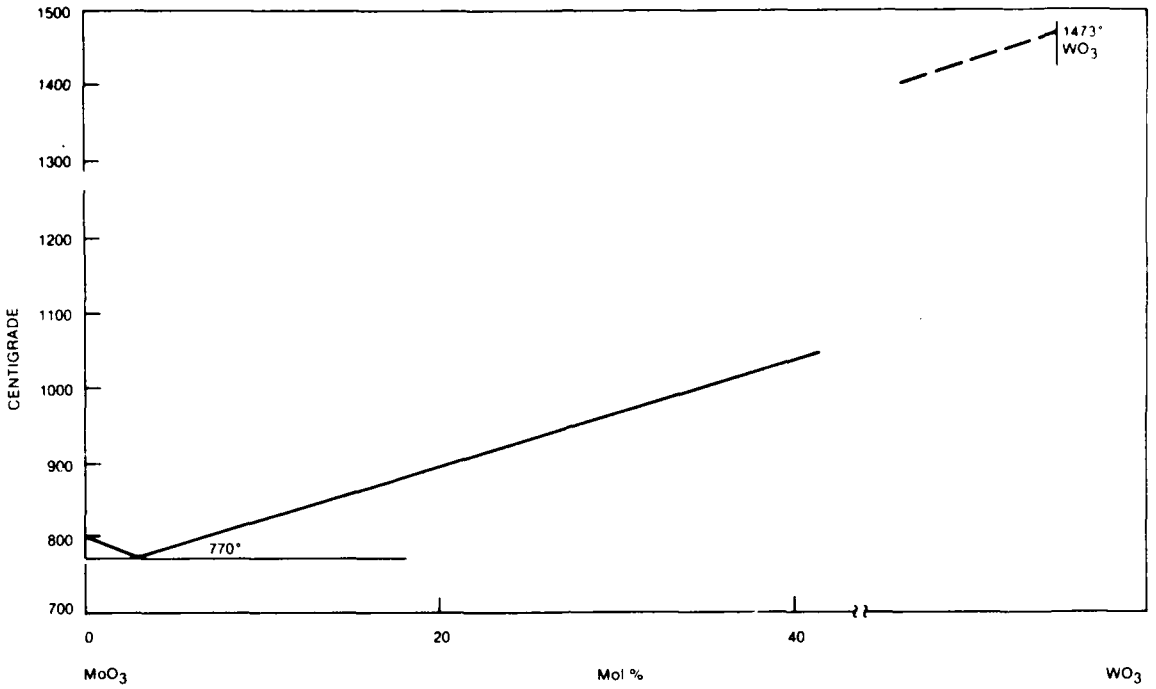

Figure 78. MoO_2-WO_3 Binary System

The failed area itself was composed of the elements of the C129Y alloy, tungsten, hafnium and columbium. The leading edge surface of both sides of the failed areas were stained brown-grey; this discoloration is typically found on burner rig specimens due to deposition of contaminants. The energy spectrum obtained of the stains showed detectable quantities of aluminum, iron and nickel. These elements were probably derived from moisture in fuel and compressed air.

The airfoil was sectioned and prepared for metallography. The cross-section at the failure is shown in Figure 80. Note a distinct demarcation line across the airfoil near the leading edge. Further metallographic examination did not reveal any additional information as to the reason for the phase difference and recourse to SEM/EDX was made. Scans made under identical parameters in both areas showed spectra that are similar with one exception.

In the low-energy region around 1.7 KeV, the emission lines of silicon (K_α and K_β), hafnium (M line) and tungsten (M line) all overlap. An expanded look at the band shape in this region is shown in Figure 81.

Note the distortion in the near gaussian peak shape in the 1.7 KeV region caused by the increased silicon X-ray emittance in the A region. Consequently, it can be deduced that with leading edge failure, silicon can diffuse rapidly through the C129Y substrate in a frontal manner, as seen in Figure 80.

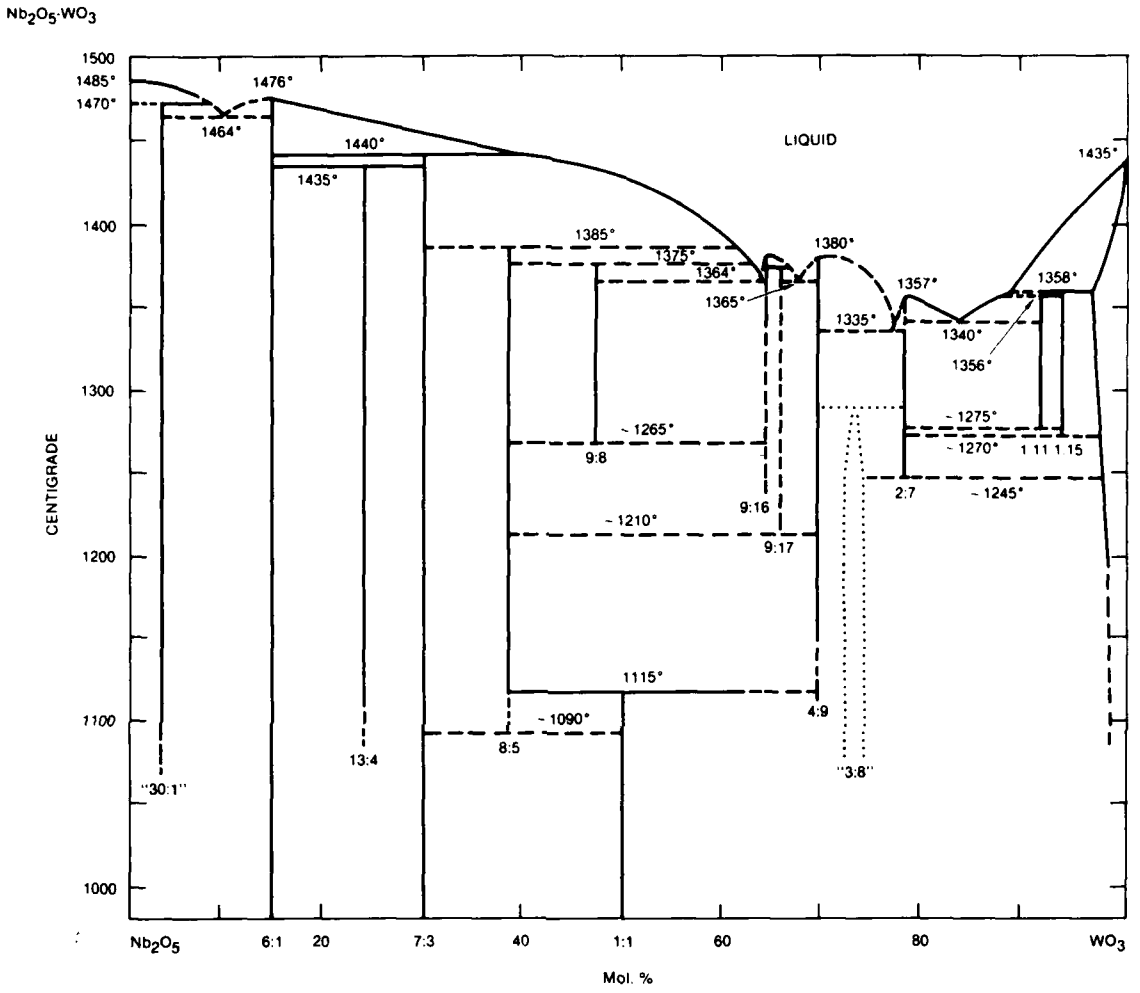

Figure 79. Nb_2O_5-WO_3 Binary System

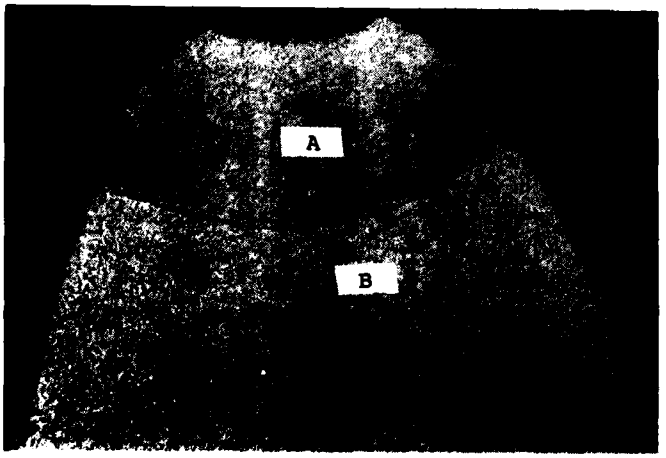

Figure 80.

Cross-Section of Failed Leading Edge on Specimen No. 1-3

Hf-HNO_3-Lactic Etch

Magnification: 20X

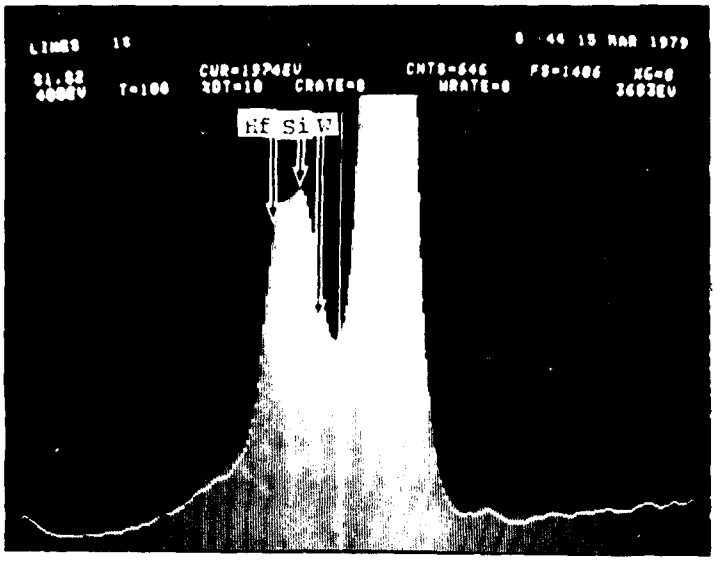

Figure 81. Energy Spectra of Two Areas Near Failed Leading Edge Of Specimen No. 1-3 (Bars = A, Dots = B)

Figure 82.

Oxidized C129Y Substrate at Center of Leading Edge Failure in Specimen No. 1-3

Hf-HNO_3-Lactic Etch

Magnification: 20X

Figure 82 shows the oxidized substrate at the center of the leading edge failure. The surface oxides exhibit a two-phase structure with intergranular diffusion from the surface, light grey regions in the substrte grain boundary. A SEM photograph of the same area (Fig. 83) shows the dark phase extending from the interface into the substrate. EDX analysis determined these areas to be tungsten-rich. In addition, comparison of peak height intensities also indicated that the two-phase surface layer has the alloy elements with a difference in relative quantities of hafnium and tungsten. The outer zone had more tugnsten but less hafnium than the inner zone. The discrete, intergranular, hafnium-rich areas extend from the substrate to the surface, which had significant porosity.

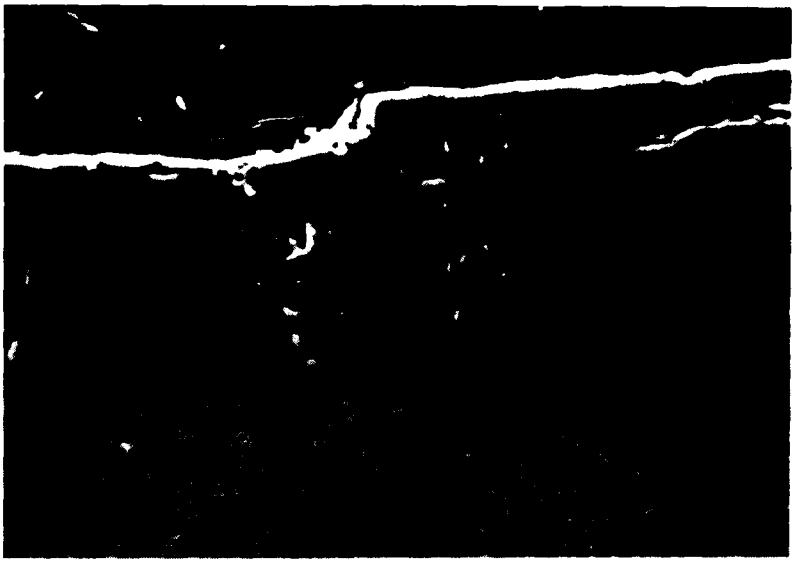

Figure 83. SEM Photomicrograph of Oxidized C129Y Substrate on Leading Edge Failure in Specimen No. 1-3 (Arrows Indicate Hafnium-Rich Areas); Magnification: 1140X

At the edge of the failed area was found partial layers of NS-4 coating. Figure 84 shows the transition from bare alloy to coating at the concave and convex edges. Note the oxides produced on the coating surface and the depletion of the outer layers of coating in the convex side. In order to examine this area in greater detail, EDX work was performed and Figure 85 shows the light grey granular areas of hafnium, both at the coating/substrate and in the coating itself. Small quantities of hafnium-rich 'pockets' are located in the oxide layer which was found to be primarily columbium and silicon.

The rest of the coating away from the leading edge area was still 100 percent intact, as can be seen in Figure 86. Note that with thermal exposure, the outermost 50 percent of the coating had developed a high degree of porosity and oxidation attack was initiated at the coating/substrate interface through the cracks in the coating. The substrate immediately below the coating appeared to be affected and the grain boundaries enhanced by diffusion reaction.

Specimen No. 5-3 (66 Hours)

Visual appearance of the leading edge failure of Specimen No. 5-3 was identical to that of Specimen No. 1-3. The diffusion of silicon through the exposed leading edge forming a siicon contaminated C129Y region was also found in this specimen, Figure 87. The two-zone surface at the leading edge previously noted in Specimen No. 1-3 was also evident here. One notable difference was the absence of tungsten diffusion into the substrate grain boundaries. (Compare Figure 88 with Figure 82). Near the edge of the failed area,

A. Concave

Hf-HNO_3-Lactic Etch

Magnification: 500X

B. Convex

Hf-HNO_3-Lactic Etch

Magnification: 200X

Figure 84. Photomicrographs of Transition From Exposed Alloy to Coated Alloy at Leading Edge Failure of Specimen No. 1-3

89. Furthermore, precipitation of a finely structured secondary phase was found near the coating interface in the alloy. Note the presence of large quantities of a dark grey phase in the coating, especially below the thick oxide layer on the right-hand side. The presence of this phase seems to be an indication of imminent coating failure as it was also found in the oxidized coating layers near the surface, see Figure 90.

Oxides (Columbium, Silicon)

Coating

Magnification: 1650X

Figure 85. SEM Photomicrograph of Edge of Failed Area on Leading Edge of Specimen No. 1-3

Figure 86.

NS-4 Coating on Convex Side of Airfoil (Specimen No. 1-3) After 57 Hours Burner Rig Testing

Hf-HNO_3-Lactic Etch

Magnification: 200X

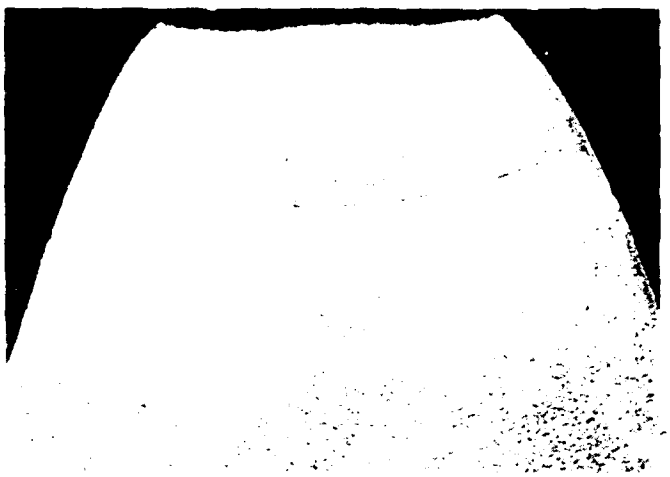

Figure 87.

Cross-Section of Failed Leading Edge on Specimen No. 5-3

Hf-HNO_3-Lactic Etch

Magnification: 500X

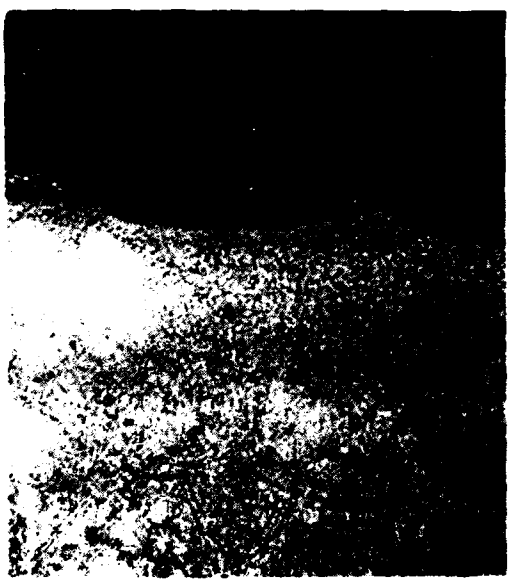

Figure 88.

Oxidized C129Y Substrate at Center of Leading Edge Failure in Specimen No. 5-3

Hf-HNO_3-Lactic Etch

Magnification: 500X

Figure 89.

Transition From Exposed Alloy to Coated Alloy at Leading Edge of Specimen No. 5-3

Hg-HNO_3-Lactic Etch

Magnification: 500X

Figure 90.

NS-4 Coated C129Y (Specimen No. 5-3) After 66 Hours of Burner Rig Testing

Hf-HNO_3-Lactic Etch

Magnification: 200X

A SEM photomicrograph of a coated surface that was still fully protected is shown in Figure 91. The coating can be divided into three zones, and each zone was scanned using similar scan parameters. The energy spectra obtained were smoothed statistically (six-point smooth) and background noise/emittance was subtracted. The final corrected spectra were converted to a titanium ratio mode; the integrated peaks for each element formed was divided by the integrated area of titanium. The reason for choosing titanium was because the amount of titanium in each zone appeared to be fairly constant. The ratio values are plotted in a bar graph in Figure 92. As expected, silicon increased in concentration from zone 1 to 3 as SiO_2 formed. Of the four coating elements, tungsten and vanadium appeared to have diffused to the coating surface with a positive gradient in that direction while most of the molybdenum remained in zone 1. Columbium and hafnium had diffused from the substrate into the coating during the thermal exposure with the highest concentrations in zone 1. The presence of columbium in the coating would result in formation of Cb_2O_5 which is more volatile and is less effective than the refractory oxides.

Specimen No. 3-4 (132 Hours)

The last specimen evaluated had the longest rig test life. A look at the leading edge cross section (Fig. 93) shows the absence of demarcation line found in Specimen Nos. 5-3 and 1-3 that marked silicon diffusion through exposed alloy surfaces into the substrate. The implication here is that the penetration at the leading edge did not expose the substrate. Examination of Figure 94 shows some damage in the coated leading edge but the extent of the damage is not clear. A closeup of the failure is shown in Figure 95 and again, fibers are noted. The light grey fibrous materials were found to be rich in titanium with tungsten and columbium. The dark background appeared

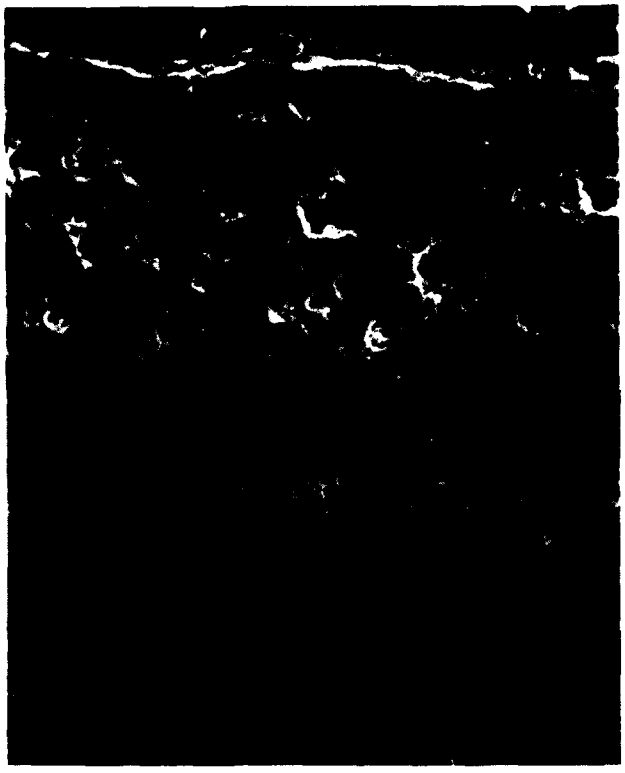

Magnification: 500X

Figure 91. SEM Photomicrograph of NS-4 Coated C129Y Alloy (Specimen No. 5-3) After 66-Hour Burner Rig Test

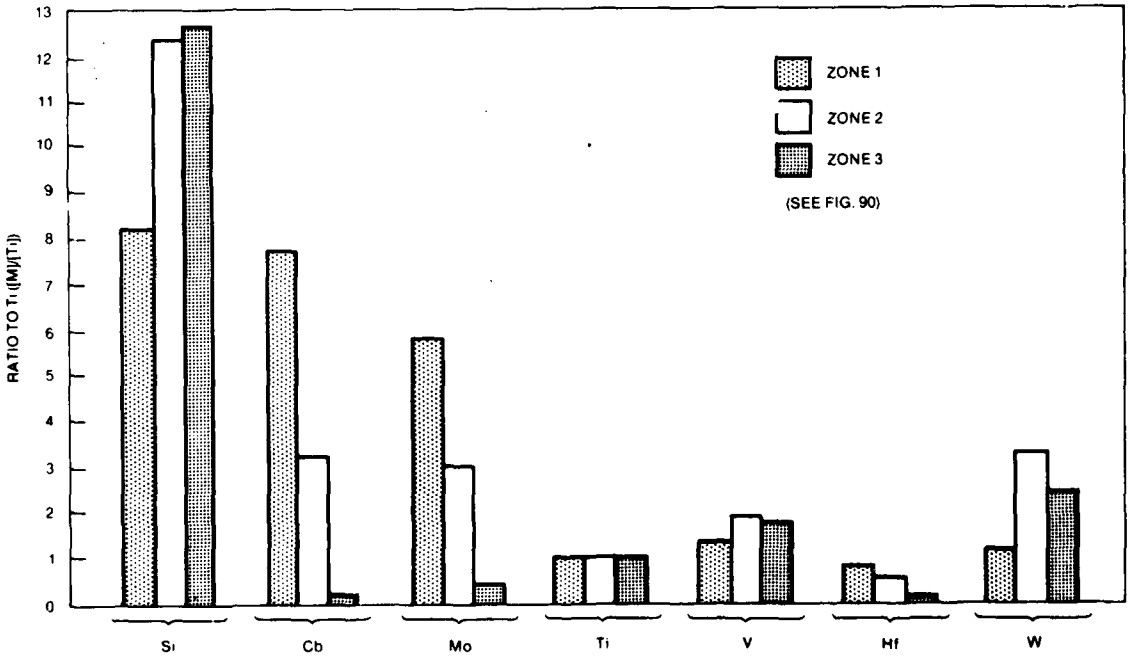

Figure 92. EDX Analysis Results of NS-4 Coating on Specimen No. 5-3

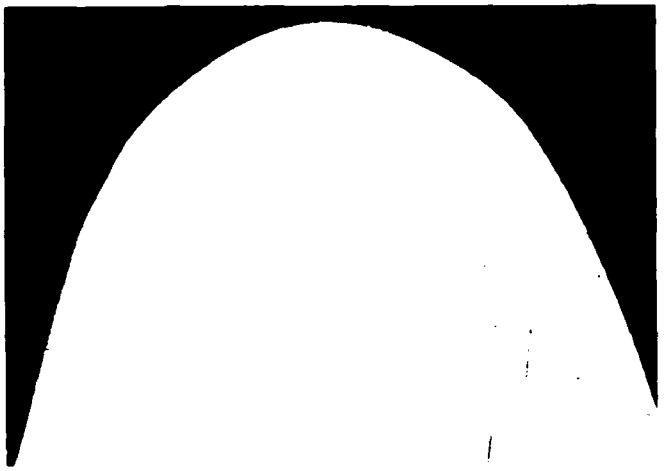

Figure 93.

Cross-Section of Failed Leading Edge on Specimen No. 3-4

$HF-HNO_3$-Lactic Etch

Magnification: 20X

to be silicided C 129Y. The dark stains found on the leading edge adjacent to the failed area (Fig. 94) were contaminants deposited by the combustor gases and included trace quantities of nickel, calcium, iron and aluminum.

After sectioning the airfoil, the leading edge was examined in cross section and the areas of maximum failure/penetration are shown in Figure 96. Complete penetration to the substrate was minimal although the remaining coating appeared to be partially oxidized. Large clumps of oxide were noted and EDX analysis indicated the presence of silicon and columbium. The NS-4 coating, or what was left of the coating, had a high columbium concentration with significant amounts of hafnium, pointing to the advanced state of degradation as a result of columbium and hafnium diffusion outward. Note the interfacial crack extending from the flaw on the left hand side in Figure 96A. It is difficult to determine the exact cause of the crack; the cracks could have been induced during cutting or were the result of thermal stresses. Small, discrete pockets of hafnium were also detected in the coating matrix.

Figure 97 shows a relatively sound coated area although evidence of oxidation attack can be noted in the outer portion of the coating.

A. Concave

Magnification: 11X

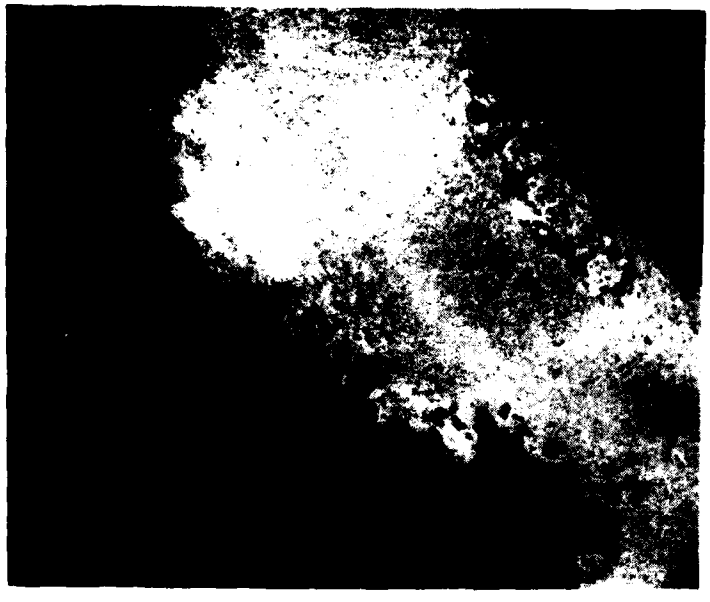

B. Convex

Magnification: 11X

Figure 94. Concave and Convex SEM Views of Failed Leading Edge on Specimen No. 3-4

Figure 95. SEM Photomicrograph of Failed Leading Edge on Specimen No. 3-4

A. SEM

Magnification: 340X

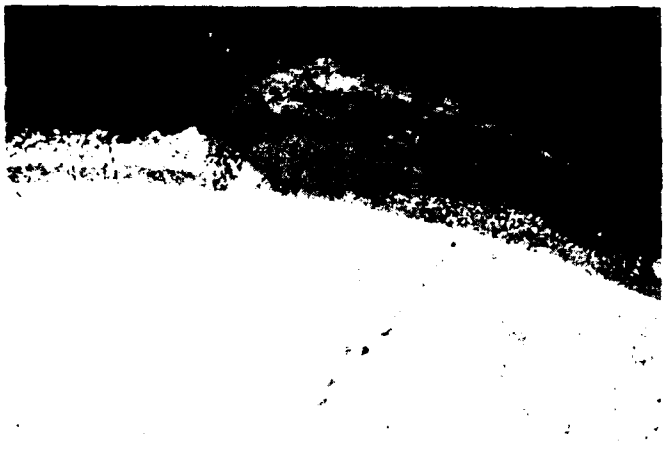

B. Hf-HNO_3-Lactic Etch

Magnification: 200X

Figure 96. Photomicrographs of Failed Area on Leading Edge of Specimen No. 3-4 Showing Oxide Formation (Arrows Indicate Hafnium-Rich Areas)

Figure 97.

NS-4 Coated C129Y After 132 Hours of Burner Rig Testing

Hf-HNO_3-Lactic Etch

Magnification: 200X

5

CONCLUSIONS AND RECOMMENDATIONS

1. It is clear from the casting effort of this program that considerably more development is needed in foundry techniques for columbium-base alloys. Any assumption that all the ills visited upon the foundry phase of the program were caused by selection of uncastable alloy is not valid unless a reasonable explanation can be advanced as to why C129Y reacts as it does.

2. The choice of C129Y above other columbium-base alloys considered is validated by the superiority of mechanical properties generated in tensile and stress-rupture tests. The choice is less desirable when viewed from the standpoint of castability, and this has shaded the results of the program to some extent. In comparing the technology of the present efforts to that of a prior casting program (Ref. 3), it is apparent that the selected alloy offers much more potential in terms of elevated-temperature strength, being competitive with ceramics and ODS superalloys. The quality of the hardware fabricated therein, however, was considerably superior to the C129Y castings. The choice of another alloy, while perhaps assisting in the foundry process, would not have yielded a mechanical property data base with advantage over other materials.

3. Difficulties in arc melting C129Y have not been resolved satisfactorily. For reasons yet unexplained, this alloy requires two to three times the amperage of other columbium-base alloys to initiate a melt.

4. In view of the difficulties encountered in melting C129Y by the consumable arc process, coupled with the observed poor fluidity of the alloy, it is suggested that an alternate melting procedure be considered in pursuing further casting work with thin sections. A method such as electron beam melting which can induce superheat into the melt is clearly indicated.

5. The use of a superheat melting technique may also have beneficial effects on strength and ductility. It was noted in X-ray dispersive analyses that the alloy was not in complete solution, hafnium, notably, being concentrated in segregations.

6. The above-mentioned fluidity problem may be, in part, related to an alloying error in the program material, i.e., virtual absence of yttrium in the material. The gettering action of this element - or the lack of same - may have had adverse effects on the castability of the alloy.

7. Despite the several difficulties in foundry procedure the C129Y castings display exceptional properties at elevated temperature and technically show superiority to cobalt- and nickel-base alloys for advanced engines.

8. Columbium-base alloy C129Y, in the cast and coated condition, displays mechanical properties in the 2000-2200°F temperature range which are the equivalent to those of cobalt-base X-45M at 1500-1800°F.

9. The alloy displays, in the absence of detrimentally high interstitial levels or physical flaws such as porosity, room-temperature ductility adequate for consideration of engineering use. It is clear, however, that impurities and defects must be closely controlled if practical applictions are to be achieved.

10. The effect of the NS-4 coating on the C129Y alloy system is minimal. Mechanical properties evaluated (tensile, stress-rupture) were virtually identical for both coated and uncoated configurations.

11. Isothermal oxidation life of NS-4 coated C129Y alloy at 760 and 1093°C is excellent, in excess of 5500 hours.

12. One-hour burner rig tests of a coated airfoil at 1316°C indicated that in rapid cycling (1 hour cycles from 1316 to <816°C), coating life was limited to about 10^2 hours. However, it should be pointed out that the test rig cannot be directly related to an engine since the temperature distribution across the airfoil does not simulate that in an engine. In the absence of the nozzle shroud and discs, one can expect tht the thermal stresses in the test is much more severe than is typically found, thus resulting in premature coating breakdown.

13. NDT methods are needed to critically examine castings and coated parts to detect flaws. Standards or criteria whereby nonacceptable defects could be judged need to be established to provide guidelines for quality control.

14. The unique condtions created by the rig test resulted in a combination of both applied stress and high thermal gradient. However, the NS-4 class of coatings for protection of columbium alloys can be readily modified and optimized to improve its resistance to thermal cycling and stress oxidation.

6

REFERENCES

1. Ohynsty, B. and Stetson, A.R., "Evaluation of Composite Materials for Gas Turbine Engines", AFML-TR-66-156, Part II, Final Report (1967).

2. Beauregard, R.J., "Feasibility Study of Columbium Alloy Castings", AMMRC Contract DAAG46-69-C-0163, Final Report (1971).

3. Humphrey, J.R. and Nievath, A.J., "Investment Casting of Columbium Alloys", AMMRC Contract DAAG46075-C-0007, Final Report (1975).

4. Shoemaker, H.E. and Stetson, A.R., "Silicide Coatings for Tantalum and Columbium Alloys", NASA Contract NAS3-9412, Final Report (1969).

5. Levy, M., Falco, J.J. and Herring, R.P., "Oxidation of Cb(Nb) and Coated Columbium Alloys", J. of Less Common Metals, 34 (1974) pp. 321-343.

6. Moore, V.S. and Stetson, A.R., "NS-4 Coating Process Development for Columbium Alloy Airfoils", AMMRC Contract DAAG46-74-C-0089, Final Report (1976).

7. Levin, E.M., Robbins, C.R. and McMurdier, H.F., "Phase Diagrams for Ceramics", Am. Ceram. Soc. (1964), 1969 Supplement.

8. Private communication, A.A. Tavassoli, KBI, to A.N. Hammer, Solar.

9. Hauffe, K., "Oxidation of Metals", Plenum Press, New York (1965).

APPENDIX A

PROCEDURES FOR HYDRIDING TITANIUM AND VANADIUM

HYDRIDING TITANIUM

The titanium sponge (-20 +50 mesh) is placed in an unlined Inconel retort which is subsequently sealed by fusion welding. Following pressurizing of the retort to 34.5 kPag with argon, the welds are soap-bubble leak checked. The retort and the palladium alloy hydrogen purifier are vacuum-argon cycle purged a minimum of three times. Under dynamic vacuum, the hydrogen purifier is heated to 454°C at which point it is back filled with hydrogen. The retort is then vacuum-hydrogen cycle purged a minimum of three times at room temperature before hydrogen pressure in the retort is adjusted to 10 mm Hg above atmospheric pressure preparatory to placing the retort in a furnace preheated to 427°C. The furnace containing the retort is then heated to 677°C over a 30-minute period. The retort is soaked in the furnace at 677°C for one hour. The hydriding reaction, however, should be complete in 30 to 40 minutes at 677°C, as indicated by the flow meter in the hydrogen supply line from the palladium purifier. The hydrogen pressure is maintained above atmospheric pressure while the retort is removed from the furnace and allowed to cool to room temperature.

HYDRIDING VANADIUM

Vanadium granules (approx. 13 mm sponge) are pickled in nitric acid, rinsed in distilled water and subsequently methanol. After vacuum drying at room temperature, the vanadium is placed in an Inconel retort which is sealed by fusion welding. After pressurization with argon, the retort is soap-bubble leak checked. The retort and palladium hydrogen purifier are vacuum-argon cycle purged a minimum of three times. After evacuation, the palladium membrane is heated and the retort vacuum-hydrogen purged as recommended in the "Hydriding Titanium" section.

With the hydrogen pressure from the palladium alloy purifier adjusted to 10 mm Hg above atmospheric pressure, the retort is inserted into a furnace preheated to 649°C. The furnace is then heated to 927°C over a one-hour period and held at temperature for a period of not less than 12 hours. After the 927°C soak, the control temperature is reduced to 593°C. Eight hours later the furnace control is reduced to 260°C. When it reaches 260°C, it is removed from the furnace and allowed to air cool while maintaining a hydrogen pressure above atmospheric pressure.

APPENDIX B

SPRAY SLURRY PREPARATION PROCEDURE

A description of the process used in preparing the slurries based on a vehicle containing an ethyl cellulose binder is given in the following paragraphs.

Thirty grams of ethyl cellulose(1) is dissolved in a mixture of 0.200ℓ of secondary butyl alcohol and 0.800ℓ of xylene. One litre of Stoddard solvent (a petroleum distillate having a boiling point range of 156 to 199°C) is added to this solution to obtain the desired vehicle, which was designated E-4.

Bewteen 0.180 and 0.220ℓ of the vehicle and the appropriate quantity of powdered elemental metals needed to give a fuids-to-solids true volume ratio of 2.5 (approx. 770 g of NS-4 powder) are added to a one quart low-silica ball mill(2) that is slightly more than half filled with balls.

After the ball mill has been tumbled for a period of 20 hours, the slip is transferred to a preweighed graduated cylinder for the determination of the specific gravity (by weighing the observed volume of slip) prior to spray application.

(1) N-200 grade ethyl cellulose as supplied by the Polymers Department, Hercules Power Company, Wilmington, Delaware.

(2) Burundum fortified mills and balls are purchased from U.S. Stoneware Company, Akron, Ohio.

TELEDYNE
WAH CHANG ALBANY

P O BOX 460
ALBANY, OREGON 97321
(503) 926-4211 TWX (510) 595-0973

APPENDIX C

Specification No.
TWCA—Cb—MS—1
Rev.
ISSUED: October 7, 1970

COLUMBIUM

Specification **Cb & Cb Alloy Plates, Sheets and Strip**

1. SCOPE

1.1 *Scope.* This specification establishes the requirements for Columbium alloy plates, sheets, and strip.

1.2 *Classification.* Columbium alloy plates, sheet, and strip procured to this specification shall be supplied in the following types:

Type	*Composition*
Cb	Cb
WC103	Cb—10Hf—1Ti
WC129Y	Cb—10Hf—10W—.1Y
Cb–1Zr	Cb—1Zr
Cb 752	Cb—10W—2.5Zr.

2. APPLICABLE DOCUMENTS

2.1 The following documents of the issue in effect on the date of invitation for bids or request for proposal, form a part of this specification to the extent specified herein.

STANDARDS

Federal

Federal Test Method Standard No. 151	Metals; Test Methods
MIL STD 271	Non-Destructive Testing (X-Ray, Sonics, Dye Penetrant)

American Society for Testing Materials

ASTM–E112	Methods for Determining Average Grain Size.

National Academy of Science

Material Advisory Board, MAB-216-M	Evaluation Test Methods for Refractory Metal Sheet Material

Aeronautical Material Specifications

AMS 2242c	Tolerance

3. REQUIREMENTS

3.1 *Materials*

3.1.1 *Production Methods.* The ingot metal shall be double Vacuum melted in a furnace of a type suited for reactive metals. The starting ingot shall be free of voids and defects as determined by ultrasonic inspection.

3.1.2 *Alloy Identification.* The identity of all alloys with respect to ingot melt number shall be maintained at all stages of fabrication.

3.1.3 *Condition.* Unless otherwise specified, all material shall be supplied in the recrystallized annealed condition in accordance with Table I.

Table I

THICKNESS	% RECRYSTALLIZATION				
	*Cb**	*WC103*	*WC129Y*	*Cb–1Zr*	*Cb752*
Less than .005	A/W	A/W	A/W	A/W	A/W
.005— .150	80	95 – 100%	95 – 100%	95 – 100%	95 – 100%
.151— .250	75	90 – 100%	90 – 100%	90 – 100%	90 – 100%
.251—1.00	50	85 – 100%	85 – 100%	85 – 100%	85 – 100%

* Material supplied in the As Worked (A/W) condition unless otherwise specified by the P/O.

3.2 *Chemical Composition.* The Chemical Composition of each alloy ingot shall conform to Table II.

Table II

Element	*Cb*	*WC103*	*WC129Y*	*Cb–1Zr*	*Cb–752*
Tungsten	500 ppm*	5000 ppm*	9–11%	500 ppm*	9–11%
Hafnium		9–11%	9–11%	200 ppm*	2000 ppm*
Tantalum	1000 ppm*	5000 ppm*	5000 ppm*	1000 ppm*	5000 ppm*
Yttrium			.05–.3%		
Titanium		.7–1.3%			
Zirconium	500 ppm*	7000 ppm*	5000 ppm*	.8–1.2%	2.0–3.0%
Carbon	100 ppm*	150 ppm*	150 ppm*	200 ppm*	150 ppm*
Oxygen	200 ppm*	250 ppm*	225 ppm*	300 ppm*	225 ppm*
Nitrogen	100 ppm*	100 ppm*	100 ppm*	100 ppm*	100 ppm*
Hydrogen	15 ppm*	15 ppm*	15 ppm*	15 ppm*	15 ppm*
Columbium	Bal.	Bal.	Bal.	Bal.	Bal.

* Maximum limits unless otherwise indicated. ppm = Parts Per Million.

3.2.1 *Product Analysis.* If specified, product analysis shall be performed on C, O_2, N with maximum levels specified as follows on Parts Per Million (ppm).

Element	*Cb*	*WC103*	*WC129Y*	*Cb–1Zr*	*Cb–752*
C	100	150	150	200	150
O_2	200	225	225	300	225
N	100	100	100	100	100
H	15	15	15	15	15

3.3 *Tensile Properties.* Elongation, yield strength, and ultimate tensile strength shall be measured at room temperature on samples transverse to final rolling direction on material which is 0.010" thick or greater. The strain rate shall be maintained at 0.005 ±0.001"/per inch per minute through the 0.2% offset yield strength and at 0.05 ±0.005"/per inch per minute thereafter. The material shall have minimum transverse tensile property values as specified in Table III.

Table III

	Cb	*WC103*	*WC129Y*	*Cb–1Zr*	*Cb–752*
Ultimate tensile strength, 1000 psi	25	54	80	35	75
Yield strength, 0.2% offset, 1000 psi	11	38	60	15	55
Elongation, % in one inch	35	20	20	20	20

3.4 *Bend Ductility.* Representative samples of the materials in final form shall withstand the following bend test at room temperatures without failure when tested according to procedures described in the most recent revision of the Materials Advisory Board report MAB-216-M, "Evaluation Test Methods for Refractory Metal Sheet Materials". The samples shall be sectioned with the long axis of the bend specimens perpendicular to the final rolling direction.

3.4.1 Sheet 0.060" in thickness and under shall be bent over a 1T radius through 105 degrees at a ram speed of one inch/per minute.

3.4.2 Sheet over 0.060" to 0.187" in thickness shall be bent over a 2T radius through 105 degrees at a ram speed of one inch/per minute.

3.5 *Grain Size.* Unless otherwise specified, the minimum average ASTM grain size number shall be in accordance with Table IV.

Table IV

Thickness	*WC103*	*WC129Y*	*Cb–1Zr*	*Cb–752*
.006 – .150"	6	6	5	6
.151 – .500"	5	5	4	5
Greater than .750"	.....	.....	.....	.....

4. DIMENSIONS AND TOLERANCES

4.1 *Dimensions and Tolerances.* Unless otherwise specified, tolerances shall be as defined in AMS 2242c.

4.2 *Flatness.* Total deviation from flatness of sheet and strip shall not exceed 6% as determined by the following formula:

$$\frac{H}{L} \times 100 = \text{percent of flatness deviation.}$$

where H = maximum distance from a flat reference deviation.
and L = minimum distance from this point to the point of contact with the reference surface.

4.3 *Marking for Identification.* Each plate, sheet, and strip shall be suitably marked with the contract number or order number, ingot melt number, specification number, and composition number.

5. QUALITY

5.1 *General.* The finished product shall be visibly free from oxide or scale of any nature, grease, oil residual lubricants, and other extraneous materials. Cracks, laps, seams, gouges, and fins shall be unacceptable.

5.2 *Surface Rework.* All surface pores, gouges, and other defects deeper than 0.005" or 3% of the thickness, whichever is smaller, shall be unacceptable. Surface imperfections may be faired smooth to remove any notch effect provided dimensional tolerances are still lmaintained.

5.3 *Edge.* The edges shall be produced by shearing, slitting or sawing. The burr height shall not exceed five (5) percent of the thickness of the material.

6. REPORTS. The supplier shall submit three certified copies of reports indicating the ingot chemistries. In addition, a certification statement will be added stating that although not tested, the material is in conformance wih the specification. Additional test for tensile yield, elongation, grain size and product analysis for oxygen, carbon, and nitrogen as well as other tests will be furnished when negotiated and specified in the purchase order.

7. PREPARATION FOR DELIVERY

7.1 *Packaging.* All material shall be packaged in a manner that will prevent damage in transit and in storage.

8. REJECTIONS. Material not conforming to any of the requirements of this specification unless otherwise agreed upon by the purchaser.

9. DEFINITIONS. For the purposes of this specification, the following definitions shall apply:

9.1 *Sheet.* Sheet is flat, rolled material up to 0.125" thick, and other material not considered strip, normally supplied in widths to 24".

9.2 *Plate.* Plate is flat, rolled material 0.125" thick or greater.

9.3 *Strip.* Strip is flat, rolled material up to 0.060" thick in widths under twelve inches (12").

APPENDIX D

PROCESS SPECIFICATION FOR THE NS-4 COATING

SPECIFICATION I

NS-4 Coating Modifier Composition

1.0 SCOPE

This specification describes the composition and processing requirements for producing the modifier powder constituent of the NS-4 oxidation-resistant coating for C129Y and other columbium- and tantalum-base alloys.

2.0 APPLICABLE DOCUMENTS

R. T. Wimber and A. R. Stetson, "Development of Coatings for Tantalum Nozzle Vanes", NASA CR-54529 (July 1967).

H. E. Shoemaker and A. R. Stetson, "Silicide Coatings for Tantalum and Columbium Alloys", NASA CR-72519 (August 1969).

3.0 REQUIREMENTS

The requirements of this specification apply to components designated as Solar controlled items applicable to S.O. 6-4444-7.

3.1 Responsibilities

3.1.1 General

Each department at Solar engaged in the manufacturing of the NS-4 oxidation-resistant coating shall be responsible for implementing the provisions of this procedure.

3.1.2 Requests to deviate from any requirement herein shall be supported by comprehensive test data to substantiate the reliability of the deviation and indicate why the deviation is necessary. No deviation to the requirements of this procedure shall be made until written approval is obtained from both the cognizant Solar department, Solar Materials Engineering Laboratory.

4.0 MATERIALS AND TEST EQUIPMENT

Tungsten <44μm powder, (O_2 2000 ppm max; Mo 250 ppm max; Fe 30 ppm max; Al, Ca, C, Si, Cr, Ni, Cu, Mn, Mg and Sn 10 ppm max each).

Molybdenum <44μm powder (O_2 2000 ppm max; W 250 ppm max; Fe 30 ppm max; Al, Ca, C, Si, Cr, Ni, Cu, Mn, Mg and Sn 10 ppm max each).

Vanadium Hydride VHx 99.5% <44μm powder (prepared from 99.5% vanadium and palladium diffused hydrogen).

Titanium Hydride TiH_2 99.5% <44μm powder (prepared from 99.5% titanium sponge and palladium diffused hydrogen).

Argon: dew point -100°C, 1 ppm O_2

Acetone: Reagent grade

Alumina Ball Mill

Fischer Sub-Sieve Sizer

10μm Sieve

Analytical Balance

Vacuum Oven: 200°C temperature limit, 13 Pa capability.

5.0 MODIFIER POWDER PREPARATION

5.1 Add powder mixture consisting of 50 weight percent tungsten, 20 weight percent molybdenum and 15 weight percent each of vanadium, 20 weight titanium hydride to alumina ball mill then wet powder with 10 weight percent xylene and mill for 22 to 26 hours.

5.2 Remove milled powder from mill and decant off excess xylene and allow remainder to evaporate.

5.3 Wash dried powder with two successive aliquots (10 weight percent) of acetone. After decanting the excess from the last wash, vacuum dry the powder at 100°C for 16 to 18 hours.

6.0 QUALITY ASSURANCE

6.1 Particle size and distribution. The Fischer sub-sieve size of the product (ASTM B330-65) shall be between 4.0 and 5.0 μm and 40 to 50 weight percent should pass a 10 μm screen.

6.2 The density of the dried powder measured by a pycnometer shall be 8.5 to 8.6 gm/cc at 20°C.

7.0 STORAGE

Store powder in a sealed container under an argon atmosphere.

SPECIFICATION II:

NS-4 Modifier Coating Application to Internal Surface of C129Y Hollow Vane

1.0 SCOPE

This specification describes the processing and composition requirements for applying the NS-4 oxidation-resistant modifier constituent to the internal surface of a hollow C129Y nozzle vane.

2.0 APPLICABLE DOCUMENTS

NS-4 Coating Modifier Composition Specification I.

V. S. Moore and A. R. Stetson, "NS-4 Coating Process Development for Columbium Alloy Airfoils", AMMRC CTR-76-8, Final Report on Contract DAAG46-74-C-0089 (March 1976).

3.0 REQUIREMENTS

The requirements of this specification apply to components designated as Solar controlled items applicable to S.O. 6-4444-7.

3.1 Responsibilities

3.1.1 General

Each department at Solar engaged in the manufacturing of the NS-4 oxidation-resistant coating shall be responsible for implementing the provisions of this procedure.

3.1.2 Requests to deviate from any requirement herein shall be supported by comprehensive test data to substantiate why the deviation is necessary. No deviation to the requirements of this procedure shall be made until written approval is obtained from both the cognizant Solar department, Solar Materials Engineering Laboratory.

4.0 MATERIALS

Abrasive Blast Cabinet with 250 to 500 μm garnet media and 0.4 to 0.55 MPa gauge air supply.

Vapor Degreaser filled with technical grade 1,1,1- trichloroethane.

Mechanical Mixer

Linear Withdrawal Apparatus with controlled range of 5 to 30 mm/min.

2-ethoxyethanol-reagent grade

Acetone reagent grade

Polymethylmethocrylate solution - Rohm and Hass B7 or equivalent

Cotton tipped swabs

Graduated cylinder - 50 cc capacity

Light cotton gloves

Analytical balance

Vacuum oven - 200°C capability, 13 Pa capability

NS-4 Modifier powder - NS-4 coating modifier specification or equivalent.

5.0 NS-4 Modifier Dipping Slurry Preparation

Blend with mechanical mixer equal volumes of the polymethylmethacrylate solution and 2-ethoxyethanol to prepare the vehicle, then add a weight of the modifier powder equal to 5.7 times the weight blended vehicle to the vehicle. Continue mixing until a viscous slurry free of lumps is obtained.

5.1 Quality Assurance

Specific gravity of the powder slurry shall be 3.9 to 4.0 at 20°C.

6.0 C129Y Surface Preparation and Application of NS-4 Modifier Powder Coating

6.1 Abrasive blast both internal and external surfaces of C129Y vane.

6.2 Vapor degrease.

6.3 Record weight of part.

6.4 Attach vane to linear withdrawal apparatus with the axis of the vane cavity inclined 20 to 30 degrees from the axis of withdrawal .

6.5 Lower vane into NS-4 modifier slurry until completely immersed and wait until slurry surface is even and smooth.

6.6 Withdraw vane at a rate of 11 millimeters per minute until completely clear of surface of slurry.

6.7 Cover slurry container to minimize evaporation when not in use.

6.8 Remove coated vane from linear withdrawal apparatus and allow to dry in air for two hours.

6.9 Using cotton gloves and cotton tipped swabs, moistened with reagent-grade acetone, carefully remove the dried slurry from the outer surfaces of the C129Y vane. Take care not to re-wet or remove the coating from the inner surface and feather a radius of the inner coating thickness at each cavity opening.

6.10 Vacuum dry the coated C129Y vane at 130°C for two hours at a pressure of less than 133 Pa.

7.0 QUALITY ASSURANCE

Weigh vacuum dried part. Modifier deposition shall be between 60 to 100 milligrams per square centimeter of internal area.

SPECIFICATION III
NS-4 Modifier Coating Application to External Surface of C129Y Vane

1.0 SCOPE

This specification describes the composition and processing requirements for applying the NS-4 oxidation-resistant modifier constituent to the external surface of a C129Y nozzle vane.

2.0 APPLICABLE DOCUMENTS

NS-4 Coating Modifier Composition Specification I

NS-4 Modifier Coating Application Specification II

3.0 REQUIREMENTS

The requirements of this specification apply to components designated as Solar controlled items applicable to S.O. 6-4444-7.

3.1 Responsibilities

3.1.1 General

Each department at Solar engaged in the manufacturing of the NS-4 oxidation-resistant coating shall be responsible for implementing the provisions of this procedure.

3.1.2 Requests to deviate from any requirement herein shall be supported by comprehensive test data to substantiate why the deviation is necessary. No deviation shall be made until written approval is obtained from both the cognizant Solar department, Solar Materials Engineering Laboratory.

4.0 MATERIALS

Abrasive Blast Cabinet with 250 to 500 μm garnet media and 0.4 to 0.55 MPa gage air supply.

Vapor degreaser filled with technical grade 1,1,1- trichloroethane.

Mechanical Mixer or Alumina Ball Mill and Balls

Spray Gun - DeVilbiss Model GGA-Series 500 with F-tip or equivalent

Air supply - 0.2 to 0.55 MPa gage

E-4 Vehicle - Ethyl cellulose, butyl alcohol, xylene, Stoddard solvent

Graduated Cylinder - 50 cc capacity

Light cotton gloves

Analytical balance

NS-4 modifier powder - NS-4 coating modifier specification I or equivalent.

5.0 NS-4 MODIFIER SPRAY SLURRY PREPARATION

Mix 75 parts by weight of the modifier powder with 25 parts by weight of the E-4 vehicle until it is free of lumps.

5.1 Quality Assurance

Specific gravity of the spray slurry shall be between 2.3 and 2.8 at 20°C.

6.0 C129Y SURFACE PREPARATION AND APPLICATION OF NS-4 MODIFIER POWDER COATING

6.1 If vane is hollow and uncoated on any surface, follow procedure in in NS-4 Modifier Coating Specification II.

6.2 If vane is hollow and internal cavity is coated, procede to Step 6.6.

6.3 If vane is solid, abrasive blast to clean surface.

6.4 Vapor degrease vane.

6.5 Record weight of cleaned vane.

6.6 Using light cotton gloves to hold vane, uniformly apply the NS-4 powder bisque to the external surfaces of the vane by spraying the NS-4 modifier spray slurry.

7.0 QUALITY ASSURANCE

Modifier deposition shall be between 60 and 100 milligrams per square centimeter of vane surface.

SPECIFICATION IV

NS-4 Coating Bonding and Formation on Surface of C129Y Vane

1.0 SCOPE

This specification describes the processing and composition requirements for bonding and forming the NS-4 oxidation-resistant coating to the surface of a C129Y nozzle vane.

2.0 APPLICABLE DOCUMENTS

NS-4 Modifier Coating Application Specification II

NS-4 Modifier Coating Application Specification III

3.0 REQUIREMENTS

The requirements of this specification apply to components designated as Solar controlled items applicable to S.O. 6-4444-7.

3.1 Responsibilities

3.1.1 General

Each department at Solar engaged in the manufacturing of the NS-4 oxidation-resistant coating shall be responsible for implementing the provisions of this procedure.

3.1.2 Requests to deviate from any requirement herein shall be supported by comprehensive test data to substantiate why the deviation is necessary. No deviation shall be made until written approval is obtained from both the cognizant Solar department, Solar Materials Engineering Laboratory.

4.0 MATERIALS

NS-4 modifier coated C129Y vanes per NS-4 Modifier Coating Application Specifications II and III.

Silicon 99.1 percent, 300 to 600 μm particle size, maximum impurities 0.34 percent Fe, 0.03 percent Ca, 100 ppm O_2.

Titanium sponge, 99.5 percent pure.

Inconel 600 retort with tungsten covered bottom and double walled liner fabricated from B66 or Cb-1Zr. Space between liner walls to be filled with titanium sponge as shown below.

Vacuum pump

Argon - 100°C dewpoint, <1 ppm O_2, <1 ppm N_2

TIG Welder

Leak Check solution - Snoop or equivalent

Oil trapped pressure release bubbler

Furnace with 1200°C capability

Vacuum furnace with 1550°C and 1.0 millipascal capabilities

Columbium or tantalum racks for holding vanes.

5.0 NS-4 MODIFIER SINTERING PROCEDURE

5.1 Load NS-4 modifier coated vanes onto columbium or tantalum racks and place in vacuum furnace, taking care not to damage the modifier bisque.

5.2 Evacuate furnace to 1.0 millipascal or less.

5.3 Increase temperature of furnace to 1516°C while maintaining a pressure less than 13 millipascals and sinter modifier coated vanes for three hours at 1516 $\pm$5°C.

5.4 Cool and reweigh parts.

6.0 QUALITY ASSURANCE

The sintered modifier weight shall be 87 to 90 percent of its initial value.

7.0 NS-4 COATING FORMATION AND BONDING PROCESS

7.1 Partially fill the innermost cavity of the Cb-1Zr or B-66 liner with the silicon powder.

7.2 Imbed the sintered NS-4 modifier coated C129Y vanes and a control coupon of C129Y coated with the sintered NS-4 modifier in the powder and cover them with the silicon powder.

7.3 Place the liner and its lid (covered with titanium sponge in the Inconel retort and seal it by TIG welding.

7.4 Leak check the weld by pressurizing with argon and watching for bubbles along weld after wetting with leak check solution.

7.5 Reweld if necessary to seal noted leaks.

7.6 Evacuate retort to at least 26 pascals and backfill with argon three times, leaving retort under an argon blanket at 102 kPa pressure with the pressure release bubbler attached to vent the excess argon.

7.7 Place retort in furnace at 1150 ± 5°C and silicide NS-4 modifier coated vanes for eight hours.

7.8 Cool and record weight of NS-4 coated C129Y vanes.

8.0 QUALITY ASSURANCE

8.1 The silicided modifier coating on the vanes shall have gained from 65 to 70 percent additional weight based on the modifier coating weight of the sintered vanes.

8.2 Metallographic examination of a test coupon must indicate that the silicided layer extends 40 to 100 μm into the C129Y substrate beneath the silicided modifier.

9.0 POST-CASTING PROTECTION

Oxidize NS-4 coated C129Y vanes in furnace for one hour at 1371 ± 15°C.

DISTRIBUTION LIST
US ARMY AVIATION RESEARCH AND DEVELOPMENT COMMAND
MANUFACTURING TECHNOLOGY (MANTECH) PROJECTS
FINAL REPORT - AVRADCOM TR 80-F-2

Commander
US Army Aviation Research & Development Command
P.O. Box 209
St. Louis, MO 63166
Attn: DRDAV-EXT (10)
Attn: DRDAV-D (1)
Attn: DRDAV-N (1)

Project Manager
Advanced Attack Helicopter
P.O. Box 209
St. Louis, MO 63166
Attn: DRCPM-AAH-TM (2)
Attn: DPCPM-AAH-TP (1)

Project Manager, Black Hawk
P.O. Box 209
St. Louis, MO 63166
Attn: DRCPM-BH-T (2)

Project Manager
CH-47 Modernization
P.O. Box 209
St. Louis, MO 63166
Attn: DRCPM-CH47M-T (2)

Project Manager
Aircraft Survivability Equipment
P.O. Box 209
St. Louis, MO 63166
Attn: DRCPM-ASF-TM (2)

Project Manager, Cobra
P.O. Box 209
St. Louis, MO 63166
Attn: DRCPM-CO-T (2)

Project Manager
Advanced Scout Helicopter
P.O. Box 209
St. Louis, MO 63166
Attn: DRDAV-ASH (2)

Project Manager
Navigation/Control Systems
Ft. Monmouth, NJ 07703
Attn: DRCPM-NC-TM (2)

Project Manager
Tactical Airborne Remotely Piloted Vehicle/Drone Systems
P.O. Box 209
St. Louis, MO 63166
Attn: DRCPM-RPV (2)

Commander
US Army Materiel Development and Readiness Command
5001 Eisenhower Avenue
Alexandria, VA 22333
Attn: DRCMT (4)

Director
Applied Technology Laboratory
Research & Technology Laboratories
Ft. Eustis, VA 23604
Attn: DAVDL-ATL-ATS (2)

Director
Research & Technology Laboratories
AVRADCOM
Moffett Field, CA 94035
Attn: DAVDL-AL-D (2)

Director
Langley Directorate
US Army Air Mobility R&D Laboratory
(AVRADCOM)
Mail Stop 266
Hampton, VA 23365
Attn: DAVDL-LA (2)

Commander
US Army Avionics Research & Development Activity
Ft. Monmouth, NJ 07703
Attn: DAVAA-) (2)

DISTRIBUTION LIST (Cont)

Director, Lewis Directorate
US Army Air Mobility R&D Labs
21000 Brookpark Road
Cleveland, OH 44135
Attn: DAVDL-LE (2)

Director
US Army Materials & Mechanics
Research Center
Watertown, MA 02172
Attn: DRXMR-PT (25)

Director
US Army Industrial Base
Engineering Activity
Rock Island Arsenal
Rock Island, IL 61201
Attn: DRXIB-MT (4)

Director
Air Force Materials Laboratory
Wright-Patterson Air Force Base
Dayton, OH 45433
Attn: AFML/LT (2)

Commander
U.S. Army Electronics Command
Ft. Monmouth, NJ 07703
Attn: DRSEL-RD-P (1)

Commander
US Army Missile Command
Redstone Arsennal, AL 35809
Attn: DRSMI-IIE (1)

Mr. P. Baumgartner
Chief, Manufacturing Technology
Bell Helicopter Textron
P.O. Box 482
Ft. Worth, TX 76101 (2)

Mr. A. S. Falcone
Chief, Materials Engineering
Bloomfield, CT 06002 (2)

Mr. R. Pickney
Manufacturing Technology
Boeing Vertol Company
P.O. Box 16858
Philadelphia, PA 19142 (2)

Commander
US Army Troop Support & Aviation
Materiel Readiness Command
4300 Goodfellow Blvd.
St. Louis, MO 63120
Attn: DRSTS-PLC (1)
Attn: DRSTS-ME (1)
Attn: DRSTS-DIL (2)

Commander
US Army Armament Command
Rock Island, IL 61201
Attn: DRSAR-PPR-1W (1)

Commander
US Army Tank-Automotive Command
Warren, MI 48090
Attn: DRSTA-RCM.1 (1)

Commander
Defense Documentation Center
Cameron Station, Building 5
5010 Duke Street
Alexandria, VA 22314 (12)

Hughes Helicopters-Summa
Centinella Ave. & Teale St.
Culver City, CA 90230
Attn: Mr. R. E. Moore
Bldg. 314, MS T-419 (2)

Sikorsky Aircraft Division
United Aircraft Corporation
Stratford, CT 06497
Attn: Mr. Melvin M. Schwartz
Chief, Mfg. Tech. (2)

Mr. J. E. Knott
General Manager
Detroit Diesel Allison
P.O. Box 894
Indianapolis, IN 46206 (2)

Mr. H. Franzen
General Electric Company
10449 St. Charles Rock Road
St. Ann, MO 63074 (2)

DISTRIBUTION LIST (Cont)

Mr. V. Strautman, Manager
Process Technology Laboratory
AVCO-Lycoming Corporation
550 South Main Street
Stratford, CT 08497 (2)

Grumman Aerospace Corporation
Plant 2
Bethpage, NY 11714
Attn: Richard Cyphers, Mgr.
Mfg. Technology (1)
Attn: Albert Grenci, Mfg.
Engineer, Dept. 231 (1)

Mr. D. M. Schwartz
Dept. 55-10, Bldg. 572
Lockheed Missiles & Space Co., Inc.
P.O. Box 504
Sunnyvale, CA 94086 (2)

Mr. Ray Traynor
Mfg Research & Development
Pratt & Whitney Aircraft Div.
United Technologies Corp.
East Hartford, CT 06108 (2)

Mr. R. Drago
Advanced Drive Systems Technology
Boeing Vertol Company
P.O. Box 16858
Philadelphia, PA 19142 (2)

Mr. H. Dorfman
Research Specialist, Mfg. Research
1111 Lockheed Way
Sunnyvale, CA 94088 (2)

Army Materials and Mechanics Research Center,
Watertown, Massachusetts 02172
COMPLEX, PRECISION CAST COLUMBIUM ALLOY GAS TURBINE ENGINE NOZZLES COATED TO RESIST OXIDATION
L. Hsu, W.G. Stevens and A.R. Stetson
Solar Turbines International, An Operating Group of International Harvester, P.O. Box 80966, San Diego, California 92138.
Technical Report AVRADCOM TR 80-F-2
illus - tables, Contract DAAG46-76-C-0053
D/A Project 1758129, AMCMS Code 1497.94.5.58129
Final Report, August 2, 1976 to August 2, 1979

AD_____

UNCLASSIFIED
UNLIMITED DISTRIBUTION

Key Words

Columbium alloys	Solid
C129Y	Cored
Castings	Burner rig
Oxidation	NS-4 coating
Nozzle vane	Tensile
Stress rupture	

The objectives of this program were to produce investment cast single vane nozzle segments in C129Y alloy (Cb-10Hf-10W0.3Y) and to coat these vanes with the NS-4 (50W-20Mo-15Ti-10V) silicide coating. Initially, both cored and solid vane segments were specified but due to problems experienced in the consumable arc process, cored vanes were deleted from the program scope. REM Metals of Albany, Oregon was the casting subcontractor and though they have had previous experience with this alloy and other columbium alloys in general, several problems developed. The electrode material supplied was low in yttrium, which might have contributed to the poor fluidity during arc melt and incomplete fill of thin walled sections. The solid nozzles and round test bars were acceptable and were used in coating processing and testing. Process specifications for both slurry spray and dip applications of the NS-4 modifier were prepared. Tensile and stress rupture tests of coated specimens displayed exceptional properties at elevated temperatures and showed superiority to cobalt-base vane alloys. Isothermal oxidation lives in excess of 5500 hours (at 760 and 1093°C) were exhibited by NS-4 coated C129Y specimens. In rig testing, under the severe thermal cycles and profiles imposed, the airfoil specimens typically survived about 100 hours.

Army Materials and Mechanics Research Center,
Watertown, Massachusetts 02172
COMPLEX, PRECISION CAST COLUMBIUM ALLOY GAS TURBINE ENGINE NOZZLES COATED TO RESIST OXIDATION
L. Hsu, W.G. Stevens and A.R. Stetson
Solar Turbines International, An Operating Group of International Harvester, P.O. Box 80966, San Diego, California 92138.
Technical Report AVRADCOM TR 80-F-2
illus - tables, Contract DAAG46-76-C-0053
D/A Project 1758129, AMCMS Code 1497.94.5.58129
Final Report, August 2, 1976 to August 2, 1979

AD_____

UNCLASSIFIED
UNLIMITED DISTRIBUTION

Key Words

Columbium alloys	Solid
C129Y	Cored
Castings	Burner rig
Oxidation	NS-4 coating
Nozzle vane	Tensile
Stress rupture	

The objectives of this program were to produce investment cast single vane nozzle segments in C129Y alloy (Cb-10Hf-10W0.3Y) and to coat these vanes with the NS-4 (50W-20Mo-15Ti-10V) silicide coating. Initially, both cored and solid vane segments were specified but due to problems experienced in the consumable arc process, cored vanes were deleted from the program scope. REM Metals of Albany, Oregon was the casting subcontractor and though they have had previous experience with this alloy and other columbium alloys in general, several problems developed. The electrode material supplied was low in yttrium, which might have contributed to the poor fluidity during arc melt and incomplete fill of thin walled sections. The solid nozzles and round test bars were acceptable and were used in coating processing and testing. Process specifications for both slurry spray and dip applications of the NS-4 modifier were prepared. Tensile and stress rupture tests of coated specimens displayed exceptional properties at elevated temperatures and showed superiority to cobalt-base vane alloys. Isothermal oxidation lives in excess of 5500 hours (at 760 and 1093°C) were exhibited by NS-4 coated C129Y specimens. In rig testing, under the severe thermal cycles and profiles imposed, the airfoil specimens typically survived about 100 hours.

Army Materials and Mechanics Research Center,
Watertown, Massachusetts 02172
COMPLEX, PRECISION CAST COLUMBIUM ALLOY GAS TURBINE ENGINE NOZZLES COATED TO RESIST OXIDATION
L. Hsu, W.G. Stevens and A.R. Stetson
Solar Turbines International, An Operating Group of International Harvester, P.O. Box 80966, San Diego, California 92138.
Technical Report AVRADCOM TR 80-F-2
illus - tables, Contract DAAG46-76-C-0053
D/A Project 1758129, AMCMS Code 1497.94.5.58129
Final Report, August 2, 1976 to August 2, 1979

AD_____

UNCLASSIFIED
UNLIMITED DISTRIBUTION

Key Words

Columbium alloys	Solid
C129Y	Cored
Castings	Burner rig
Oxidation	NS-4 coating
Nozzle vane	Tensile
Stress rupture	

The objectives of this program were to produce investment cast single vane nozzle segments in C129Y alloy (Cb-10Hf-10W0.3Y) and to coat these vanes with the NS-4 (50W-20Mo-15Ti-10V) silicide coating. Initially, both cored and solid vane segments were specified but due to problems experienced in the consumable arc process, cored vanes were deleted from the program scope. REM Metals of Albany, Oregon was the casting subcontractor and though they have had previous experience with this alloy and other columbium alloys in general, several problems developed. The electrode material supplied was low in yttrium, which might have contributed to the poor fluidity during arc melt and incomplete fill of thin walled sections. The solid nozzles and round test bars were acceptable and were used in coating processing and testing. Process specifications for both slurry spray and dip applications of the NS-4 modifier were prepared. Tensile and stress rupture tests of coated specimens displayed exceptional properties at elevated temperatures and showed superiority to cobalt-base vane alloys. Isothermal oxidation lives in excess of 5500 hours (at 760 and 1093°C) were exhibited by NS-4 coated C129Y specimens. In rig testing, under the severe thermal cycles and profiles imposed, the airfoil specimens typically survived about 100 hours.

Army Materials and Mechanics Research Center,
Watertown, Massachusetts 02172
COMPLEX, PRECISION CAST COLUMBIUM ALLOY GAS TURBINE ENGINE NOZZLES COATED TO RESIST OXIDATION
L. Hsu, W.G. Stevens and A.R. Stetson
Solar Turbines International, An Operating Group of International Harvester, P.O. Box 80966, San Diego, California 92138.
Technical Report AVRADCOM TR 80-F-2
illus - tables, Contract DAAG46-76-C-0053
D/A Project 1758129, AMCMS Code 1497.94.5.58129
Final Report, August 2, 1976 to August 2, 1979

AD_____

UNCLASSIFIED
UNLIMITED DISTRIBUTION

Key Words

Columbium alloys	Solid
C129Y	Cored
Castings	Burner rig
Oxidation	NS-4 coating
Nozzle vane	Tensile
Stress rupture	

The objectives of this program were to produce investment cast single vane nozzle segments in C129Y alloy (Cb-10Hf-10W0.3Y) and to coat these vanes with the NS-4 (50W-20Mo-15Ti-10V) silicide coating. Initially, both cored and solid vane segments were specified but due to problems experienced in the consumable arc process, cored vanes were deleted from the program scope. REM Metals of Albany, Oregon was the casting subcontractor and though they have had previous experience with this alloy and other columbium alloys in general, several problems developed. The electrode material supplied was low in yttrium, which might have contributed to the poor fluidity during arc melt and incomplete fill of thin walled sections. The solid nozzles and round test bars were acceptable and were used in coating processing and testing. Process specifications for both slurry spray and dip applications of the NS-4 modifier were prepared. Tensile and stress rupture tests of coated specimens displayed exceptional properties at elevated temperatures and showed superiority to cobalt-base vane alloys. Isothermal oxidation lives in excess of 5500 hours (at 760 and 1093°C) were exhibited by NS-4 coated C129Y specimens. In rig testing, under the severe thermal cycles and profiles imposed, the airfoil specimens typically survived about 100 hours.

Army Materials and Mechanics Research Center,
Watertown, Massachusetts 02172
COMPLEX, PRECISION CAST COLUMBIUM ALLOY GAS TURBINE ENGINE NOZZLES COATED TO RESIST OXIDATION
L. Hsu, W.G. Stevens and A.R. Stetson
Solar Turbines International, An Operating Group of International Harvester, P.O. Box 80966, San Diego, California 92138.
Technical Report AVRADCOM TR 80-F-2
illus - tables, Contract DAAG46-76-C-0053
D/A Project 1758129, AMCMS Code 1497.94.5.58129
Final Report, August 2, 1976 to August 2, 1979

AD_____

UNCLASSIFIED
UNLIMITED DISTRIBUTION

Key Words

Columbium alloys	Solid
C129Y	Cored
Castings	Burner rig
Oxidation	NS-4 coating
Nozzle vane	Tensile
Stress rupture	

The objectives of this program were to produce investment cast single vane nozzle segments in C129Y alloy (Cb-10Hf-10W0.3Y) and to coat these vanes with the NS-4 (50W-20Mo-15Ti-10V) silicide coating. Initially, both cored and solid vane segments were specified but due to problems experienced in the consumable arc process, cored vanes were deleted from the program scope. REM Metals of Albany, Oregon was the casting subcontractor and though they have had previous experience with this alloy and other columbium alloys in general, several problems developed. The electrode material supplied was low in yttrium, which might have contributed to the poor fluidity during arc melt and incomplete fill of thin walled sections. The solid nozzles and round test bars were acceptable and were used in coating processing and testing. Process specifications for both slurry spray and dip applications of the NS-4 modifier were prepared. Tensile and stress rupture tests of coated specimens displayed exceptional properties at elevated temperatures and showed superiority to cobalt-base vane alloys. Isothermal oxidation lives in excess of 5500 hours (at 760 and 1093°C) were exhibited by NS-4 coated C129Y specimens. In rig testing, under the severe thermal cycles and profiles imposed, the airfoil specimens typically survived about 100 hours.

Army Materials and Mechanics Research Center,
Watertown, Massachusetts 02172
COMPLEX, PRECISION CAST COLUMBIUM ALLOY GAS TURBINE ENGINE NOZZLES COATED TO RESIST OXIDATION
L. Hsu, W.G. Stevens and A.R. Stetson
Solar Turbines International, An Operating Group of International Harvester, P.O. Box 80966, San Diego, California 92138.
Technical Report AVRADCOM TR 80-F-2
illus - tables, Contract DAAG46-76-C-0053
D/A Project 1758129, AMCMS Code 1497.94.5.58129
Final Report, August 2, 1976 to August 2, 1979

AD_____

UNCLASSIFIED
UNLIMITED DISTRIBUTION

Key Words

Columbium alloys	Solid
C129Y	Cored
Castings	Burner rig
Oxidation	NS-4 coating
Nozzle vane	Tensile
Stress rupture	

The objectives of this program were to produce investment cast single vane nozzle segments in C129Y alloy (Cb-10Hf-10W0.3Y) and to coat these vanes with the NS-4 (50W-20Mo-15Ti-10V) silicide coating. Initially, both cored and solid vane segments were specified but due to problems experienced in the consumable arc process, cored vanes were deleted from the program scope. REM Metals of Albany, Oregon was the casting subcontractor and though they have had previous experience with this alloy and other columbium alloys in general, several problems developed. The electrode material supplied was low in yttrium, which might have contributed to the poor fluidity during arc melt and incomplete fill of thin walled sections. The solid nozzles and round test bars were acceptable and were used in coating processing and testing. Process specifications for both slurry spray and dip applications of the NS-4 modifier were prepared. Tensile and stress rupture tests of coated specimens displayed exceptional properties at elevated temperatures and showed superiority to cobalt-base vane alloys. Isothermal oxidation lives in excess of 5500 hours (at 760 and 1093°C) were exhibited by NS-4 coated C129Y specimens. In rig testing, under the severe thermal cycles and profiles imposed, the airfoil specimens typically survived about 100 hours.